ORGANIC/INORGANIC HYBRID AMINE AND SULFONIC ACID TETHERED SILICA MATERIALS: SYNTHESIS, CHARACTERIZATION AND APPLICATION

A Dissertation
Presented to
The Academic Faculty

by

Jason Christopher Hicks

In Partial Fulfillment
of the Requirements for the Degree
Doctor of Philosophy in the
School of Chemical & Biomolecular Engineering

Georgia Institute of Technology
December, 2007

ORGANIC/INORGANIC HYBRID AMINE AND SULFONIC ACID TETHERED SILICA MATERIALS: SYNTHESIS, CHARACTERIZATION AND APPLICATION

Approved by:

Dr. Christopher W. Jones, Advisor
School of Chemical & Biomolecular Engineering
Georgia Institute of Technology

Dr. Sankar Nair
School of Chemical & Biomolecular Engineering
Georgia Institute of Technology

Dr. William Koros
School of Chemical & Biomolecular Engineering
Georgia Institute of Technology

Dr. Marcus Weck
School of Chemistry & Biochemistry
Georgia Institute of Technology

Dr. Andrew Lyon
School of Chemistry & Biochemistry
Georgia Institute of Technology

Date Approved: August 17, 2007

ACKNOWLEDGEMENTS

This work could not have been completed without the help of many individuals. I would like to start by thinking my advisor, Chris Jones. I owe many thanks to Chris for developing me as a scientist who strives for excellence. He gave me independence while guiding me through the rough patches. I have appreciated and enjoyed working with him. I also thank my committee members, Dr. William Koros, Dr. Andrew Lyon, Dr. Sankar Nair, and Dr. Marcus Weck for their advice and support. I also thank Marcus for initiating many scientific debates/discussions during group meetings. I would also like to thank Dr. Mike McKittrick for training me in the lab and being a great friend! I hope he continues to have success with his career.

I also thank previous and current members of the Jones group. I would like to thank Benn Wilson, John Richardson, Chris Gill and Dr. Henry Cheng for making many of the bad days better.

I would like to thank my parents, John and Debbie Hicks, for all of your love and support. Without your guidance I would not have accomplished many of my goals. I would also like to thank my big brother, Jon Hicks, for encouraging me to make as much money as possible. I also thank my Siberian Husky, Kaia, for keeping me company all of those nights I worked at home.

Most importantly, I thank my favorite group member, best friend, and fiancée, Rebecca Shiels. Without you, I could not have accomplished all that I have. I specifically thank you for having such amazing editing skills. You saved me countless

hours during this process. For this, I am forever grateful and indebted to you. I love you so very much!

TABLE OF CONTENTS

LIST OF TABLES

LIST OF FIGURES

LIST OF ABBREVIATIONS

AEAPTMS	N-(3-(trimethoxysilyl)propyl)ethane-1,2-diamine
APTMS	3-aminopropyltrimethoxysilane
$B(Ar)_F$	tris(pentafluorophenyl)borane
BET	Brunauer-Emmet-Teller
BJH	Bopp-Jancso-Heinzinger
CGC	constrained-geometry catalyst
Cp	cyclopentadiene
Cp'	tetramethylcyclopentadiene
CP MAS	cross polarization magic angle spinning
D.I.	deionized
DSC	differential scanning calorimetry
FAB	perfluoro(aryl)boranes
FT-	Fourier transform-
HAS	hyperbranched aminosilica
HMDS	1,1,1,3,3,3-hexamethyldisilazane
IR	infrared
MAO	methylaluminoxane
MCM-41	type of periodic mesoporous silica
MPTMS	3-mercaptopropyltrimethoxysilane
MS	mass spectroscopy
MTMS	methyltrimethoxysilane
NETL	National Energy Technology Laboratory
NMR	nuclear magnetic resonance

PBA	1-pyrenebutyric acid
PCA	1-pyrenecarboxylic acid
PE	poly(ethylene)
PEI	polyethyleneimine
ppm	parts per million
SBA-15	type of periodic mesoporous silica
SCA	spherical capacitor analyzer
SEM	scanning electron microscopy
SMO	sulfated metal oxide
TEOS	tetraethyl orthosilicate
TGA	thermogravimetric analysis
TIBA	triisobutylaluminum
TMA	trimethylaluminum
UV-Vis	ultraviolet-visible spectroscopy
XPS	X-ray photoelectron spectroscopy
XRD	X-ray diffraction

SUMMARY

The major goals of this thesis were to: (1) create a site-isolated aminosilica material with higher amine loadings than previously reported isolation methods, (2) use spectroscopic, reactivity, and catalytic (olefin polymerization precatalysts) probes to determine isolation of amine groups on these organic/inorganic hybrid materials, (3) synthesize an organic/inorganic hybrid material capable of activating Group 4 olefin polymerization precatalysts, and (4) synthesize a high amine loaded organic/inorganic hybrid material capable of reversibly capturing CO_2 in a simulated flue gas stream.

The underlying motivation of this research involved the synthesis and design of novel amine and sulfonic acid materials. Traditional routes to synthesize aminosilicas have led to the formation of a high loading of multiple types of amine sites on the silica surface. Part of this research involved the creation of a new aminosilica material via a protection/deprotection method designed to prevent multiple sites, while maintaining a relatively high loading. As a characterization technique, fluorescence spectroscopy of pyrene-based fluorophores loaded on traditional aminosilicas and site-isolated aminosilicas was used to probe the degree of site-isolation obtained with these methods. Also, this protection/deprotection method was compared to other reported isolation techniques with heterogeneous Group 4 constrained-geometry inspired catalysts (CGCs). It was determined that the degree of separation of the amine sites could be controlled with protection/deprotection methods. Furthermore, an increase in the reactivity of the amines and the catalytic activity of CGCs built off of the amines was determined for aminosilicas synthesized by a protection/deprotection method. The second part of this

work involved developing organic/inorganic hybrid materials as heterogeneous Brønsted acidic cocatalysts for activation of olefin polymerization precatalysts. This was the first reported organic/inorganic hybrid sulfonic acid functionalized silica material capable of activating metallocenes for the polymerization of ethylene when small amounts of an alkylaluminum was added. Lastly, an organic/inorganic hybrid hyperbranched aminosilica material capable of capturing carbon dioxide from flue gas streams was synthesized. This material was determined to capture CO_2 with capacities higher than currently reported aminosilica adsorbents.

.

.

CHAPTER 1

INTRODUCTION

1.1 Organic/Inorganic Hybrid Materials

The focus of this dissertation is the synthesis and characterization of organic/inorganic hybrid materials, as well as the engineering of these hybrid materials for applications in polymerization catalysis and adsorption. For the purposes of this work, I will define an organic/inorganic hybrid material as a material that consists of an inorganic support with organic functionalities covalently tethered to the support or covalently bound within the framework. Organic/inorganic hybrid materials are important because they can be designed at a molecular level to perform many processes including catalysis,[1] adsorption,[2-5] separation,[6] drug delivery[7] and sensing[7]. They are also used as supports off of which one may construct more complex materials such as dendrons and organometallic catalysts.[8-18] Due to their many different building blocks as well as the countless ways to combine the building blocks together, organic/inorganic hybrid materials will continue to have high importance in the future. This work focuses on the synthesis, characterization, and application of organic/inorganic hybrid amine and sulfonic acid functionalized silica materials.

There were four specific goals that motivated the presented research. The first of these was the development of a site isolated aminosilica with higher amine loadings than previously reported methods. While these earlier methods allowed the preparation of either highly loaded amines or site-isolated amines, a satisfactory method for achieving high loading with relatively uniform amine spacing in the same material has not been

previously reported. This topic is introduced is section 1.2 of this Introduction, and new advances are described in Chapter 2.

The second goal of this work was the characterization of the degree of amine isolation on the new aminosilica material described in Chapter 1 along with other leading aminosilica materials by examining their spectroscopic signatures, their reactivity toward further functionalization, and their utility as support materials for grafted olefin polymerization precatalysts. While reactivity studies are informative and are commonly performed, I have found that the addition of new spectroscopic data has provided greater insight into the nature of the surface species. These results are presented in Chapter 3. These results are complemented with reactivity studies centered around the immobilization of olefin polymerization precatalysts on the aminosilica materials. An introduction to tethered olefin polymerization precatalysts as well as a background on the development of olefin polymerization catalysts can be found in this Introduction in sections 1.3.1 and 1.3.2. My results pertaining to the reactivity of the aminosilica supported catalysts in olefin polymerizations may be found in Chapter 4.

The third goal of this work was the synthesis of an organic/inorganic hybrid material capable of activating Group 4 olefin polymerization precatalysts. Previously, activators, or cocatalysts, have been ill-defined, difficult to synthesize, extremely unstable, or have suffered from extensive leaching from the support into solution under reaction conditions. An introduction to this topic is presented in this chapter in section 1.3.3 as a continuation of the olefin polymerization section (1.3). My results involving the synthesis of the first organic/inorganic hybrid reported as a successful dual

cocatalyst/support for single-site olefin polymerization precatalysts are presented in Chapter 5.

The final goal was synthesizing a highly loaded aminosilica material capable of reversibly capturing CO_2 in a simulated flue gas stream. Aqueous amine solutions have been utilized in the past to reversibly capture CO_2, but these processes have required a substantial amount of energy to be recyclable. Therefore, solid materials with similar CO_2 adsorbing properties have become very attractive. A key hurdle preventing implementation of these solid materials has been their low CO_2 capacities. An introduction to this topic is presented in this Introduction in section 1.4. My results demonstrating a high capacity solid amine material are presented in Chapter 6.

Thus, this thesis demonstrates an expansion in both understanding of the structure of advanced hybrid materials as well as new engineering applications for this class of materials.

1.1.1 Inorganic Support Material: Silica

The inorganic portion of the organic/inorganic hybrid material plays an important role in the overall properties of the material. Key attributes of the support material for the goals I have described above are that it should be (1) inert to chemical reactions with the solvent, (2) robust over a wide range of reaction temperatures and pressures, (3) easily functionalized without destruction of the material, and (4) low in cost. Amorphous silica materials are common supports that satisfy these requirements. The most important characteristic of silica materials for the work described here is the ease with which one can tether organic functionalities onto the support material. The silica surface has highly

reactive silanol (Si – OH) groups onto which organic functionalities may be reacted (Figure 1.1), allowing for the formation of organic/inorganic hybrid materials. The silica material can have a mixture of isolated silanols (1.1A), geminal silanols (1.1B), vicinal silanols (1.1C), and siloxane bridges (1.1D). All of these surface species can be modified to form organic/inorganic hybrid materials.

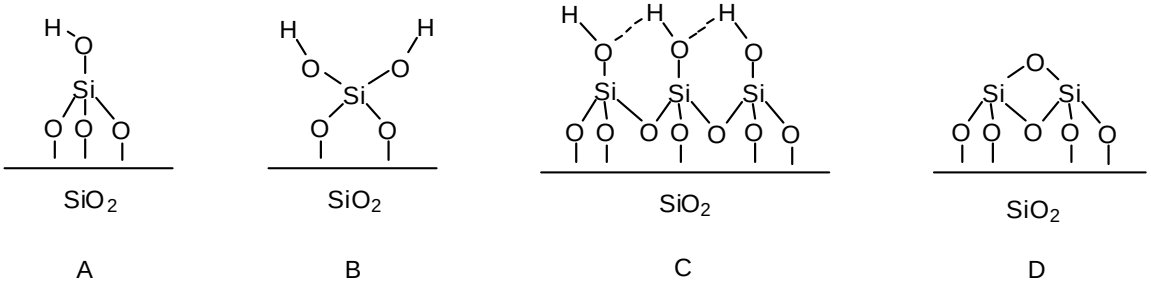

Figure 1.1. Types of silica surface Si-O species.

1.1.2 Synthesis of Mesoporous Silica Supports

Typically, amorphous silica supports are synthesized by the polymerization of $Si(OR)_4$ (tetraalkyl orthosilicate, where R is the alkyl chain) to form a network of SiO_2 groups (Figure 1.2).[19] The structure and properties of the silica are controlled by the reaction conditions and the alkoxy groups on the silicate used to make the material. Although commercial amorphous silicas meet the design criteria, their main disadvantage is a broad distribution of pore diameters. To address this problem, periodic mesoporous silicas have been developed. These mesoporous silicas can be synthesized with a smaller distribution of pore diameters while also maintaining high surface areas (~ 700 – 900

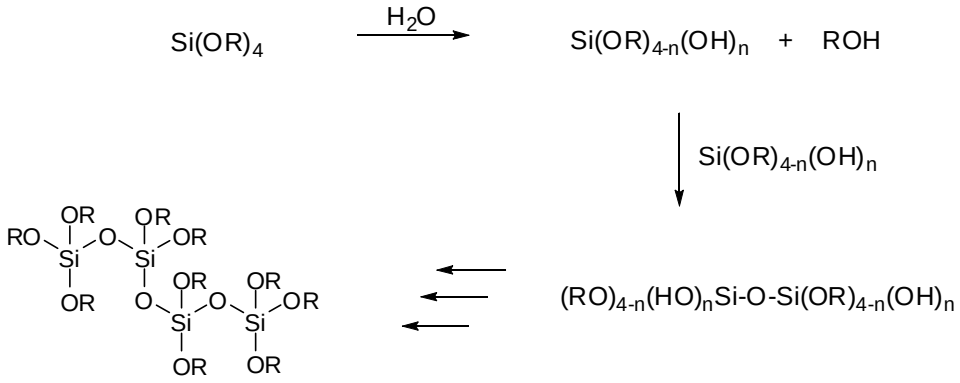

Figure 1.2. Amorphous SiO_2 framework.

m^2/g). The experiments discussed in this dissertation will predominately utilize periodic mesoporous silicas, where the mesopores range between 20 and 500 Å. These materials were initially discovered by Beck and coworkers who synthesized a silica material, MCM-41, with a regular, controllable pore size.[20] In one example from this group, the pores were unidirectional and hexagonally aligned and resulted in a material with a very high surface area (~ 700 m^2/g).

Another periodic mesoporous silica is SBA-15. SBA-15 is the material used in the work described in this thesis.[21] The key to the synthesis of this material is the use of a non-ionic triblock copolymer (Pluronic 123), which serves as a structure directing agent. Specifically, the triblock copolymer forms micelles in an acidic aqueous ethanol solution (Figure 1.3A). After dispersion of the micelles, tetraethyl orthosilicate (TEOS, $Si(OEt)_4$) is added as the silica source, and it polymerizes around the micelles to form the inorganic framework (Figure 1.3B and 1.3C). TEOS is used as the silica source because it prevents the silica material from being contaminated with residual halogen compounds that can be

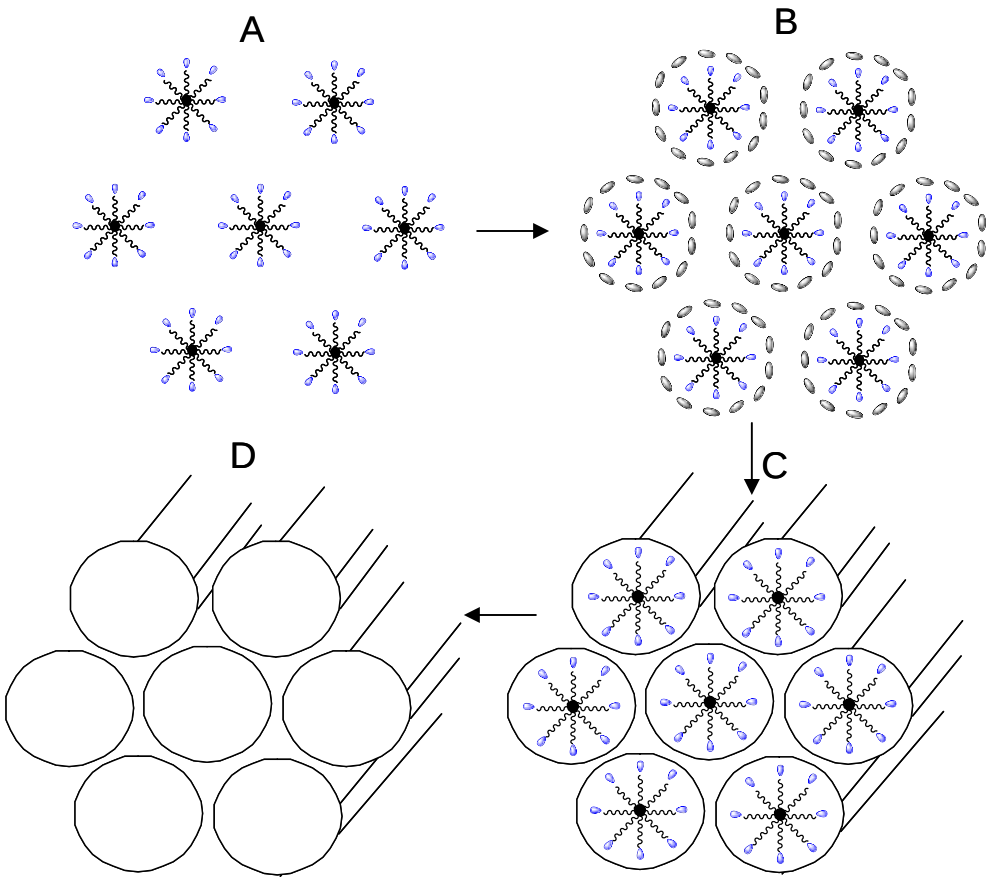

Figure 1.3. Synthesis of SBA-15.

incorporated when other silica sources, such as $SiCl_4$, are used. Subsequently, the copolymer is removed from the support material by calcinations in air and it leaves behind a unidirectional, hexagonally aligned mesoporous silica material (Figure 1.3D). The triblock copolymer directs the silica source to form according to the shape and size of the micelles, allowing for control of the pore size in the silica product.

1.2 Organic/Inorganic Hybrid Aminosilicas

Possibly the most well-studied class of organic/inorganic hybrid materials is aminosilicas. These are materials where primary, secondary, or tertiary amine functionalities are attached to the silica support via an alkyl or aryl linker. Due to the simplicity of their syntheses, aminosilicas have been studied for many different applications. For instance, aminosilica materials have been used in catalysis,[1] adsorption,[2-5] separations,[6] and as supports for more advanced organic synthesis, resulting silica-tethered organometallic catalysts or dendrons.[8-18] This section will focus on discussing the various syntheses of 3-aminopropylsilyl-functionalized silica materials (Figure 1.4).

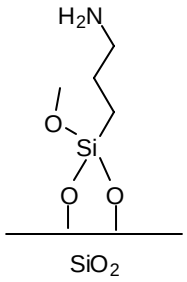

Figure 1.4. Example of 3-aminopropylsilyl-fuctionalized silica materials.

Typically, aminosilicas are synthesized by one of two routes: (1) co-condensation of an aminopropylalkoxysilane with the silica source to form the silica material[22], or (2) grafting[20] of the aminopropylalkoxysilane to the post-synthesized silica material. The difference between the two methods chiefly involves the location of the amine organic functionalities on the silica support with the co-condensed material having amine groups

on the surface and within the walls of the silica framework and the grafted material only having amine groups on the surface (Figure 1.5).[23] The co-condensation method usually

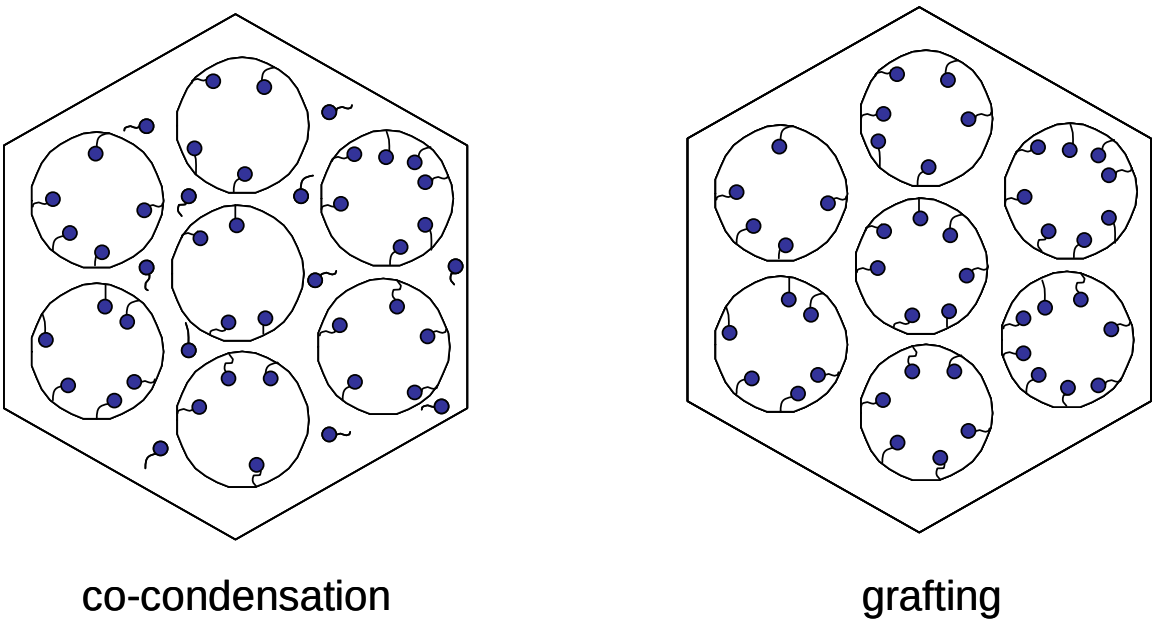

Figure 1.5. Aminosilicas via co-condensation or grafting.

begins by mixing dilute quantities of an aminopropylalkoxysilane and silica precursor with a structure directing agent to form the pore structure. After the silica precursor and aminopropylalkoxysilane co-polymerize, the structure directing agent can be removed via a solvent extraction to give functionalized porous channels. This method has allowed for the ability to easily alter the loading of the amino groups on the surface. However, in some cases, the aminopropylsilane can damage the structural integrity of the material.[24] Another drawback is that the location of the organic group may or may not be accessible, especially when high quantities of the aminopropylalkoxysilane are used.[23]

Grafting of aminopropylalkoxysilanes to preformed silica structures is possibly the easiest approach to form aminopropylalkoxysilyl-groups tethered to a support. Knözinger and Rumpf first reported the synthesis of an amine-grafted silica material by refluxing (2-aminoethyl)-aminopropyltrimethoxysilane (AEAPTMS) with silica in 1978.[25] Grafting of the aminopropylalkoxysilane directly to the silica surface occurs through a reaction between the surface silanols (Figure 1.1) and the alkoxysilane. As shown in Figure 1.6, the alkoxy portion of the silane reacts directly with the surface

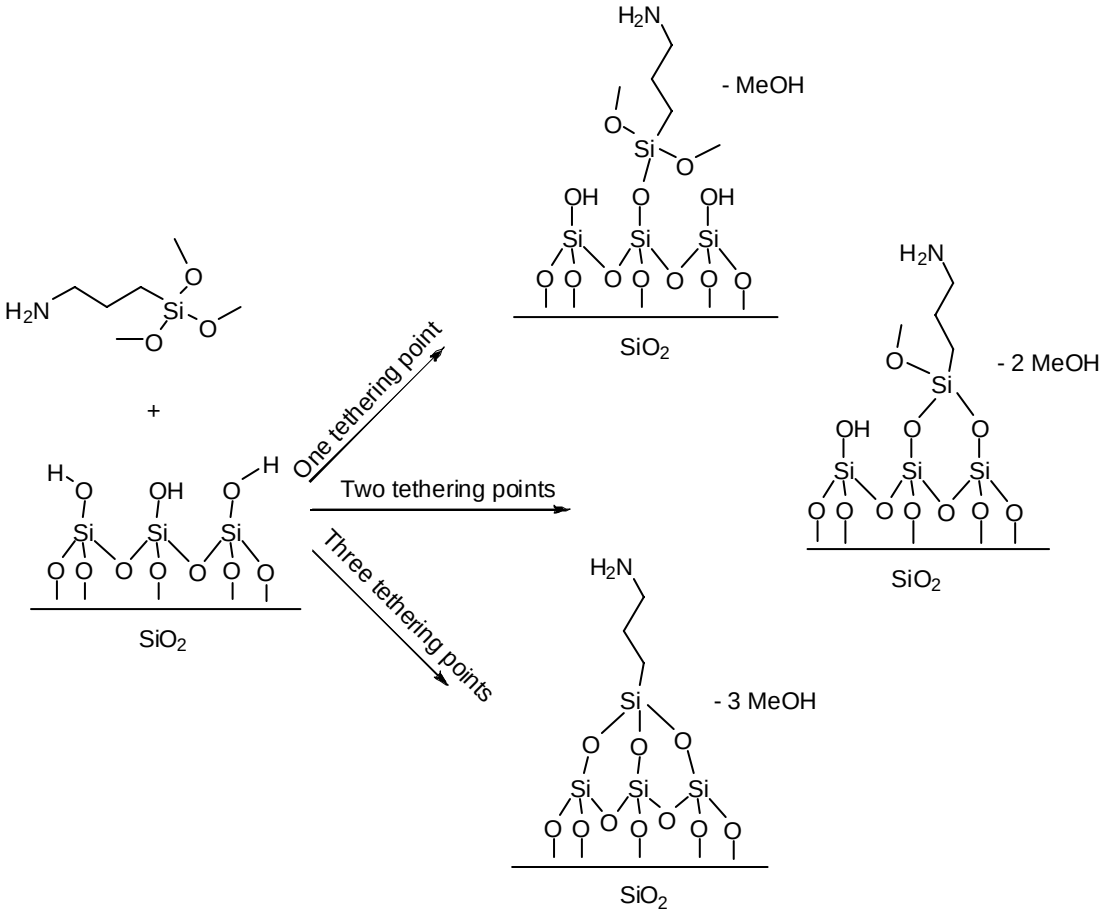

Figure 1.6. Reaction of 3-aminopropyltrimethoxysilane (APTMS) with silica.

silanol evolving alcohol (methanol in this case). The silane is therefore grafted to the surface via a covalent bond with an oxygen atom from the surface. This oxygen can either be from a reactive silanol or a siloxane bridge (Figure 1.1). Depending on the proximity of the surface silanols to one another and depending on how many alkoxy groups are on the silane, up to three tethering linkages can be formed. The resulting material is stable towards most organic solvents and moderate temperatures (~ 200 ^{o}C).

One method to produce aminosilicas with high loadings of amine groups involves the addition of water to create a wet silica surface.[26, 27] The water on the surface "activates" the aminopropylalkoxysilane before its reaction to the surface. This activation occurs through the reaction of water with the alkoxysilane (R'Si(OR)$_3$) to form an R'Si(OR)$_2$-OH compound and the corresponding alcohol (ROH) (Figure 1.7).

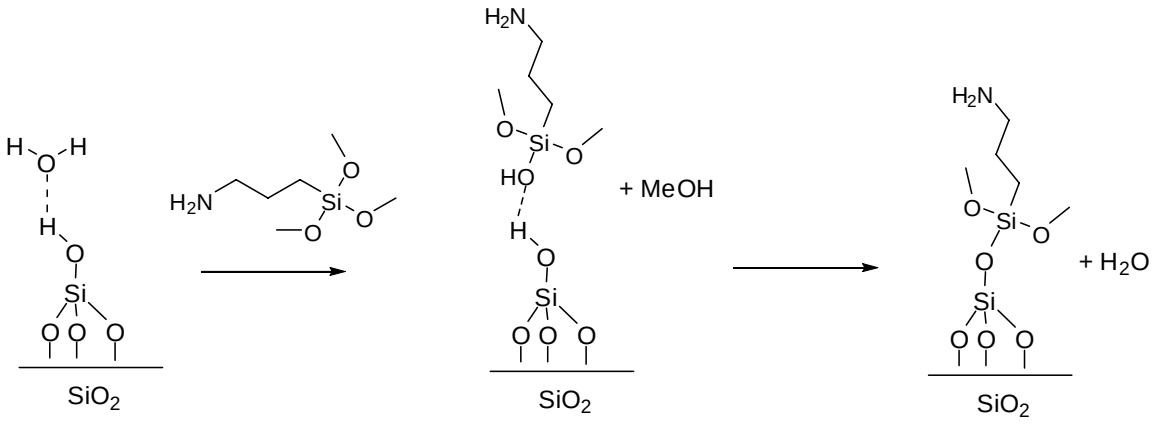

Figure 1.7. Grafting of APTMS in the presence of water.

Subsequently, the R'Si(OR)$_2$-OH group can react with a surface silanol (Si-OH) group to form a covalent bond with the surface. Unfortunately, the alkoxysilane can oligomerize

uncontrollably in the presence of water.[26, 28] Therefore, the resulting material is synthesized with a high loading of amines, but the configuration of the amines on the surface is uncontrollable (Figure 1.8). When the aminopropylalkoxysilane groups

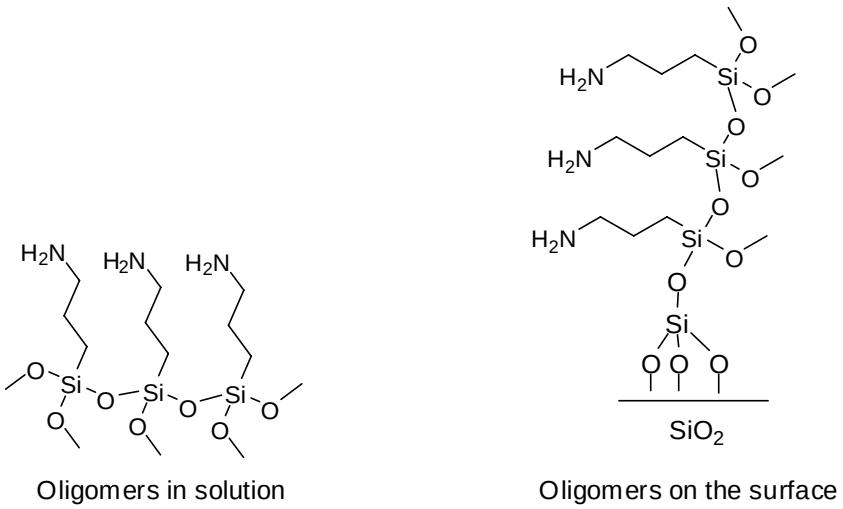

Figure 1.8. Alkoxysilane oligomers.

oligomerize, it can make it difficult for substrates to access all of the amine sites, resulting in an aminosilica with poor amine efficiency in further reactions.

Tripp and coworkers discovered that the addition of a base (triethylamine, ethylenediamine, or 3-aminopropyltrimethoxysilane (APTMS)) activated the silanols for reaction with the alkoxysilane.[28] The advantage of this method to produce high amine loadings is that it can be performed in the absence of water. It was proposed that as the amines become relatively close to the surface, they form hydrogen bonds with the surface silanols (Figure 1.9). The hydrogen bonding activates the silanols to react with a nearby

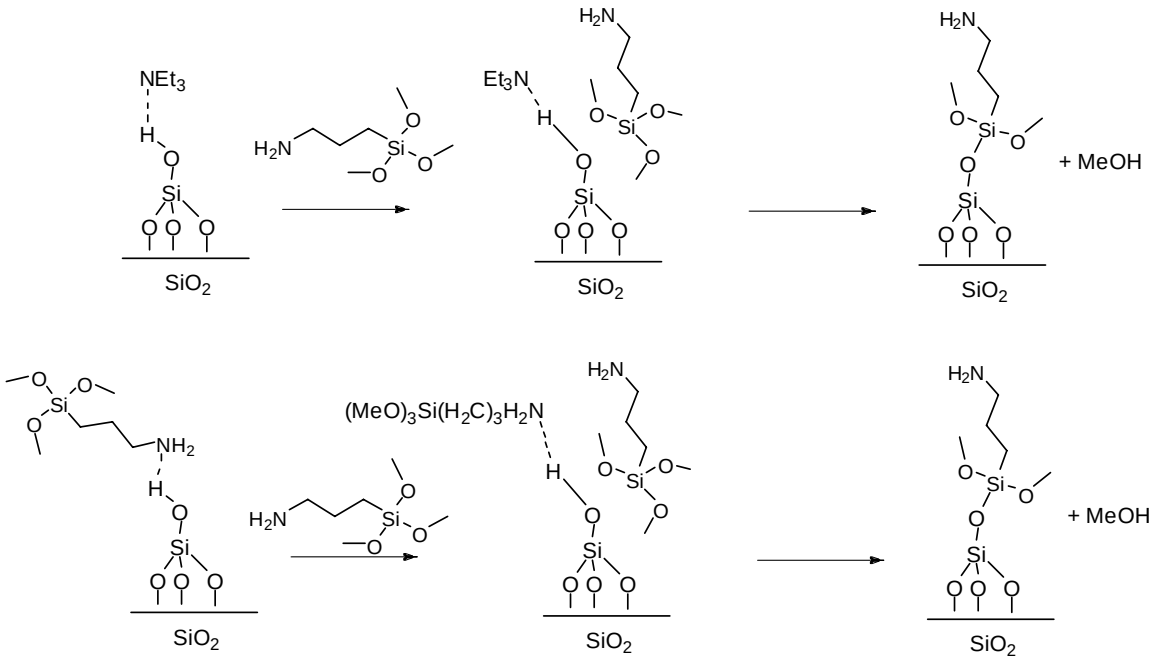

Figure 1.9. Activation of silanols with triethylamine or APTMS.

alkoxysilane. Since water was not present, the silanes were not able to oligomerize in solution or on the surface of silica, and a relatively high loading of surface amines (0.2 – 2.7 mmol NH_2/g) could be achieved.[28]

The disadvantage of forming high amine loaded materials with 3-aminopropyltrimethoxysilane is the formation of multiple types of amine sites on the silica surface. For instance, when APTMS and silica are mixed in toluene (the traditional method of preparing an aminosilica material), the amine groups can hydrogen bond in solution and produce amine sites on the surface that hydrogen bond with one another or with the surface silanols (Figure 1.10). Therefore, the resulting aminosilica has different types of amine environments on the surface ranging from closely packed, interacting amines to isolated amines. The disadvantage with these materials is the differences in accessibility and reactivity of the amine groups. McKittrick et al. determined that

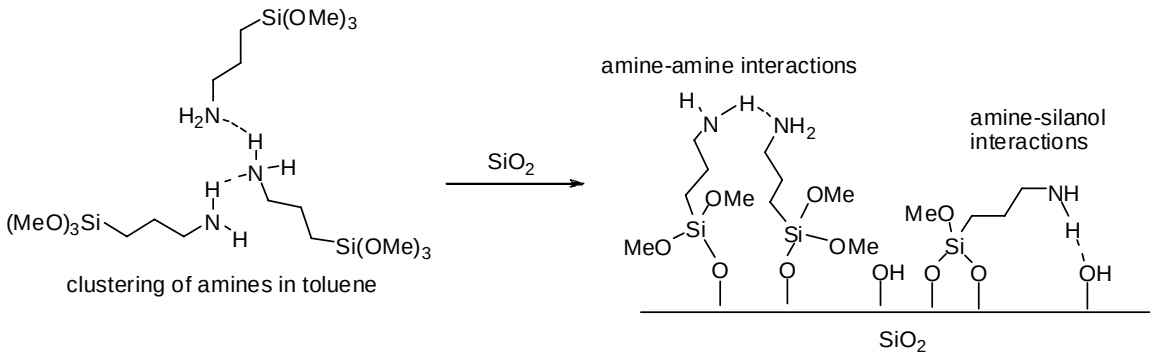

Figure 1.10. Various types of amine sites on traditional aminosilicas.

aminosilicas synthesized via a traditional method produced materials with some inaccessible amine sites.[11]

In order to create grafted aminosilicas with uniform, accessible amine functionalities, protection/deprotection methods have been developed which prevent amine-amine interactions and cap excess surface silanols to prevent amine-silanol interactions. For instance, Wulff et al. created spaced amines on silica by immobilizing a template capable of being hydrolyzed (Figure 1.11).[29, 30] The template was formed via the reaction between two equivalents of 4-(methoxydimethylsilyl)aniline and one equivalent of 4,4'-methylenedibenzaldehyde. After reaction of the protected amine template with the surface, the protecting group was removed with an acid solution to

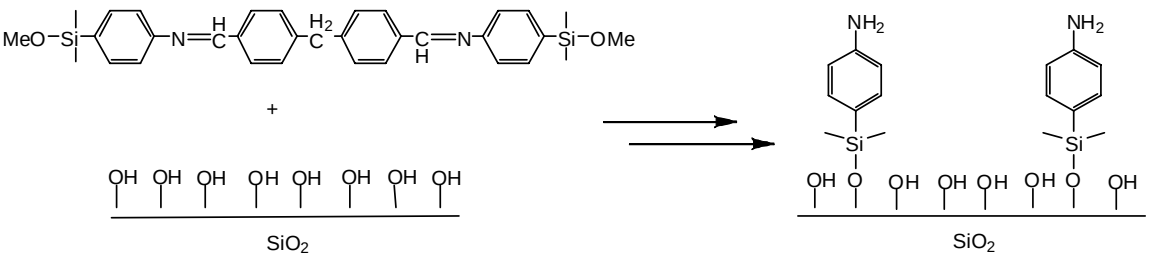

Figure 1.11. Spaced amines via Wulff's method.

form the resulting spaced, primary amine (Figure 1.11). However, very dilute concentrations of the template were required to ensure separation of most amine groups, because if high concentrations were used, two templates could react with the surface side by side, producing a distribution in amine separation (Figure 1.12). This method thus required amine loadings of less than 0.2 mmol NH_2/g to form spaced amines.

Katz and coworkers have synthesized aminosilicas using a molecular imprinting

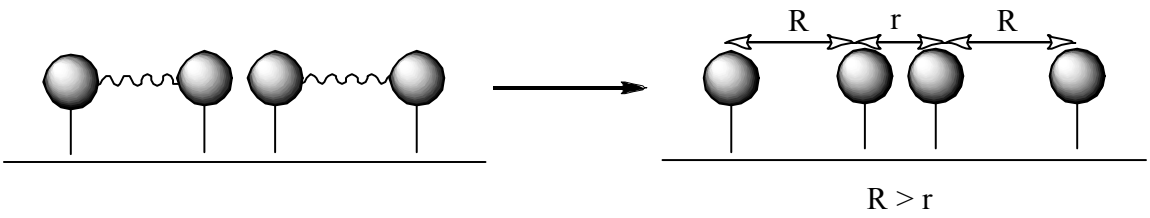

Figure 1.12. Various amine spacing with Wulff's method.

approach to produce isolated amines.[31-33] Their approach utilized a co-condensation method for forming protected amines within the framework of bulk, amorphous, microporous silica. After synthesis of the material, the protecting group was cleaved by thermolysis (heating to 250 ^oC under N_2) or addition of trimethylsilyiodide (Figure 1.13). Two disadvantages exist for these materials: (1) loadings of less than 0.25 mmol NH_2/g and (2) difficulties for large molecules to access amine sites in microporous materials.

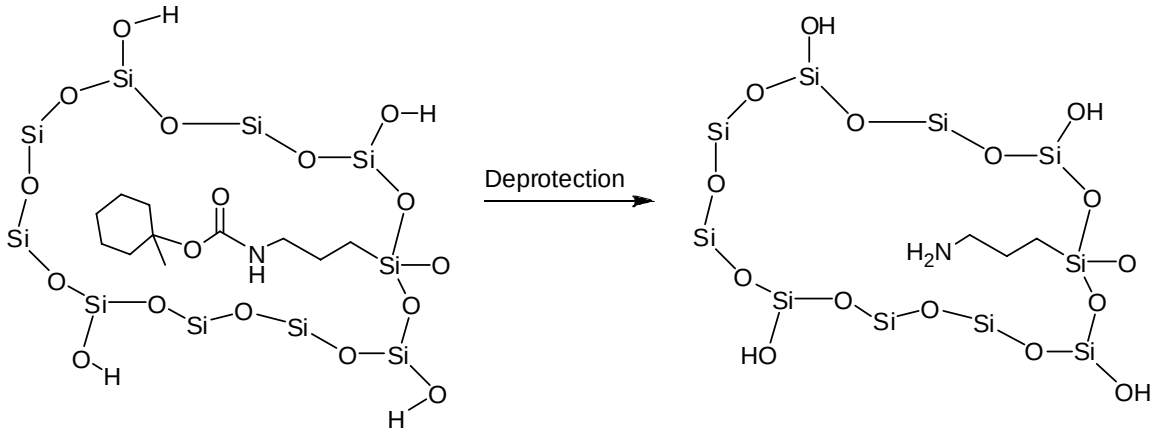

Figure 1.13. Molecular imprinting.

McKittrick and Jones developed a method to protect the primary amine of APTMS by reacting it with 3,3,3-triphenylpropanal to form a tritylimine with an alkoxysilane tail.[11, 34] The tritylimineakoxysilane was tethered to silica in a simple one step reaction. Next, the unreacted silanols on the surface were capped with 1,1,1-3,3,3-hexamethyldisilazane to prevent amine-silanol interactions. Subsequently, the protecting group was cleaved to produce trityl-spaced amine groups on the surface. This method reduced or eliminated amine-silanol interactions and amine-amine interactions (Figure 1.14). Although the amine loading was roughly twice that of previously reported spacing methods (~0.4 mmol NH_2/g material), this method was deficient in amine loading compared to traditional methods (~1.2 mmol NH_2/g material).

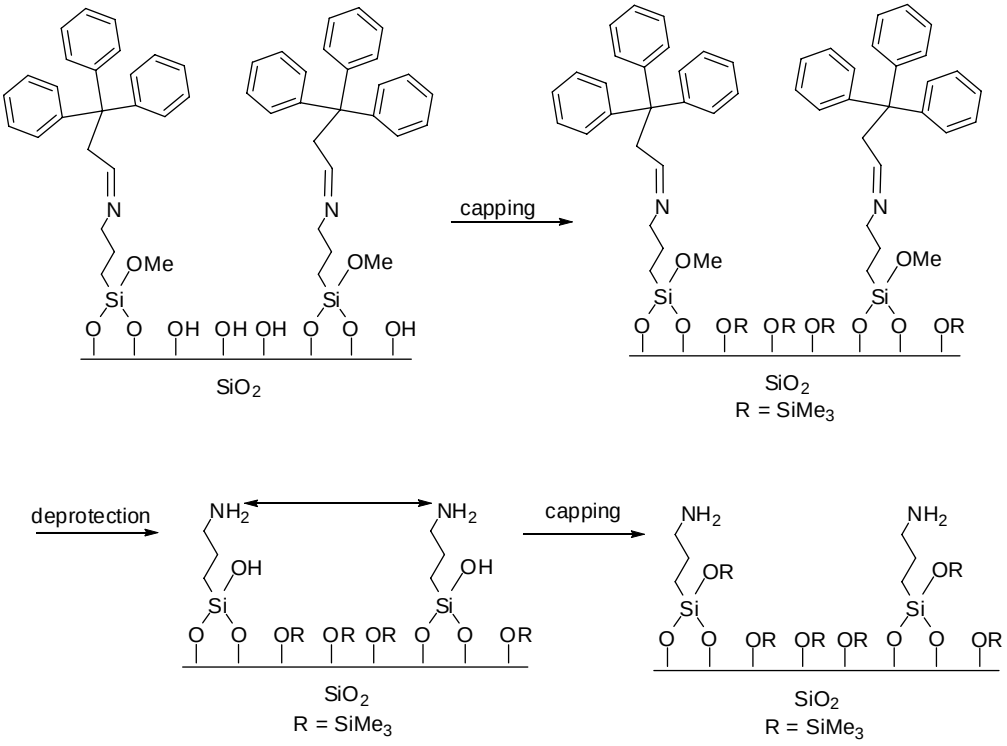

Figure 1.14. Trityl-spaced aminosilicas.

In summary, many techniques have been investigated for the synthesis of aminosilicas. While all the methods address different properties of the materials and optimize certain parameters, none have yet been able to produce a material with a high amine loading and spaced amine sites.

1.3 Tethering Olefin Polymerization Catalysts and Cocatalysts to Inorganic Oxides

As mentioned above, one of the uses of aminosilicas is for support materials off of which organometallic catalysts may be synthesized. Organometallic olefin polymerization precatalysts are one such group of catalysts often tethered to aminosilicas

or other support materials. Just as their homogeneous counterparts, these precatalysts are activated to their catalytic form with a cocatalyst which is added to the reaction mixture. The art of tethering olefin polymerization precatalysts to solid supports (usually oxides) is possibly one of the most robust approachs to constructing heterogeneous surface bound precatalysts. Current tethering methodologies account for the nature of the support material (usually silica or alumina), the length of the spacer from the surface anchor, the separation between tethered functional groups, the type of reactive silane used to tether to the surface (usually alkoxysilanes or chlorosilanes), and the type of ligand covalently bound to the surface. Tethering has attracted a large amount of attention mainly due to the ideal situation of completely preventing catalyst leaching in commonly used slurry phase processes. Furthermore, the presence of fixed tethers can, in principle, be used as building blocks to construct very well-defined, single-site supported complexes that are more amenable to structural characterization, leading to an understanding of molecular level structure-property relationships.

There are two main routes typically used to tether olefin polymerization precatalysts: (1) building the precatalyst off of the surface using a stepwise grafting approach, and (2) tethering a preformed precatalyst directly to the inorganic surface.[18, 35-37] One of the main disadvantages with the first method involves the number of tedious and, in many cases, non-stoichiometric steps required to create the active catalyst on the surface. Another drawback involves the possible formation of deactivated precatalysts through their interactions with the support material (such as reaction of the precatalyst with surface silanols on silica). The second method requires the synthesis of a highly pure homogeneous precatalyst with the appropriate organic and inorganic groups capable

of reacting with the support's surface. This can be difficult because, many times, the formation of a pure tetherable precatalyst is not insignificant, and the synthetic and purification procedures are rather extensive and economically unfavorable. In addition, this tethering method can produce multiple types of active and inactive metal sites on the surface after immobilization due to interactions between the metal and the surface during the grafting step (especially when using early transition metals). Characterization of the synthesized materials can also be very difficult. This is because metal-center characterization techniques either provide limited data (e.g. UV-Vis) or require detailed *in situ* experimental investigations (e.g. EXAFS).

1.3.1 Introduction to Olefin Polymerizations

Before venturing into the development of well-defined tethered olefin polymerization catalysts, it is important to understand the historical progress of the various catalysts used to make polyolefins. Advances in the polyolefin industry have been prolific since the discovery of Ziegler-Natta catalysts in 1953. Polyolefins are an exceptionally important class of materials, as over 15 million tons of poly(ethylene) and poly(propylene) have been produced annually since 2001.[38] The most common of the Ziegler catalysts is $TiCl_3/Et_2AlCl$. It is active at 25°C and 1 atm whereas traditional non-catalytic polyolefin production requires harsh conditions (200°C, 1000 atm). Since the Ziegler-Natta discoveries, research in this area has involved developing new catalysts designed to produce polyolefins with ordered stereochemistry (tacticity), with low polydispersities, and with high molecular weights. However, the formulation of such catalytic systems is arduous.

Ziegler discovered that ethylene could be polymerized to high molecular weights using titanium tetrachloride, $TiCl_4$, with aluminum alkyl compounds as cocatalysts.[39] Breslow and Newburg discovered the first homogeneous metallocene, bis-(cyclopentadienyl)titanium dichloride, which blocked two potential active sites forming a single-site precatalyst. The metallocene polymerized ethylene in the presence of diethylaluminum chloride, although the activity was inferior to the Ziegler-Natta catalysts.[40] Without diethylaluminum chloride, no polymerization was observed with the metallocene.[41] This very important discovery led others to investigate metallocene activation. Using detailed kinetic analyses, isotopic labeling, and advanced spectroscopic techniques, Breslow and Long proposed that metallocene activation occurs in multiple steps (Figure 1.15).[42] First, the diethylaluminum chloride (cocatalyst) performs a ligand exchange with the bis-(cyclopentadienyl) titanium dichloride (precatalyst) compound to alkylate the titanium. Once alkylated, the bulk alkyl aluminum interaction with the chloride ligand polarizes the Ti-Cl bond and allows for insertion of the monomer. Later electrochemical experiments showed that the active metal complex is actually a cation.[36] These metal alkyl aluminum systems were important because they elucidated the nature of the active metal intermediate, but they were not optimal due to their lower activity.

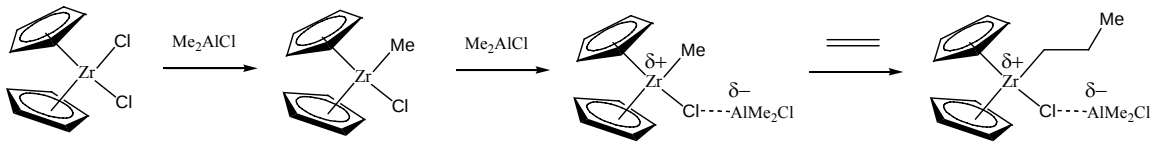

Figure 1.15. Initial proposed mechanism for single-site precatalyst activation.

Sinn and Kaminsky found that bis-(cyclopentadienyl) dimethyl zirconium and trimethylaluminum in the presence of water produces a very active, halide-free catalyst.[43] This lead to the discovery of methylaluminoxane (MAO). Methylaluminoxane is formed by the controlled hydrolysis of trimethylaluminum to form oligomeric $[\text{-Al(Me)-O-}]_n$ with molecular weights of 20 kg/mol[44]. Because MAO produces highly active metallocenes, it has received much attention as a cocatalyst. However, it is a difficult compound to characterize precisely, and many proposed structures exist.[36, 44]

Perfluoroarylboranes, $B(Ar)_F$, are a newer group of well-defined cocatalysts used to activate precatalysts. Massey and Park reported the synthesis of tris(pentafluorophenyl)borane in 1964.[45] In the early 1990's, Marks and coworkers discovered that the strongly Lewis acidic nature of tris(pentafluorophenyl)borane could activate Group 4 metallocenes by abstracting an alkyl group from the metal.[46, 47] As shown in Figure 1.16, the zirconocene cation initially contains 16 e^- (Figure 1.16 A). The Lewis acidic borane removes one of the methyl groups, resulting in an activated 14 e^- zirconocene (Figure 1.16 B). Once the methyl group is removed, it is possible to form an α-agostic interaction between the metal and a hydrogen atom on the remaining methyl group can form that stabilizes the electron deficient metal. An ethylene molecule can now be added to the metal; it will donate two π electrons, returning the metal to a 16 e^- configuration (Figure 1.16 C). A strained four coordinate species is then formed (Figure 1.16 D). The strain is sufficient to break the Zr – Me bond and return the catalyst to the active 14 e^- configuration (Figure 1.16 E and F). At this point, another ethylene monomer can insert and continue the production of a longer polymer.

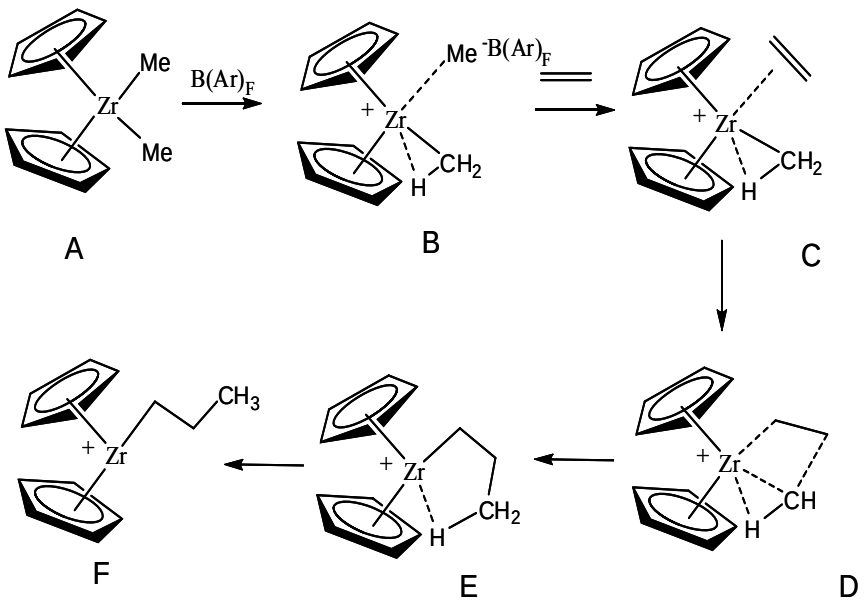

Figure 1.16. Activation and polymerization mechanism.

The dominant method for chain-termination of the growing polymer chain in this system is β-hydride elimination (Figure 1.17).[48] β-Hydride elimination occurs through the interaction between the metal center and a hydrogen atom on the β carbon. When this happens, the metal bonds to the hydrogen and an olefin is eliminated as the leaving group. In some cases, the resulting olefin can subsequently be reintroduced as a long chain monomer for additional chain growth.

Borates are another large class of cocatalysts related to boranes. Borates are negatively charged, four-coordinate boron complexes usually stabilized by a large trityl cation, typically $[Ph_3C]^+[B(C_6F_5)_4]^-$ in polymerization studies. Borate cocatalysts have yielded highly active olefin polymerization metallocene catalysts,[49] but their limited hydrocarbon solubility makes it difficult to activate the metal in solution, and their poor thermal stability leads to a limited range of usability.[50]

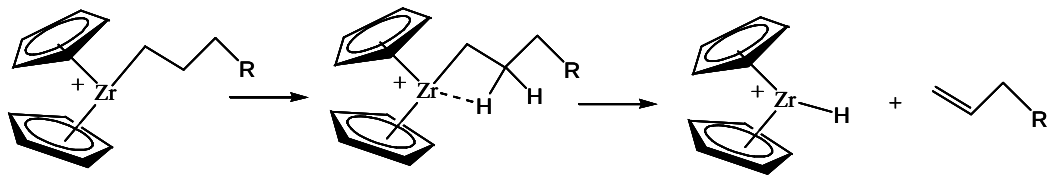

Figure 1.17. Chain termination via β-hydride elimination.

1.3.2 Tethering Olefin Polymerization Catalysts

1.3.2.1 Surface Tethered Metallocene Precatalysts

Industrially, there are many drawbacks to using homogeneous catalysts for polymerizations. For instance, polymer morphology, in many cases, cannot be easily controlled. Also, the use of homogeneous catalysts in solution leads to reactor fouling by deposition of high molecular weight polyolefins on the walls of the reactor. To alleviate some of these problems, the precatalyst can be immobilized on a solid support to produce a heterogeneous system. When the catalyst is tethered to the support, the polymerization occurs on the surface and in the pores of the support material. The precatalyst on the surface allows for better control of the polymerization by restricting the mobility of the catalyst, giving better polymer morphology than homogeneous systems. Tethering the precatalyst also prevents the deactivation that free moving catalysts exhibit in solution from bimolecular interactions.

Soga and coworkers authored the first literature reports of tethered olefin polymerization precatalysts.[51-60] In these reports, silica-tethered indenyl ligands were built off of the surface by first reacting the silica with $SiCl_4$, followed by the addition of a

lithium salt of indene.[58] This method was used to synthesize an indenyl ligand bound to the surface that could be deprotonated by the addition of n-butyllithum and subsequently metallated with a zirconium source (Figure 1.18). Afterwards, the resulting tethered precatalyst was activated by addition of either MAO or triisobutylaluminum (TIBA) in order to produce isotactic polypropylene. However, both isotactic and atactic polypropylene were formed. In order to determine the cause of the formation of both isotactic and atactic polypropylene, the authors suggested that detailed characterization of the tethered precatalyst was needed to determine the structure of the precatalysts actually tethered to the silica support. The same method was used to tether neodymocene precatalysts on silica for the polymerization of ethylene.[59] The neodymocene precatalysts were activated with different alkylating agents (ranging from triisobutylaluminum, trimethylaluminum, BuMgEt, nBuLi, MeLi, to MAO), producing catalytic activities up to

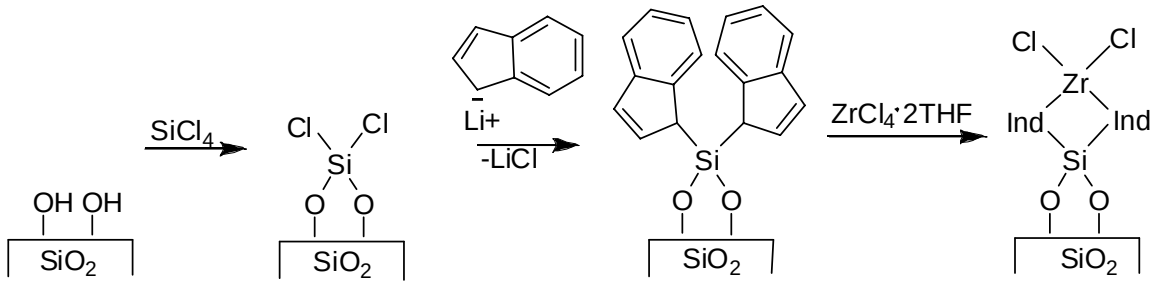

Figure 1.18. Silica grafted indenyl ligands.

90 kgPE/(mol Nd ·hr). However, the polydispersities (PDIs) of the polyethylene were broad (and most likely bimodal), ranging between 2 – 17 (M_w/M_n). So, although the researchers reported the first successful tethered olefin polymerization catalysts many

years ago, their performance did not achieve the targets of complete control of tacticity and low PDI, nor were the solid catalysts thoroughly characterized.

Later, Soga and coworkers reported a method to graft olefin polymerization precatalysts on 3-aminopropylsilyl-modified silica surfaces.[60] First, 3-aminopropyltrimethoxysilane was reacted to the silica surface. Afterwards, Cp^*TiCl_3 was added to interact with the surface amine functionalities. The authors synthesized a heterogeneous precatalyst as a control by reacting the homogeneous precatalyst (Cp^*TiCl_3) directly to the silica surface. Leaching was tested with both supports/precatalysts. The leaching studies showed that a greater fraction of the complex was lost on the Cp^*TiCl_3-SiO_2 support compared to the Cp^*TiCl_3/NH_2-SiO_2 support (5.4 and 1.7 mol % respectively), due to MAO. In both cases, however, only trace amounts of poly(ethylene) were recovered using the leached components. The authors reported that MAO can more easily break surface Ti-O bonds than Ti-N bonds, based on the amount of titanium leached. These studies indicated that the use of an aminosilica as a support material could facilitate the optimization of the tethered catalyst's performance in terms of stability against leaching and incorporation of a co-monomer, although control of the tacticity was still not achieved.

Pakkanen and coworkers developed a method that used the reaction of $Cp(CH_2)_3Si(OEt)_3$ in the gas phase with the silica surface to graft the cyclopentadienyl ligand.[61, 62] The success of the surface reaction was determined by FT-IR and ^{13}C CPMAS NMR. The surface bound cyclopentadiene species were reacted with nBuLi to form the deprotonated cyclopentadienyl ligand (LiCp, Figure 1.19). Subsequently, reaction of $CpZrCl_3$ with the surface LiCp groups formed a tethered precatalyst. This

precatalyst produced polyethylene with relatively narrow PDIs when activated by methylaluminoxane (MAO, Al/Zr 1500 or 2000).[43] As a control material, $CpZrCl_3$ was reacted directly to the silica surface and activated with MAO. It was concluded that the surface tethered Cp moieties provided a better support material to form the heterogeneous precatalyst because the control material had much less catalytic activity. However, multiple types of sites were expected to exist on the silica surface due addition of nBuLi. The nBuLi was suggested to react with remaining Si-OEt groups to yield LiOEt and Si-

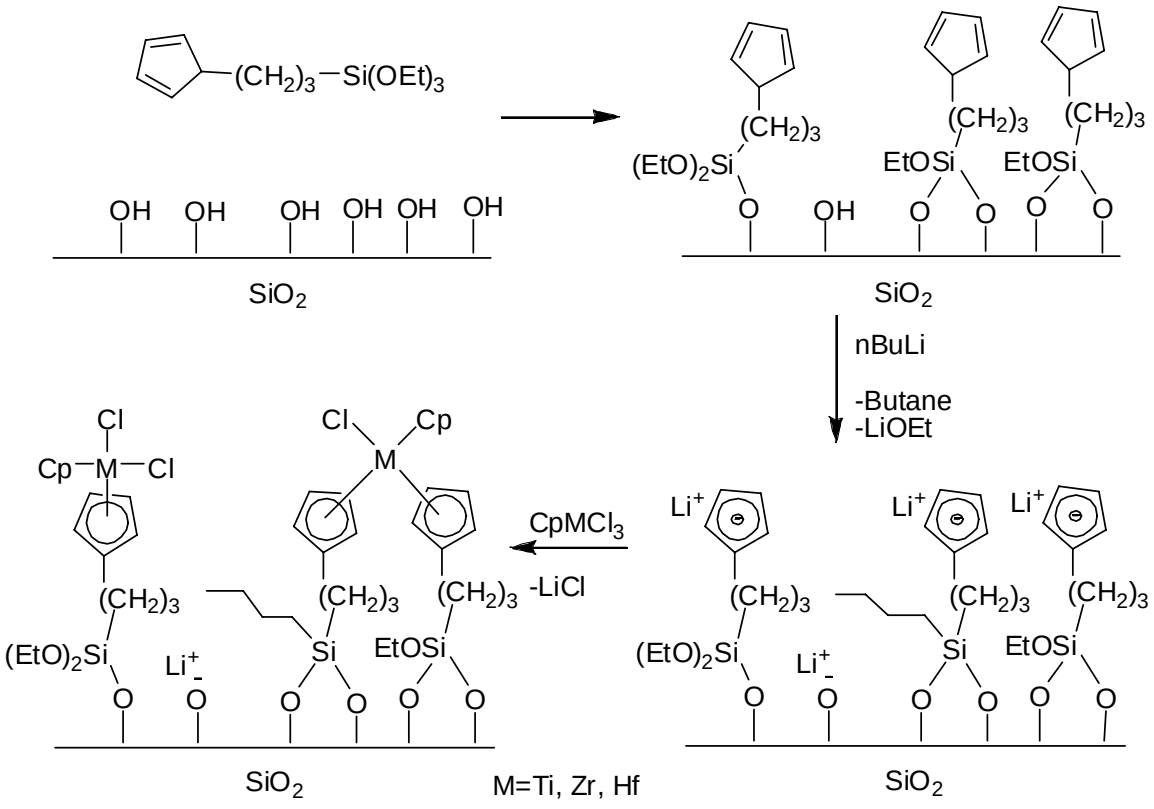

Figure 1.19. Multi-step grafting of metallocenes on silica.

Bu surface groups. Therefore, the lithium salt by-product (LiOEt) could react with the precatalyst ($CpZrCl_3$) to form $CpZr(OEt)Cl_2$, which can also react with the silica surface. The authors did not comment on leaching of the metal precatalyst in this study; however, they discovered that the addition of the Cp functionality to the surface before the addition of the precatalyst improved catalyst performance.

Using a similar strategy, Pakkanen and coworkers were able to eliminate the use of the very harsh organolithium agent (nBuLi) by using a metal amide complex [$Zr(NMe_2)_4$ or $Ti(NMe_2)_4$] to bind to the cyclopentadienyl-modified silica (Figure 1.20).[9, 63] The use of the metal amide complex also eliminated one step in the synthesis. The productivities of the titanium-based heterogeneous precatalysts, when activated by MAO, were comparable to a homogeneous control, $(CH_3)_3SiCpTi[N(CH_3)_2]_3$, for production of linear high density poly(ethylene). However, the activity of the catalyst was greatly dependent on the Al/Ti ratio, as Al/Ti ratios of 4000 produced an order of magnitude increase in

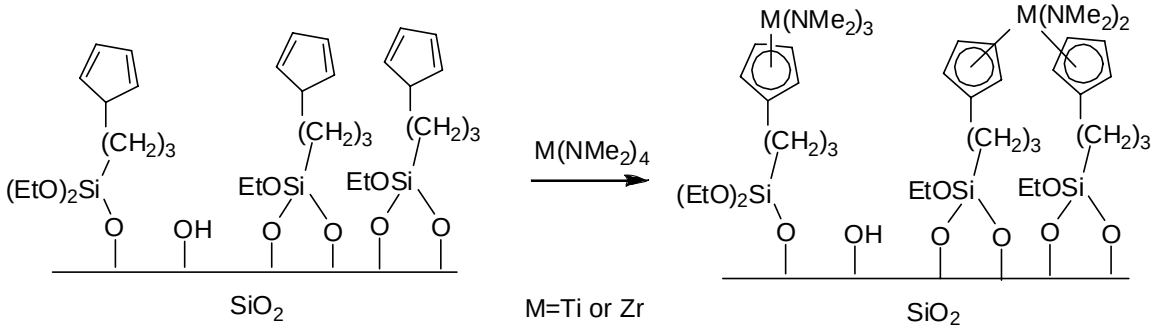

Figure 1.20. Metallation of surface Cp groups.

catalytic activity compared to ratios of 1000. Leaching of the metal precatalyst from the surface with the addition of MAO was not addressed by the authors. This work simplified the immobilized catalyst synthesis and eliminated the problems associated with the use of n-butyllithium.

Bortolussi et al. patented a process to tether Group 4 metal precatalysts by first reacting nBuLi with silica and subsequently adding 6,6-dimethylfulvene (Figure 1.21).[64] The result produced a supported cyclopentadienyl ring that could be used to tether the metal complex ($ZrCl_4 \cdot 2THF$). Afterwards, an additional reaction with cyclopentadienyllithium produces the tethered metallocene precatalyst, through a ligand exchange with the chloro group. When triisobutylaluminum and N,N-dimethylaluminum tetra(pentafluorophenyl)borate were added as the homogeneous cocatalysts/activators, the supported zirconocene produced poly(ethylene) with a productivity of 3,580 g PE/g catalyst. Alt and coworkers reported the synthesis of tethered mono- and bis-fluorenyl zirconocene precatalysts on silica (Figure 1.22).[65] They synthesized the fluorenyl

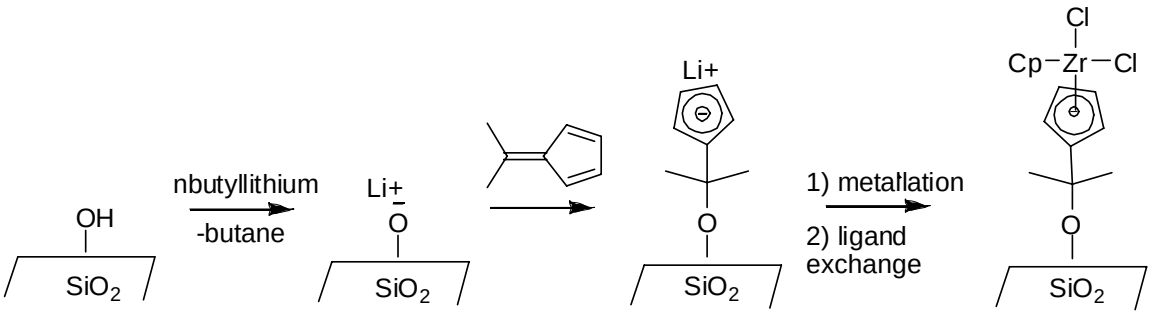

Figure 1.21. Grafting Cp ligands on silica with nBuLi.

tethered precatalysts by reacting the fluorenyl-chlorosilane to 600 ^{o}C pretreated silica. The nBuLi deprotonated the ligand for addition of either Cp*$ZrCl_3$ or $ZrCl_4$. The silica-tethered zirconium catalysts produced poly(ethylene) with higher molecular weights and less reactor fouling than to the homogeneous catalysts, when activated with MAO. However, the homogeneous catalysts were more active than the silica tethered catalysts. These published reports show additional methods that could be used to tether active olefin polymerization catalysts could be tethered to the surface.

Herrmann and coworkers tethered $CpZr(NMe_2)_3$ precatalysts on $Si(Ind)(CH_3)_2Cl$ and 1,1,1,3,3,3-hexamethyldisilazane (HMDS) modified silica surfaces to probe the

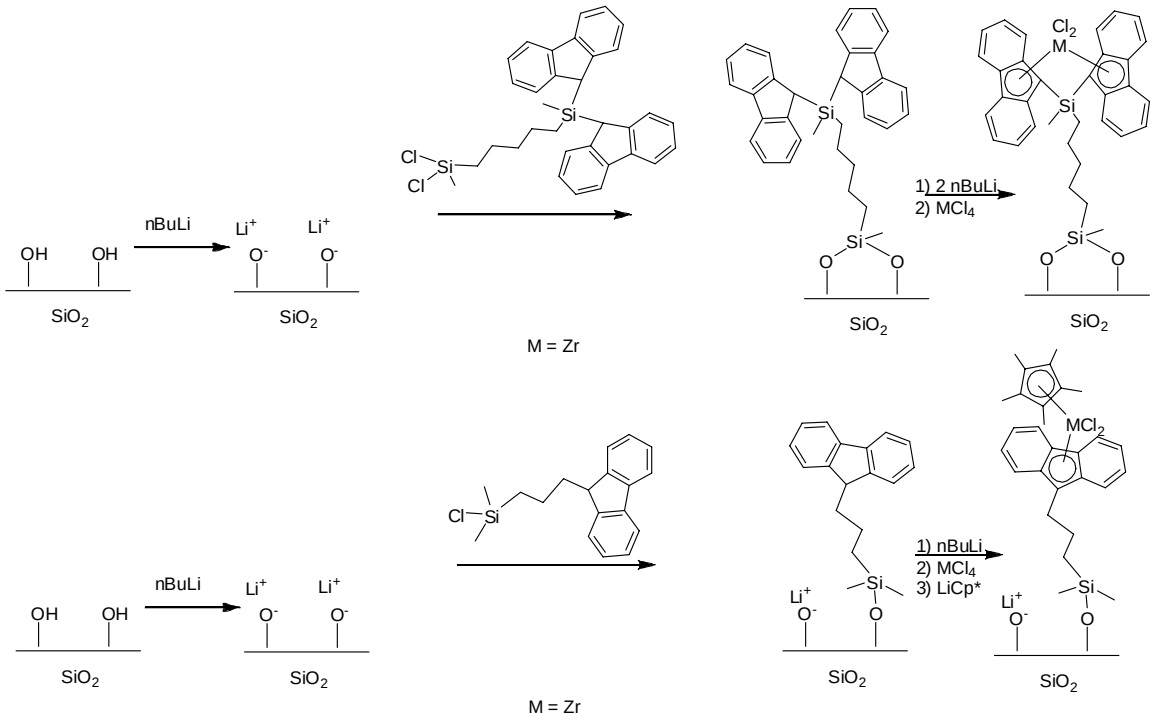

Figure 1.22. Silica grafted fluorenyl ligands.

function of surface polarity on catalytic activity.[66] HMDS was added after the indenyl-silane in order to reduce side reactions with the transition metal and the silica support by removing reactive surface silanols. The authors indicated that after the silanols were capped, a support material with mainly monografted complexes was produced, which produced lower polydispersities for the polymerization of ethylene when activated by MAO. When the precatalyst was synthesized on an uncapped silica support, more bigrafted precatalysts were formed (between the metal and the indenyl ligand and the metal and the surface silanols) which produced more stable, but less active catalysts when activated by MAO (Figure 1.23). Thus, it was determined that HMDS prevented side reactions of the precatalyst with the surface and to produced a more "single-site"

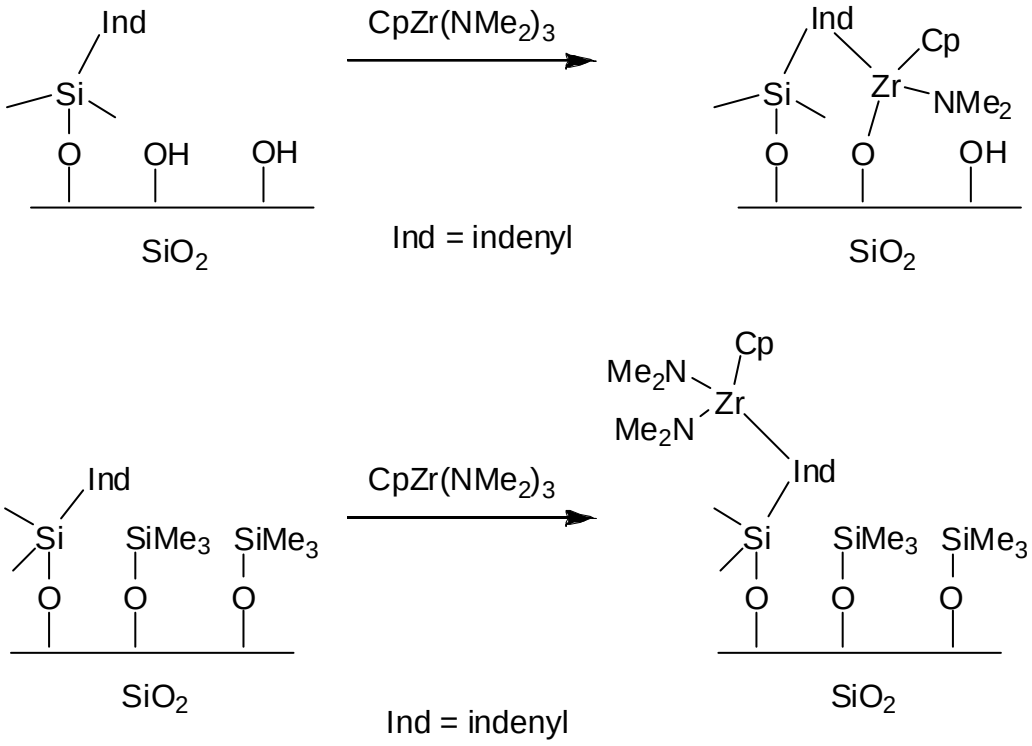

Figure 1.23. Comparison between silanol capped and uncapped surfaces.

polymerization precatalyst. However, the decreased stability of the precatalysts when using the capping method was a major disadvantage.

Suzuki and coworkers synthesized an isospecific ansa-zirconocene covalently tethered on silica to polymerize propylene.[67, 68] The authors tethered zirconocene precatalysts by three different methods: (1) formation of an ansa-zirconocene with a chlorosilane functionality that can react to the surface, (2) pretreatment of the silica with Me_3SiCl followed by addition of the ansa-zirconocene, and (3) tethering $Me_2(Cl)Si(CH=CH_2)$ to the surface and using these olefins to couple with the ansa-zirconocene via hydroboration. The order of decreasing activity for the various techniques described in this study was 3 > 2 > 1, when activated by MAO. This work provided a nice comparison of the various immobilization methods and how the various methods affected the catalyst's activity.

Collins and coworkers used hydrosilylation techniques to tether various zirconocenes to the silica (Figure 1.24).[69] Two different synthetic methods were studied: 1) grafting silica with Me_2SiHCl followed by addition of a zirconocene with a $(CH_2=CH)SiMe$ bridge, or 2) grafting silica with $Me_2(Cl)Si\text{-}R\text{-}(CH=CH_2)$ (where R is an alkyl chain) and coupling this supported olefin to a synthesized homogeneous ansa-metallocene complex containing a silicon hydride via hydrosilylation. As reported, various supported precatalysts with different ligands and lengths from the surface to the metal could be formed. The more active the catalysts were synthesized with longer lengths of the tether (when activated by MAO for polymerization of propylene). However, MAO leached the catalysts from the surface at elevated temperatures (up to 50% leached at 70 ^{o}C). The leaching was minimized to approximately 10% when lower

temperatures were studied. Therefore, an immobilized catalyst with a longer tether offers promise for an active, more stable catalyst.

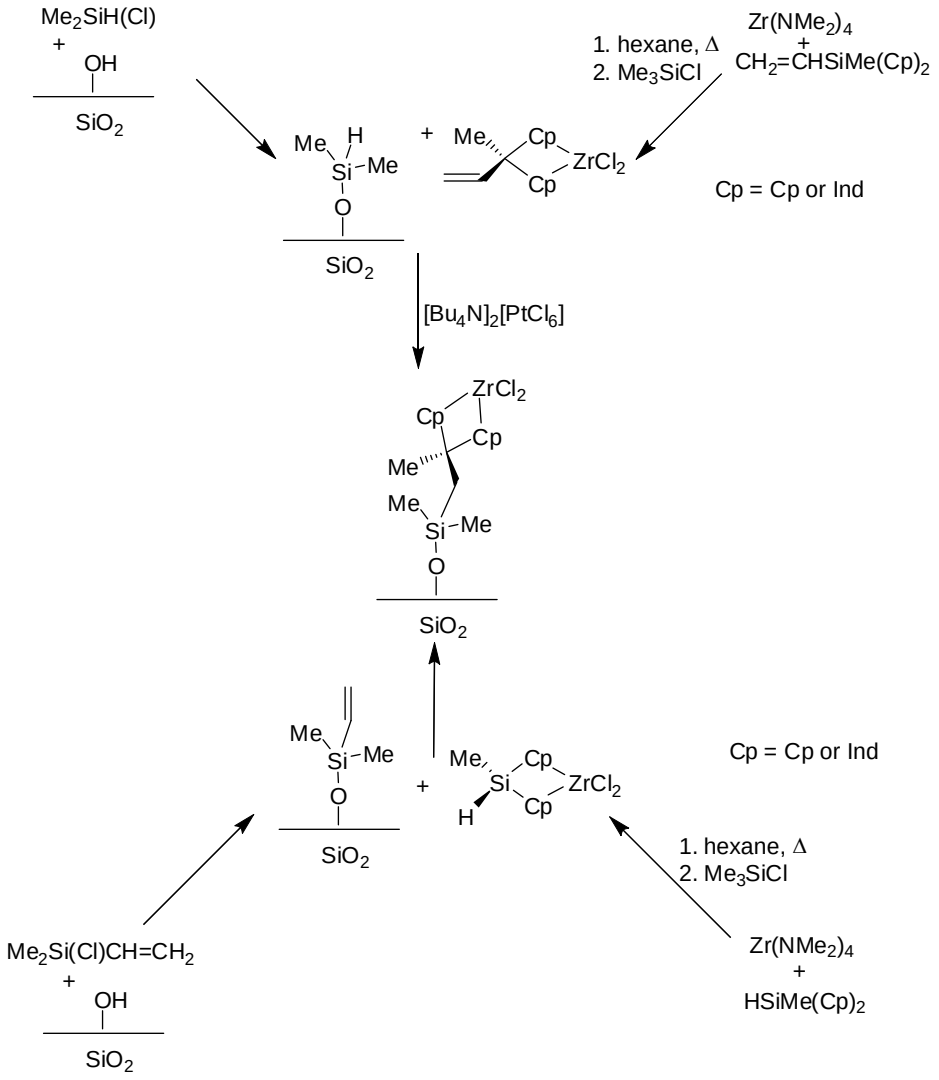

Figure 1.24. Grafting using hydrosilylation chemistry.

1.3.2.2 Surface Tethered Constrained Geometry Precatalysts

As previously mentioned, Soga and coworkers reported an aminopropylsilyl-modified silica as a support to immobilize Cp^*TiCl_3 precatalysts.[60] Based on their efforts, Pakkanen and coworkers attempted the synthesis of heterogeneous constrained geometry catalysts (CGCs) using aminopropylsilyl-modified silica to build the cyclopentadienyl ligand (Figure 1.25).[8, 70] CGCs are interesing because they offer advantages over typical metallocene precatalysts because the ligand structure provides enhanced access of the monomer to the metal center. Therefore, the production of higher molecular weight poly(ethylene) and branched poly(ethylene) can be obtained. Pakkanen and coworkers reported the deprotonation of the aminosilica surface with nBuLi.[70] Afterward, either $Me_2Si(C_5Me_4H)Cl$ or $MeHSi(C_5Me_4H)Cl$ was added to react with the deprotonated surface amines (LiCl formed as a side product). The materials were characterized by many techniques: ^1H, ^{13}C and ^{29}Si solid state NMR and FTIR spectroscopy. The results indicated that nBuLi deprotonated the amines and reacted with siloxane bridges and/or unreacted ethoxy groups from the aminosilane. The reaction of either $Me_2Si(C_5Me_4H)Cl$ or $Me(H)Si(C_5Me_4H)Cl$ directly with the amine groups on the silica surface was also studied to prevent the side reactions associated with nBuLi,.[8] However, the HCl formed interacted with the amine groups to form a protonated salt and cleavaged of the Cp-Si bond. Due to the cleavage of the Cp-Si bond, Zr-, Hf-, and Ti-CGCs were synthesized with the nBuLi treatment of the aminopropylsilyl-modified silica.[10, 71, 72] The Group 4 metal CGCs were compared for ethylene polymerization when attached to $Me_2Si(C_5Me_4H)Cl$ (or Cp') modified aminosilicas.[10] When the tethered CGC precatalysts were activated by MAO, the productivities of the catalysts were higher for

Zr-CGC and Hf-CGC than for the Ti-CGC. Actually, very little polyethylene was recovered with the heterogeneous Ti-CGC, when activated with MAO. The heterogeneous Zr-CGC was approximately twice as active as the Hf version. It was thought that the Ti-CGC was inferior multiple types of inactive titanium sites were created. However, this was solely speculation, as the various structures of the tethered CGCs were not verified in the report.[10] Although these various tethered precatalysts were able to form poly(ethylene), much of the surface was left with unreacted amine groups. This created at least two different functionalities on the surface capable of deactivating the metal center through strong coordination. Thus, to obtain heterogeneous single-site catalysts, the metal/amine ratio must be unity. Furthermore, since the authors did not verify the existence of CGCs on the surface, these materials should be referred to as

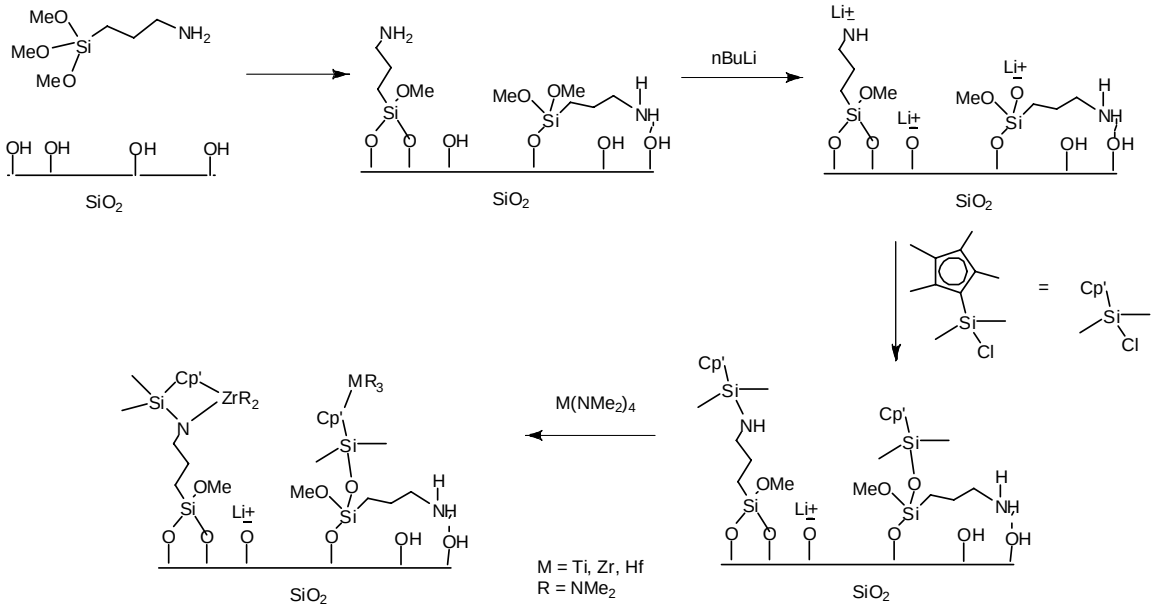

Figure 1.25. Traditional method to form silica tethered CGCs.

CGC-inspired[12, 14-17] rather than CGCs.

Eisen and coworkers reported a method to produce a homogeneous, tetherable titanium constrained-geometry catalyst (Figure 1.26).[73] The homogeneous precatalyst showed high activity for the polymerization of ethylene when activated by MAO. However, once grafted to either SiO_2 or Al_2O_3, a decrease in activity was observed. The advantages of this over other tethering methods previously described are as follows: (1) the amine to metal ratio is unity, (2) the lack of nBuLi prevents the creation of many types of metal sites, (3) the reaction between the surface and the alkoxy silane groups on the complex does not create by-products that destroy the material, and (4) the tethered CGC requires a one surface reaction step. Although this method had some advantages, the main disadvantage occurred because of the interaction between the Ti-CGC and the surface silanols which caused inactive sites on the surface.[73] In each of the previous reports, the creation of multiple types of metal/surface sites were possible in each material. Therefore, a "truly" heterogeneous single-sited catalyst was not created.

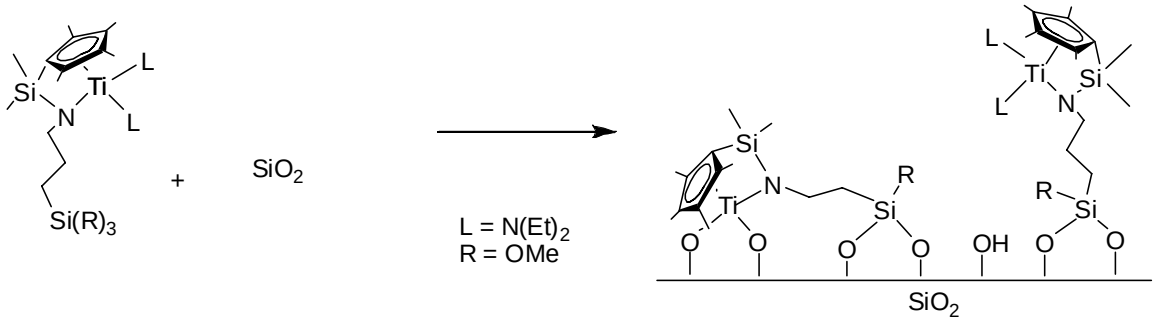

Figure 1.26. Ti-CGC silane coupling to silica surface.

McKittrick designed a method to create "site-isolation" between the amine sites of aminosilicas by using a protection/deprotection strategy to space the amine groups prior to addition of the metal precatalyst (Figure 1.14).[11, 34] Multiple surface treatments were used to achieve amine-separation on the surface and in the pores of the silica: (1) synthesis of the protected homogeneous aminopropyltrialkoxysilane with a trityl protecting group, (2) reaction of the protected aminopropyltrimethoxysilane to the silica support, (3) capping silanols with HMDS to prevent amine-silanol interactions and metal-silanol interactions, (4) deprotection of the protecting group site-isolation of the surface tethered amines, and (5) an additional capping step with HMDS. The protection/deprotection materials were characterized by FT-Raman spectroscopy, ^{13}C and ^{29}Si CP/MAS NMR, and thermogravimetric analysis (TGA). Together, these techniques indicated that the protecting groups were cleaved in virtually quantitative yield.[11]

McKittrick created the trityl-protection/deprotection strategy to form "site-isolated" single-site Group 4 CGC-inspired complexes on SBA-15 (Figure 1.27).[12, 14-17, 74] The authors reported the use of $Me_2(Cl)Si(C_5Me_4)$ along with 2,6-di-*tert*-butylpyridine (as a proton sponge) to trap the HCl evolved from the amine reaction. After addition of the metal source, $Ti(NEt_2)_4$, and exchange of the diethylamino-ligands for Cl-groups (with Me_2SiCl_2), a trityl-separated titanium-inspired CGC was formed on the surface to use as a heterogeneous olefin polymerization precatalyst. The tethered CGC was primarily activated with the combination of tris(pentafluorphenyl)borane[45-47, 75] and a trialkylaluminum complex (TMA or TIBA) because MAO caused significant leaching. As reported, virtually quantitative addition of the Ti complex to the amine sites was achieved (nearly 1 for the Ti/N ratio), due to the amine separation. As evidenced by the

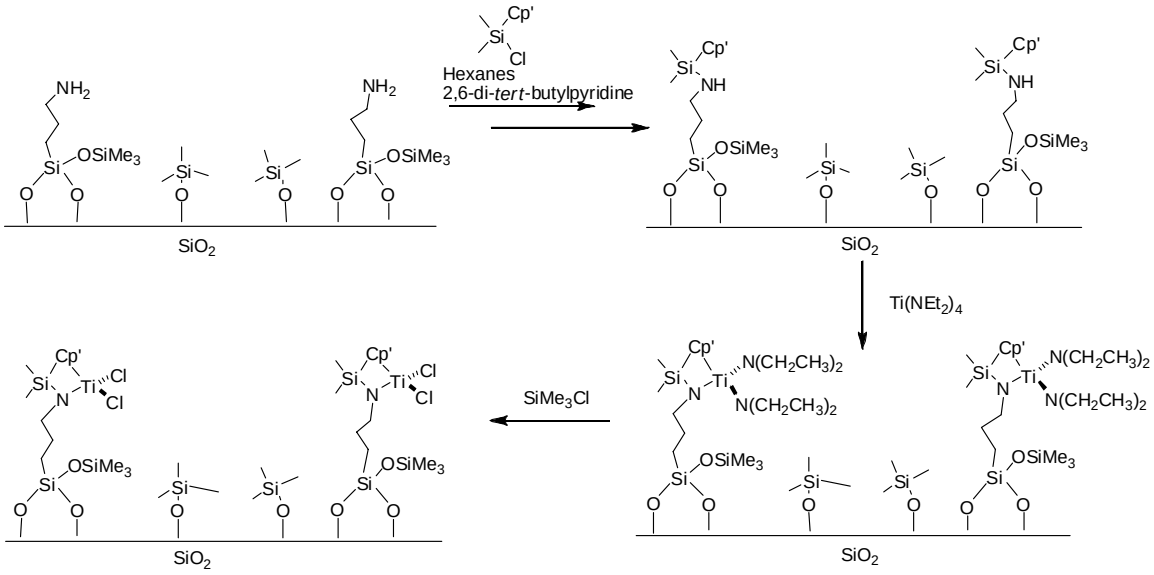

Figure 1.27. Multi-step formation of single-sited CGCs.

reported data, the productivity of the titanium-inspired constrained-geometry catalyst was nearly 5 times greater than using Eisen's method on mesoporous silica[73] and 10-15 times greater than using the traditional route of synthesizing unprotected aminosilicas[8, 10, 70-72] for polymerization of ethylene previously described.[12, 15] Furthermore, a traditional approach[8] to produce tethered CGC-inspired materials produced an inactive catalyst for the copolymerization of ethylene-norbornene.[16] However, if the "spacing" protocol of the aminosilica was used, the incorporation of both norbornene and ethylene was found in

the collected polymer. Therefore, the properties of the tethered organometallic catalysts through spatial separation was obtained with the trityl protection/deprotection method.

The aforementioned research performed in tethered Group 4 olefin polymerization precatalysts primarily focused on different methods to tether various metal complexes to a solid support. However, leaching experiments of the tethered precatalysts was generally absent in most reports. The goal of tethering the precatalyst to the support is to produce a catalyst with the advantages of both traditional heterogeneous and homogeneous catalysts, especially focusing on high activity (similar to homogeneous catalysts) and prevention of reactor fouling (similar to heterogeneous catalysts). Much research has emphasized these goals. However, leaching experiments and molecular-scale characterization of the metal is generally absent in most reports. If more was known about the "true" catalytic sites on the surface, it could make it possible to develop even more efficient or tailored catalysts.

1.3.3 Heterogeneous Olefin Polymerization Cocatalysts

Utilizing heterogeneous cocatalysts is a more versatile method to produce heterogeneous olefin polymerization catalysts, as various precatalysts can be used with a single tethered cocatalyst/support. However, the predominant location of reports in this area is the patent literature. Therefore, it is difficult, many times, to elucidate the exact tethered cocatalyst suggested in the vaguely constructed reports.

1.3.3.1 Non-Tethered Heterogeneous Olefin Polymerization Cocatalysts

In initial studies of cocatalyst grafting by Chien and He, MAO was reacted directly with the silica surface, followed by addition of the precatalyst (Figure 1.28).[76] Use of this cocatalyst led to heterogeneous catalysts with good activities.[37] However, one difficulty with this method arose when determination of the nature of the metal bound to the support was attempted. Since MAO itself is ill-defined and is used in huge excess (on the order of 100-500 equivalents are required to effectively activate the precatalyst), it is virtually impossible to study the supported active transition metal. Although these amounts are much lower than what is utilized with typical homogeneous systems, this is still a very large excess of required MAO. As one of the goals of this work was to develop catalytic systems which are more well-defined, a cocatalyst that could be immobilized directly onto a surface was sought.

In the quest to create well-defined cocatalysts on surfaces, immobilization of $B(Ar)_F$ on silica and alumina supports has garnered some attention. Collins and coworkers reacted tris(pentafluorophenyl)borane with surface silanols on silica (Figure

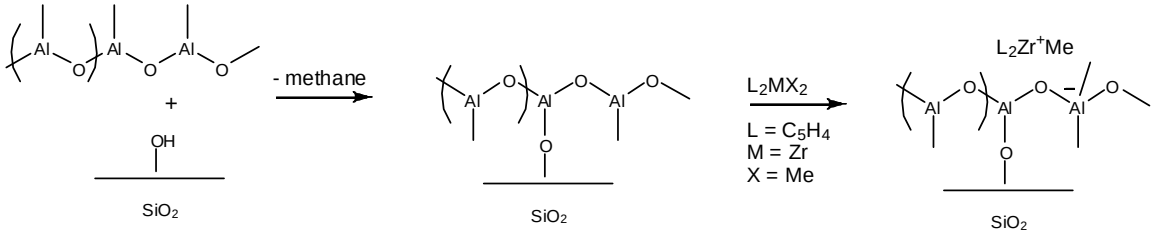

Figure 1.28. Reaction of MAO with the silica surface.

1.29).[77] When the silica immobilized borate was stirred with bis(cyclopentadienyl) dimethyl zirconium in toluene at -78°C, no metal leaching was observed. However, it was proposed that without a tertiary amine (i.e. N,N-dimethylaniline) present during the borane immobilization, the reaction with the surface is reversible and leads to significant cocatalyst leaching.

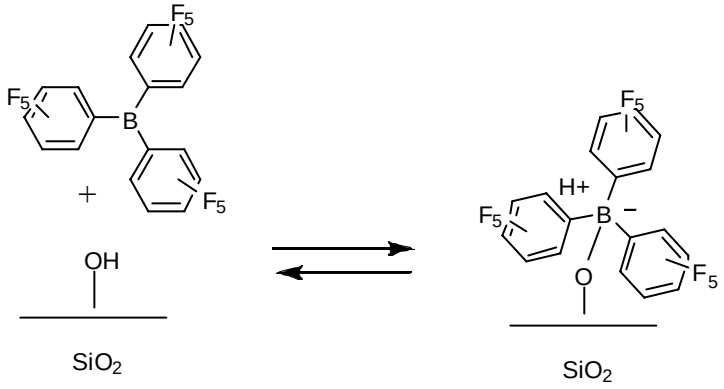

Figure 1.29. Formation of a silica-modified borate.

Other work in this field has involved the use of nBuLi to deprotonate the silica surface before adding the borane.[78] When used with a titanium constrained-geometry catalyst (CGC), the resulting supported borate produced high molecular weight polyethylene with a narrow polydispersity. This borate modified material raises two main concerns: 1) the butyllithium is strong enough to destroy the silica surface by opening siloxane bridges[8], and 2) ratios of 2:1 boron to metal were needed to optimize the activation of the CGC. This suggests that not all of the borates on the surface are accessible or reactive since the homogeneous system requires only 1:1 borane to metal.

Thus, a synthetic scheme designed to enhance accessibility of co-catalyst sites could improve catalytic performance.

Inorganic solids have also been utilized as MAO-free solid activator/supports.[79, 80] Marks and coworkers pioneered much of the work in sulfated metal oxides (SMOs) as support/activators for olefin polymerizations due to the SMOs very high Brønsted acidity.[81-84] Marks and coworkers showed that by a metal-carbon protonolysis, an active olefin polymerization catalyst can be prepared (Figure 1.30). The solid acids were useful as combined support/activators, fulfilling two requirements of a typical polymerization recipe (precatalyst/cocatalyst/support). The most effective examples of these cocatalysts/supports are derived from relatively expensive metal oxides such as zirconia or tin oxide.[84]

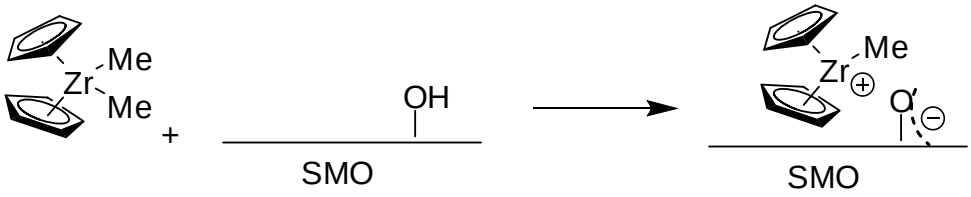

Figure 1.30. Sulfated-metal oxide as activator/support.

1.3.3.2 Tethered Olefin Polymerization Cocatalysts

Although many heterogeneous cocatalysts have been reported in the open literature, reports of tethered organic/inorganic hybrid materials proficient in activating Group 4 olefin polymerization precatalysts can only be found in the patent literature. For instance, work in this field was first reported by Turner, who allegedly tethered various borane cocatalysts to silica.[85] However, the patent only reported the synthesis of poly(styrene), poly(p-methylstyrene), and poly(vinylbenzene) supported boranes and will thus not be covered. Fritze et al. reported the synthesis of tethered boranes on silica by grafting with either chlorosilane or ethoxysilane.[86] However, the silica tethered boranes were not used as cocatalysts in this report. Hinkouma and coworkers reported the synthesis of silica tethered borates by using surface reactive chlorosilane linkers for the activation of metallocenes with triisobutylaluminum present.[87-89] Further work in this area was reported by Carnahan and coworkers.[90-92] In their syntheses, the tetherable borane cocatalysts were created with a hydroxyl substituent that was reacted to silica passivated with either a trialkylaluminum and/or a silane with Si-H groups (Figure 1.31). Afterwards, $[NHMe_2Ph]^+[(C_6F_5)_3B(C_6H_4\text{-}p\text{-}OH)]^-$ was added to the support.[90] The PDI of the polyethylene was determined as 2.47.

Other reports involved the synthesis of tethered borates by a method using protic substituents on the boron center capable of reacting with alkylaluminum passivated silica surfaces (Figure 1.32).[93, 94] For example, triethylammonium tris(pentafluorophenyl)(4-hydroxyphenyl)borate was reacted with an alkylaluminum (i.e. trimethylaluminum) passivated silica material to activate a titanocene for the olefin polymerizations. The tethered cocatalyst was capable to forming very active titanium catalysts for olefin homo- and copolymerizations. Another method reported by Jacobsen and coworkers involved the synthesis of $[(p\text{-}HOC_6H_4)B(C_6F_5)_3][NHMe(C_{18\text{-}22}H_{37\text{-}45})_2]$. This borate was reacted

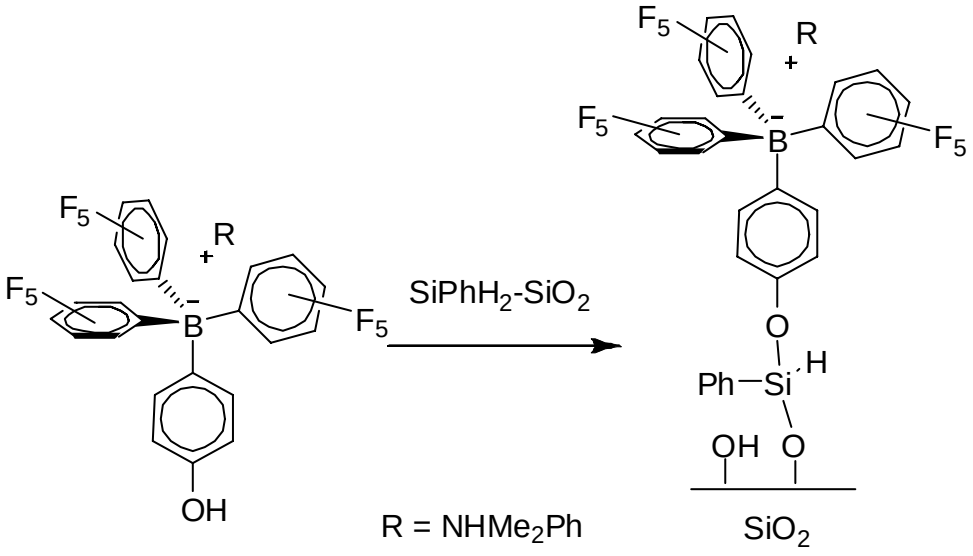

Figure 1.31. Silane-modified silica to form tethered borates.

with the titanium precatalyst before reaction with the triethylaluminum passivated silica.[95] The borate synthesized with the long chain ammonium salt was found to be a couple of orders of magnitude more soluble in hydrocarbon solvents (i.e. toluene) than the triethylammonium version. Other methods to create tethered boron complexes were reported involving the reaction between the cocatalyst and the surface via a hydroxyl functionality from the ammonium salt, $[HOC_6H_4NMe_2H]^+[B(C_6F_5)_4]^-$, with the alkylaluminum passivated silica.[96] Alternatively, the ammonium salt could be tethered directly to the silica support.[97]

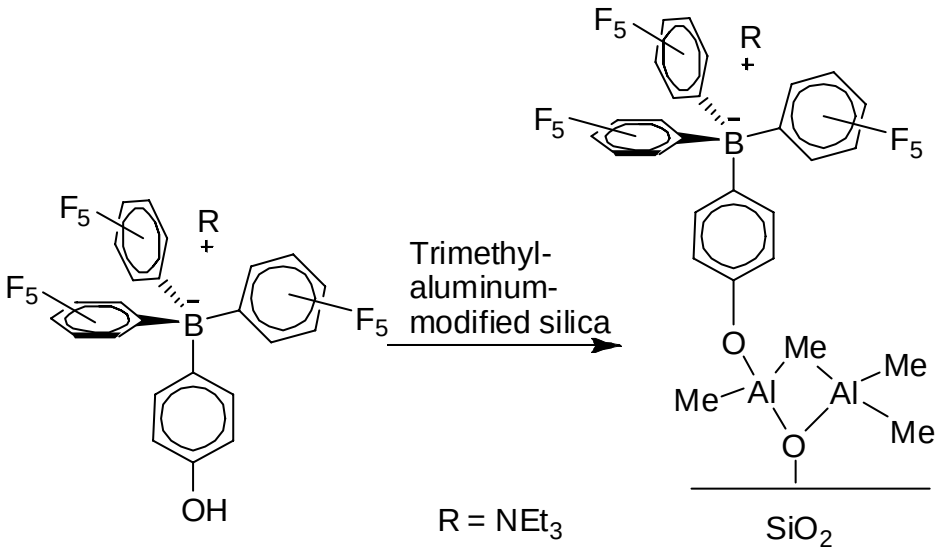

Figure 1.32. Trimethylaluminum-modified silica to form tethered borates.

In the majority of these inventions, a trialkylaluminum passivated silica material was required to form the tethered cocatalyst. It is very difficult to deduce from the patents the exact nature of the immobilized cocatalysts, as trialkylaluminums tend to form 3-, 4-, and 5-coordinate interactions with the surface, not yielding a specific structure of the tethered cocatalyst.[98] Thus, the structures of the tethered groups are unknown when using a trialkylaluminum passivated silica surface. Furthermore, most of the previous work has involved either physisorbing or tethering Lewis acids on the support. However, SMOs were found to activate metallocenes by using its strong Brønsted acidity. It would be advantageous to synthesize a tethered Brønsted acid cocatalyst on a cheaper support (silica) capable of activating olefin polymerization precatalysts without significant reactor fouling.

1.4 Organic/Inorganic Hybrids as Solid Sorbents for CO_2 Capture

In addition to support materials for organic or organometallic catalysts, aminosilicas are also used as absorbents for separation processes. One specific application is the use of amine groups as absorbents for gaseous carbon dioxide. Currently, the possibility for a global climate change due to an increase in greenhouse gases has generated international concern. The most concern is focused on the increased concentration of carbon dioxide in the atmosphere. Since the 1750s, the CO_2 concentration in the atmosphere has increased from 277 ppm to 377 ppm.[99] If this trend continues, the concentration of CO_2 in the atmosphere could possibly double by 2050.[100] The main cause of the increased concentration of CO_2 is our primary source of energy, fossil fuels. The greatest portion of emissions from these energy sources is typically

released to the environment from power plants (whose flue gases consist of CO_2, N_2, H_2O, and O_2). Consequently, to reduce the potential for a drastic, undesirable climate change, it is a global necessity to reduce CO_2 emissions. There are multiple ways to address this: (1) consume lower amounts of fossil fuels, (2) use renewable energy sources (such as wind, nuclear energy, biomass), (3) plant more trees and vegetation to consume the CO_2, and (4) capture CO_2 before it is released from the source. This section will focus mainly on the capture of CO_2 from flue gas streams.

In theory, it is simple to collect CO_2 from a flue gas stream which typically contains 10-15 % of CO_2. However, because of the low concentration of CO_2 in the flue gas stream, large volumes of emission gases must be treated. Also, impurities such as SO2 in the flue gas steam dictate the type of CO_2 capture methods that can be employed, due to the possible contamination with sulfur compounds. Due to these difficulties, multiple methods to capture the CO_2 have been reported: (1) absorption of CO_2 with aqueous amines,[101] (2) adsorption of CO_2 onto solid materials,[102, 103] (3) separation of CO_2 from the other flue gases with membranes.[104] Of the above capture methods, absorption of CO_2 with aqueous amines is the most common; this technology has been known since 1961. However, when aqueous amines are used as recyclable absorbents, the desorption of the CO_2 from the aqueous system requires a very high amount of energy due to the high heat capacity of water, ~ 4000 J/(kg*K). According to calculations by the National Energy Technology Laboratory, use of aqueous amines as the predominant CO_2 capture method would increase the cost of electricity from a newly built power plant by 25 – 84 %.[105] Due to the high cost of implementing aqueous amines technology, more research has looked at developing amine-modified silica materials as solid recyclable

sorbents for CO_2 capture since the heat capacity of silica is ~ 20 % the heat capacity of water.

Tsuda and Fujiwara reported the first aminosilica used as a solid CO_2 capture sorbent.[106] Specifically, they bound polyethyleneimine (PEI) to a silica precursor. Subsequently, the PEI-silica precursor was polymerized with water to form a gel (Figure 1.33). This material was used to reversibly bind CO_2.[106] The gel was able to bind CO_2 with adsorption capacities ranging between 0.3 – 0.7 mmol CO_2/(g gel). However, when the gel was dispersed in dimethylformamide (DMF) or water, the adsorption capacity was either 5.1 mmol CO_2/(g gel) or 5.0 mmol CO_2/(g gel), respectively. Although the capacities are better in DMF and water, the use of solvents negates much of the benefit of

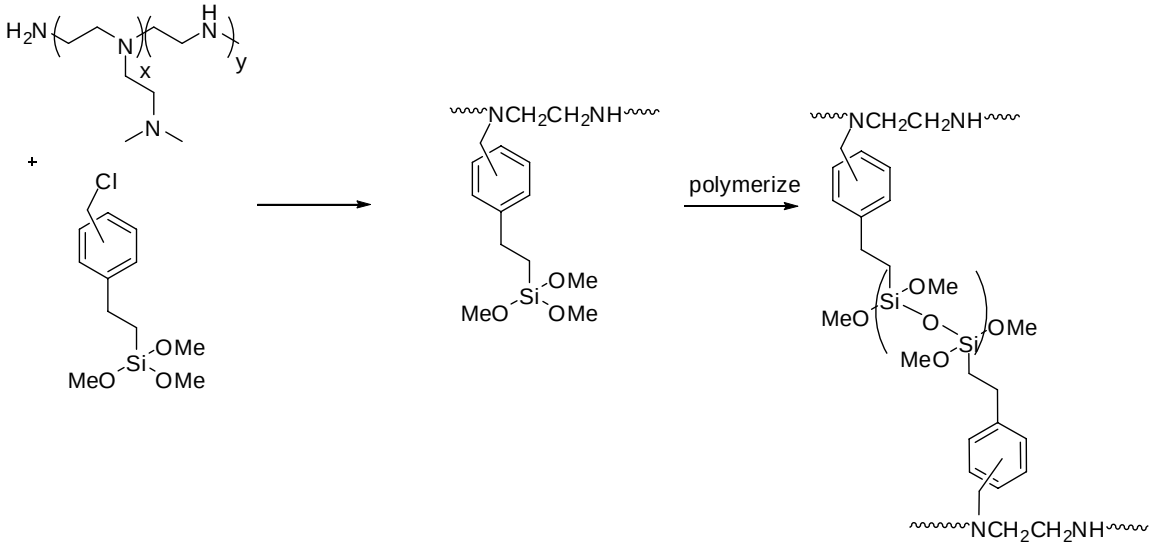

Figure 1.33. First reported amine-modified silica sorbent for CO_2 capture.

using solid sorbents.

Leal and coworkers reported the use of a traditionally functionalized aminopropylsilyl-functionalized silica material as a sorbent for reversible binding of CO_2.[102] As indicated in their report, the primary amines (~ 1.2 mmol NH_2/g) on the surface were able to reversibly bind CO_2 with a capacity of approximately 0.7 mmol CO_2/g, when CO_2 was desorbed at 100 ^oC. The most interesting results they found pertained to the interactions between the amines and the CO_2 in and not in the presence of water. For instance, in a strictly dry CO_2 environment, two SiO_2-R-NH_2 groups were needed to bind one CO_2 molecule, forming an ammonium carbamate species (SiO_2-R-NH-C(O)O^- $^+NH_3$-R-SiO_2). However, in the presence of water, only one surface amine was required to bind one CO_2 molecule to form an ammonium bicarbonate species (SiO_2-R-NH_3^+ HCO_3^-). Overall, the report determined that the presence of water increased the amine's efficiency to capture CO_2. Other SiO_2-R-NH_2 sorbents have been studied that proposed similar amine/CO2 interactions.[107-111] FT-IR experiments of the CO_2/SiO_2-R-NH_2 interaction were reported by Chang et al.[103] Again, the aminopropylsilyl-tethered silica material was found to reversibly bind CO_2. However, rather than forming only an ammonium carbamate (dry conditions) or an ammonium bicarbonate (wet conditions), five total amine/CO_2 interactions were identified by FT-IR (Figure 1.34). The capacity of the aminopropylsilyl-tethered silica was reported to be approximately 0.4 mmol CO_2/g in humidified CO_2.

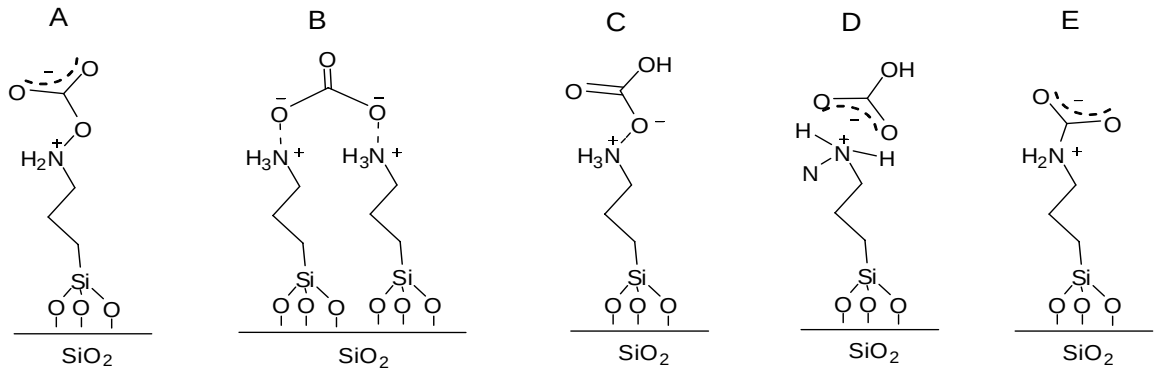

Figure 1.34. Various proposed amine/CO_2 interactions: monodentate carbonate (A), bidentate carbonate (B), monodentate bicarbonate (C), bidentate bicarbonate (D), carbamic acid (E).[103]

Other research groups have attempted to synthesize aminosilica sorbents that reversibly bind CO_2 with higher capacities (capacities > 2 mmol CO_2/g). Many groups used a tetherable silane with greater numbers of amine functionalities (such as diaminosilanes and triaminosilanes). For instance, Zheng and coworkers[112] and Chuang and coworkers[113] independently synthesized ethylenediamine-tethered to SBA-15 sorbents that could reversibly bind CO_2 with capacities twice that of the monoamine-functionalized SBA-15 materials.[113] Both Sayari and coworkers[114, 115] and Chafee and coworkers[116] reported CO_2 capture using diethylenetriamine[propyl(silyl)]-functionalized mesoporous silicas (SiO_2-CH_2-CH_2-CH_2-NH-CH_2-CH_2-NH-CH_2-CH_2-NH_2).[114-116] Chaffee and coworkers found that the triamine-functionalized silica was stable up to 170 ^oC and had capacities higher than the diamine- or monoamine-grafted materials.[116] Sayari and coworkers reported the triamine-functionalized silica sorbent to have capacities of 2.65 mmol CO_2/g (dry 5 % CO_2/N_2) and 2.94 mmol CO_2/g (humid 5% CO_2/N_2).[114] The use of the triamine-functionalized silica materials was successful in

forming a high amine content (~ 6 mmol N/g)[114] on the surface capable of reversibly binding CO_2.

Another synthetic method to produce CO_2 capture sorbents is impregnation of soluble polyamines into the pores of the support.[117-121] With typical impregnation methods, a true organic/inorganic hybrid material as defined earlier in this chapter is not produced due to the lack of a covalent bond with the surface. Impregnation is solely a method of physically adsorbing (physisorbing) organic species on the surface and in the pores of the inorganic support. For example, Song and coworkers synthesized a PEI impregnated MCM-41 support by mixing MCM-41 with a solution of polyethyleneimine/methanol.[117-120] The methanol was removed under vacuum, leaving the PEI-impregnated silica sorbent (Figure 1.35). As reported by Song and coworkers,

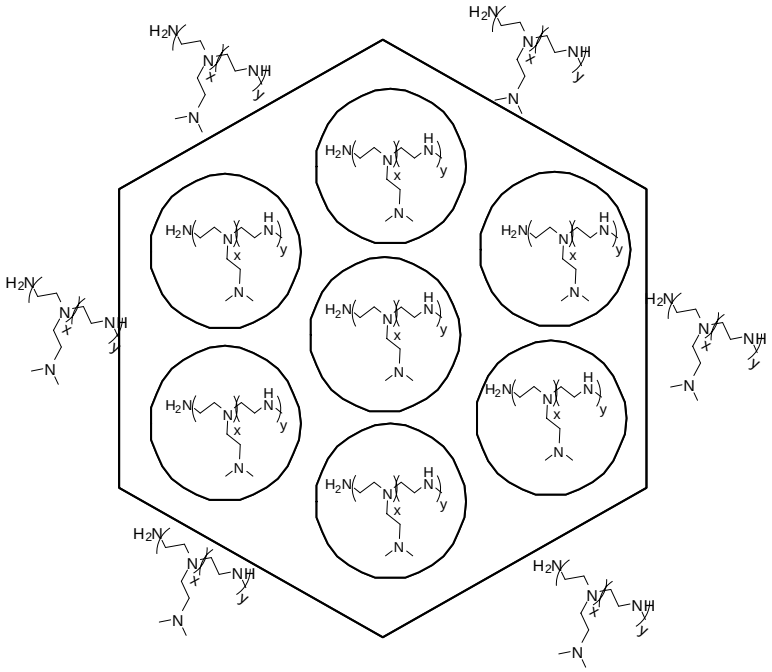

Figure 1.35. PEI-modifed silica via impregnation.

the MCM-41-PEI materials were able to capture CO_2 reversibly with capacities of approximately 3 mmol CO_2/g when a 50 wt % of PEI was impregnated in the support.[117-120] However, they found that the MCM-41-PEI material captured CO_2 with the highest capacities at 75 ^oC. The grafted aminosilicas, however, performed better at lower temperatures (~ 25 ^oC) as opposed to higher temperatures (~ 75 ^oC). The PEI impregnated materials most likely have higher capacities at 75 ^oC because the polymer can swell and become more mobile within the pore. However, at lower temperatures, the diffusion through the pore is hindered because the PEI within the pore is less mobile.

Impregnation was also reported by Zhu and coworkers as a method to capture high amounts of CO_2 per gram of sorbent.[121] In this report, SBA-15 was used as the support. Rather than calcining the material (removing the surfactant from the pores prior to further treatment), tetraethylenepentamine (TEPA) was impregnated into the as-synthesized SBA-15 material (Figure 1.36). The surfactant in the mesopores of the silica material was used to disperse the TEPA. This material captured CO_2 with capacities of approximately 3.9 mmol CO_2/g with a 50 wt % TEPA impregnated support. It was suggested that the hydroxyl groups of the poly(ethylene oxide)-poly(propylene oxide)-poly(ethylene oxide) surfactant were able to help CO_2 adsorb to the material, indicating that hydrophilic materials enhance adsorption capacities.[121] However, this material suffered from decreased capacity when recycled. It is possible that either some TEPA is lost during the desorption step at 100 ^oC or that the surfactant decomposes during the desorption step. This phenomenon could be prevented by covalently bonding the amine and the hydrophilic portion to the surface.

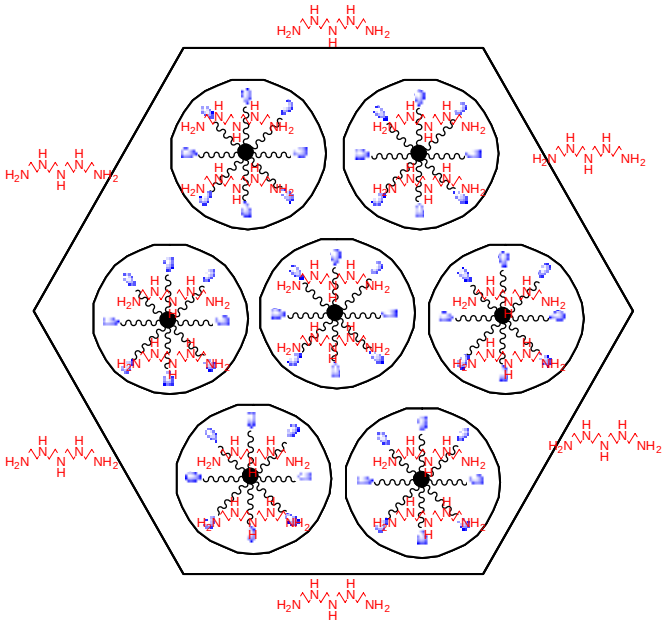

Figure 1.36. TEPA-modified as-synthesized silica via impregnation.

The following list summarizes many of the important results reported in the open literature that could assist in the molecular design or analysis of new aminosilica sorbents:

- water increases the adsorption capacity for most aminosilicas
- desorption temperatures range between 80 – 120 ^{o}C
- for polymer impregnated materials, higher capacities are found at higher temperatures due to swelling of the polymer in the pores
- larger pores (> 10 nm) typically showed an increase in CO_2 capacities
- pure CO_2 provides the highest capacities (although flue gas streams typically have concentrations of ~ 10 – 15 %)
- capacities in flow systems are usually higher than TGA measurements due to diffusion limitations in most TGA instruments

1.5 Thesis Goals

The major goals of this thesis were to create, characterize the structure, and use new organic/inorganic hybrid material in engineering applications, including specifically:

1. Creating a site-isolated aminosilica material with higher amine loadings than previously reported isolation methods
2. Using spectroscopic, reactivity, and catalytic (olefin polymerization precatalysts) probes to determine isolation of amine groups on these organic/inorganic hybrid materials
3. Synthesizing an organic/inorganic hybrid material capable of activating Group 4 olefin polymerization precatalysts.
4. Synthesizing an organic/inorganic hybrid material with ultra-high amine loading that is capable of reversibly capturing CO_2 in a simulated flue gas stream.

The overall goal of this work involves the synthesis of novel organic/inorganic hybrid materials. Chapter 2 discusses the synthesis and characterization of a site-isolated aminosilica that has loadings similar to traditional one-step methods. Chapters 3 and 4 compare the isolated aminosilica (Chapter 2) with other amine isolation techniques with spectroscopic (fluorescence), reactivity (small molecule reactions with the surface amine groups), and catalytic (formation of heterogeneous constrained-geometry-inspired precatalysts) probes to determine amine isolation and accessibility. Chapter 5 involves the synthesis of the first organic/inorganic hybrid sulfonic acid-functionalized silica material capable of activating Group 4 olefin polymerization precatalysts when small

amount of alkylaluminum are present. The application of aminosilicas as CO_2 capture materials is found in Chapter 6. A new organic/inorganic hybrid aminosilica material is discussed which reversibly captures CO_2 from simulated flue gas streams. Overall, this dissertation focuses on the synthesis, characterization and application of aminosilica and sulfonic acid-functionalized silica materials.

1.6 References

1. Wight, A. P.; Davis, M. E., *Chem. Rev.* **2002,** 102, 3589.

2. Evans, J.; Zaki, A. B.; El-Sheikh, M. Y.; El-Safty, S. A., *J. Phys. Chem. B* **2000,** 104, 10271.

3. Kramer, J.; Garcia, A. R.; Driessen, W. L.; Reedijk, J., *Chem. Commun.* **2001**, 2420.

4. Walcarius, A.; Etienne, M.; Bessiere, J., *Chem. Mater.* **2002,** 14, 2757.

5. Voss, R.; Thomas, A.; Antonietti, M.; Ozin, G. A., *J. Mater. Chem.* **2005,** 15, 4010.

6. Yoo, S.; Lunn, J. D.; Gonzalez, S.; Ristich, J. A.; Simanek, E. E.; Shantz, D. F., *Chem. Mater.* **2006,** 18, 2935.

7. Davis, M. E.; Katz, A.; Ahman, W. R., *Chem. Mater.* **1996,** 8, 1820.

8. Juvaste, H.; Iiskola, E. I.; Pakkanen, T. T., *J. Mol. Catal. A* **1999,** 150, 1.

9. Timonen, S.; Pakkanen, T. T.; Iiskola, E. I., *J. Organomet. Chem.* **1999,** 582, 273.

10. Juvaste, H.; Pakkanen, T. T.; Iiskola, E. I., *Organometallics* **2000,** 19, 4834.

11. McKittrick, M. W.; Jones, C. W., *Chem. Mater.* **2003,** 15, 1132.

12. McKittrick, M. W.; Jones, C. W., *J. Catal.* **2004,** 227, 186.

13. Acosta, E. J.; Carr, C. S.; Simanek, E. E.; Shantz, D. F., *Adv. Mater.* **2004,** 16, 985.

14. Yu, K. Q.; McKittrick, M. W.; Jones, C. W., *Organometallics* **2004,** 23, 4089.

15. McKittrick, M. W.; Jones, C. W., *J. Am. Chem. Soc.* **2004,** 126, 3052.

16. McKittrick, M. W.; Jones, C. W., *Chem. Mater.* **2005,** 17, 4758.

17. McKittrick, M. W.; Yu, K. Q.; Jones, C. W., *J. Mol. Catal. A* **2005,** 237, 26.

18. Severn, J. R.; Chadwick, J. C.; Duchateau, R.; Friederichs, N., *Chem. Rev.* **2005,** 105, 4073.

19. Kickelbick, G., *Prog. Polym. Sci.* **2003,** 28, 83.

20. Beck, J. S.; Varfuli, J. C.; Roth, W. J.; Leonowicz, M. E.; Kresge, C. T.; Schmitt, K. D.; Chu, C. T.-W.; Olson, D. H.; Sheppard, E. W.; McCullen, S. B.; Higgins, J. O.; Schlenker, J. L., *J. Am. Chem. Soc.* **1992,** 114, 10834.

21. Zhao, D.; Huo, Q.; Feng, J.; Chmelka, B. F.; Stucky, G. D., *J. Am. Chem. Soc.* **1998,** 120, 6024.

22. Burkett, S. L.; Sims, D. D.; Mann, S., *Chem. Commun.* **1996**, 1367.

23. Fryxell, G. E., *Inorg. Chem. Commun.* **2006,** 9, 1141.

24. Doyle, A. M.; Hodnett, B. K., *J. Non-Crystalline Solids* **2006,** 352, 2193.

25. Knozinger, H.; Rumpf, E., *Inorganica Chemica Acta* **1978,** 30, 51.

26. Unger, K. K.; Kinkel, J. N., *J. Chromatogr.* **1984,** 316, 193.

27. Luechinger, M.; Prins, R.; Pirngruber, G. D., *Micropor. Mesopor. Mater.* **2005,** 85, 111.

28. Kanan, S. M.; Tze, W. T. Y.; Tripp, C. P., *Langmuir* **2002,** 18, 6623.

29. Wulff, G.; Heide, B.; Helfmeier, G., *J. Am. Chem. Soc.* **1986,** 108, 1089.

30. Wulff, G.; Heide, B.; Helfmeier, G., *React. Polym.* **1987,** 6, 299.

31. Katz, A.; Davis, M. E., *Nature* **2000,** 403, 286.

32. Bass, J. D.; Anderson, S. L.; Katz, A., *Angew. Chem. Int. Ed.* **2003,** 42, 5219.

33. Bass, J. D.; Katz, A., *Chem. Mater.* **2003,** 15, 2757.

34. Zaitsev, V. N.; Skopenko, V. V.; Kholin, Y. V.; Konskaya, N. D.; Mernyi, S. A., *Zh. Obshch. Khim.* **1995,** 65, 529.

35. Chien, J. C. W., *Top. Catal.* **1999,** 7, 23.

36. Chen, E. Y.-X.; Marks, T. J., *Chem. Rev.* **2000,** 100, 1391.

37. Hlatky, G. G., *Chem. Rev.* **2000,** 100, 1347.

38. Crabtree, R. H., *The Organometallic Chemistry of the Transition Metals*. John Wiley & Sons: New York, 2001.

39. Ziegler, K.; Hozkamp, E.; Breil, H.; Martin, H., *Angew. Chem.* **1955,** 541.

40. Breslow, D. S.; Newburg, N. R., *J. Am. Chem. Soc.* **1957,** 79, 5072.

41. Natta, G.; Pino, P.; Mazzanti, G.; Giannini, U., *J. Am. Chem. Soc.* **1957,** 79, 2975.

42. Long, W. P., *J. Am. Chem. Soc.* **1959,** 81, 5312.

43. Sinn, H.; Kaminsky, W.; Vollmer, H. J.; Woldt, R., *Angew. Chem. Int. Edit.* **1980,** 19, 390.

44. Stellbrink, J.; Niu, A.; Allgaier, J.; Richter, D.; Koenig, B. W.; Hartmann, R.; Coates, G. W.; Fetters, L. J., *Macromolecules* **2007**, in press.

45. Massey, A. G.; Park, A. J., *J. Organomet. Chem.* **1964,** 2, 245.

46. Yang, X.; Stern, C. L.; Marks, T. J., *J. Am. Chem. Soc.* **1994,** 116, 10015.

47. Yang, X.; Stern, C. L.; Marks, T. J., *J. Am. Chem. Soc.* **1991,** 113, 3623.

48. Resconi, L.; Cavallo, L.; Fait, A.; Piemontesi, F., *Chem. Rev.* **2000,** 100, 1253.

49. Chien, J. C. W.; Tsai, W. M.; Rausch, M. D., *J. Am. Chem. Soc.* **1991,** 113, 8570.

50. Jia, L.; Yang, X.; Stern, C. L.; Marks, T. J., *Organometallics* **1995,** 14, 3135.

51. Soga, K.; Kim, H. J.; Shiono, T., *Macromol. Chem. Phys.* **1994,** 195, 3347.

52. Soga, K.; Arai, T.; Nozawa, H.; Uozumi, T., *Macromol. Symp.* **1995,** 97, 53.

53. Soga, K., *Macromol. Symp.* **1995,** 89, 249.

54. Soga, K., *Macromol. Symp.* **1996,** 101, 281.

55. dos Santos, J. H. Z.; Ban, H. T.; Teranishi, T.; Uozumi, T.; Sano, T.; Soga, K., *J. Mol. Catal. A* **2000,** 158, 541.

56. dos Santos, J. H. Z.; Ban, H. T.; Teranishi, T.; Uozumi, T.; Sano, T.; Soga, K., *Appl. Catal. A* **2001,** 220, 287.

57. dos Santos, J. H. Z.; Uozumi, T.; Teranishi, T.; Sano, T.; Soga, K., *Polymer* **2001,** 42, 4517.

58. Soga, K.; Kim, H. J.; Shiono, T., *Macromol. Rapid Commun.* **1994,** 15, 139.

59. Jin, J.; Uozumi, T.; Soga, K., *Macromol. Rapid Commun.* **1995,** 16, 317.

60. Uozumi, T.; Toneri, T.; Soga, K.; Shiono, T., *Macromol. Rapid Commun.* **1997,** 18, 9.

61. Iiskola, E. I.; Timonen, S.; Pakkanen, T. T.; Harkki, O.; Lehmus, P.; Seppala, J. V., *Macromolecules* **1997,** 30, 2853.

62. Iiskola, E. I.; Timonen, S.; Pakkanen, T. T.; Harkki, O.; Seppala, J. V., *Appl. Surf. Sci.* **1997,** 121, 372.

63. Timonen, S.; Pakkanen, T. T.; Iiskola, E. I., *J. Mol. Catal. A.* **1999,** 148, 235.

64. Bortolussi, F.; Boisson, C.; Spitz, R.; Malinge, J.; Broyer, J.-P. U.S. Patent Appl. 2004/0147692, **2004**.

65. Alt, H. G.; Schertl, P.; Koppl, A., *J. Organomet. Chem.* **1998,** 568, 263.

66. Schneider, H.; Puchta, G. T.; Kaul, F. A. R.; Raudaschl-Sieber, G.; Lefebvre, F.; Saggio, G.; Mihalios, D.; Herrmann, W. A.; Basset, J. M., *J. Mol. Catal. A* **2001,** 170, 127.

67. Suzuki, N.; Asami, H.; Nakamura, T.; Huhn, T.; Fukuoka, A.; Ichikawa, M.; Saburi, M.; Wakatsuki, Y., *Chem. Lett.* **1999**, 341.

68. Suzuki, N.; Yu, J.; Shioda, N.; Asami, H.; Nakamura, T.; Huhn, T.; Fukuoka, A.; Ichikawa, M.; Saburi, M.; Wakatsuki, Y., *Appl. Catal. A* **2002,** 224, 63.

69. Tian, J.; Soo-Ko, Y.; Metcalfe, R.; Feng, Y. D.; Collins, S., *Macromolecules* **2001,** 34, 3120.

70. Juvaste, H.; Iiskola, E. I.; Pakkanen, T. T., *J. Organomet. Chem.* **1999,** 587, 38.

71. Juvaste, H.; Pakkanen, T. T.; Iiskola, E. I., *J. Organomet. Chem.* **2000,** 606, 169.

72. Juvaste, H.; Pakkanen, T. T.; Iiskola, E. I., *Organometallics* **2000,** 19, 1729.

73. Galan-Fereres, M.; Koch, T.; Hey-Hawkins, E.; Eisen, M. S., *J. Organomet. Chem.* **1999,** 580, 145.

74. Jones, C. W.; McKittrick, M. W.; Nguyen, J. V.; Yu, K. Q., *Top. Catal.* **2005,** 34, 67.

75. Ewen, J. A.; Elder, M. J. Eur. Patent Appl. 0,427,697, **1991**; U.S. Pat. 5,561,092, **1996**.

76. Chien, J. C. W.; He, D., *J. Poly. Sci. Poly. Chem.* **1991,** 29, 1603.

77. Tian, J.; Wang, S.; Feng, Y.; Li, J.; Collins, S., *J. Mol. Catal. A.* **1999,** 144, 137.

78. Musikabhumma, K.; Spaniol, T. P.; Okuda, J., *Macromol. Chem. Phys.* **2002,** 203, 115.

79. Garces, J. M.; Sun, T., *Catal. Commun.* **2003,** 4, 97.

80. Lee, K.-S.; Oh, C.-G.; Yim, J.-H.; Ihm, S.-K., *J. Mol. Catal. A* **2000,** 159, 301.

81. Ahn, H.; Marks, T. J., *J. Am. Chem. Soc.* **1998,** 120, 13533.

82. Ahn, H.; Nicholas, C. P.; Marks, T. J., *Organometallics* **2002,** 21, 1788.

83. Nicholas, C. P.; Ahn, H.; Marks, T. J., *J. Am. Chem. Soc.* **2003,** 125, 4325.

84. Nicholas, C. P.; Marks, T. J., *Langmuir* **2004,** 20, 9456.

85. Turner, H. W. U.S. Patent 5,427,991, **1995**.

86. Fritze, C.; Kuber, F.; Bohnen, H. U.S. Patent 6,329,313, **2001**.

87. Hinkouma, S.; Miyake, S.; Ono, M.; Inazawa, S. U.S. Patent 5,869,723, **1999**.

88. Ishigaki, S.; Hinkouma, S. Eur. Pat. Appl. 1,359,166, **2003**.

89. Ishigaki, S.; Hinkouma, S. PCT Int. Pat. Appl. 03/035708, **2003**.

90. Carnahan, E. M.; Carney, M. J.; Neithamer, D. R.; Nickias, P. N.; Shih, K.-Y.; Spencer, L. PCT Int. Appl. 97/19959, **1997**.

91. Carnahan, E. M.; Neithamer, D. R.; Shankar, R. B. PCT Int. Appl. 00/63262, **2000**.

92. Shih, K.-Y. U.S. Patent 6,184,171, **2001**.

93. Jacobsen, G. B.; Matsushita, F.; Spencer, L.; Wauteraerts, P. L. U.S. Patent 2001/0039320, **2001**.

94. Jacobsen, G. B.; Wijkens, P.; Jastrezebski, J. T. B. H.; van Koten, G. U.S. Patent 5,834,393, **1998**.

95. Jacobsen, G. B.; Stevens, T. J. P.; Loix, H. H. U.S. Patent 6,271,165, **2001**.

96. Carnahan, E. M.; Neithamer, D. R. PCT Int. Appl. 01/58969, **2001**.

97. Kaneko, T.; Sato, M. U.S. Patent 5,807,938, **1998**.

98. Scott, S. L.; Church, T. L.; Nguyen, D. H.; Mader, E. A.; Moran, J., *Top. Catal.* **2005,** 34, 109.

99. Marland, G.; Boden, T. A.; Andres, R. J. Global, Regional, and National Fossil Fuels CO_2 Emissions. Trends: A Compendium of Data on Global Change, Oak Ridge, TN: Oak Ridge National Laboratory, 2006, http://cdiac.ornl.gov/trends/emis/tre_glob.htm.

100. Nielsen, R. Nuclear Power Plants. 2006, http://home.iprimus.com.au/nielsens/.

101. Astarita, G., *Chem. Eng. Sci.* **1961,** 16, 202.

102. Leal, O.; Bolivar, C.; Ovalles, C.; Garcia, J. J.; Espidel, Y., *Inorganica Chemica Acta* **1995,** 240, 183.

103. Chang, A. C. C.; Chuang, S. S. C.; Gray, M.; Soong, Y., *Energy & Fuels* **2003,** 17, 468.

104. Liu, L.; Chakma, A.; Feng, X., *Chem. Eng. J.* **2004,** 105, 43.

105. National Energy Technology Laboratory (NETL). http://www.netl.doe.gov/index.html.

106. Tsuda, T.; Tsuyoshi, F., *J. Chem. Soc. Chem. Commun.* **1992**, 1659.

107. Gray, M. L.; Soong, Y.; Champagne, K. J.; Pennline, H. W.; Baltrus, J.; Stevens Jr., R. W.; Khatri, R.; Chuang, S. S. C., *Int. J. Environ. Techol. Manage.* **2004,** 4, 82.

108. Gray, M. L.; Soong, Y.; Champagne, K. J.; Pennline, H. W.; Baltrus, J.; Stevens Jr., R. W.; Khatri, R.; Chuang, S. S. C.; Filburn, T., *Fuel Proc. Technol.* **2005,** 86, 1449.

109. Khatri, R. A.; Chuang, S. S. C.; Soong, Y.; Gray, M., *Energy & Fuels* **2006,** 20, 1514.

110. Kim, S.; Ida, J.; Guliants, V. V.; Lin, J. Y. S., *J. Phys. Chem. B* **2005,** 109, 6287.

111. Knowles, G. P.; Graham, J. V.; Delaney, S. W.; Chaffee, A. L., *Fuel Proc. Technol.* **2005,** 2005, 1435.

112. Zheng, F.; Tran, D. N.; Busche, B. J.; Fryxell, G. E.; Addlemann, R. S.; Zemanian, T. S.; Aardahl, C. L., *Ind. Eng. Chem. Res.* **2005,** 44, 3099.

113. Khatri, R. A.; Chuang, S. S. C.; Soong, Y.; Gray, M., *Ind. Eng. Chem. Res.* **2005,** 44, 3702.

114. Harlick, P. J. E.; Sayari, A., *Ind. Eng. Chem. Res.* **2007,** 46, 446.

115. Harlick, P. J. E.; Sayari, A., *Ind. Eng. Chem. Res.* **2006,** 45, 3248.

116. Knowles, G. P.; Delaney, S. W.; Chaffee, A. L., *Ind. Eng. Chem. Res.* **2006,** 45, 2626.

117. Xu, X.; Song, C.; Andresen, J. M.; Miller, B. G.; Scaroni, A. W., *Micropor. Mesopor. Mater.* **2003,** 62, 29.

118. Xu, X.; Song, C.; Andresen, J. M.; Miller, B. G.; Scaroni, A. W., *Energy & Fuels* **2002,** 16, 1463.

119. Xu, X.; Song, C.; Miller, B. G.; Scaroni, A. W., *Ind. Eng. Chem. Res.* **2005,** 44, 8113.

120. Xu, X.; Song, C.; Miller, B. G.; Scaroni, A. W., *Fuel Proc. Technol.* **2005,** 86, 1457.

121. Yue, M. B.; Chun, Y.; Cao, Y.; Dong, X.; Zhu, J. H., *Adv. Funct. Mater.* **2006,** 16, 1717.

CHAPTER 2

CONTROLLING THE DENSITY OF AMINE SITES ON SILICA SURFACES USING BENZYL SPACERS[†]

2.1 Introduction

As previously discussed, by utilizing traditional methods to synthesize aminopropylsilyl-functionalized materials, the creation of a final material with multiple types of amines is likely, with the presence of some isolated amines but the majority of the species being (A) hydrogen bonded or (B) interacting with silanols (Figure 2.1). To create truly well-defined functional materials, it is thus important to prevent these interactions by separating the amines and capping excess surface silanols. Many groups have attempted to synthesize aminosilicas in an effort to control the types of amine sites formed by spacing the amines with protecting groups. The main disadvantage of the previously reported amine-spacing methods[1-5] is that the loading of the amine

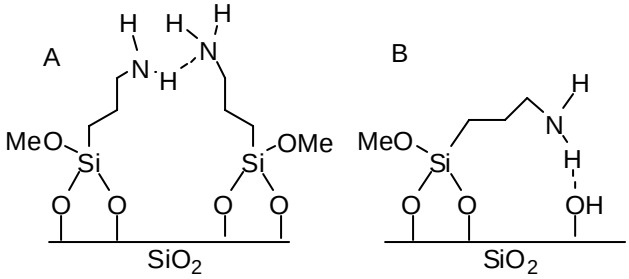

Figure 2.1. Multiple types of amine sites present on silica include (A) amine-amine and (B) amine-silanol interactions.

[†]Reproduced in part with permission from Langmuir, 2006, 22, 2676. Copyright 2006 American Chemical Society.

functionalities is greatly reduced on the support material, as amine-spacing is controlled in part by keeping the total loading of amines low. By keeping the amine concentration low on the surface, the proximity of the individual amines to each other is limited statistically. However, when traditional silane grafting approaches are employed, a large amount of aminosilanes can be deposited on the surface via reaction with silanols or siloxane bridges, allowing the pendant amines to group together on the surface close enough to interact with their nearest neighbor (which we describe as "clustering"). It would thus be advantageous to maximize the amine loading on the surface while spacing the amine groups far enough apart in hopes of preventing the clustering of amines or the interaction of the amines with surface silanols. Previously, use of a trityl spacer allowed the creation of an aminosilica material with amines that were spaced far enough apart on the surface to allow for unique amine reactivity patterns.[6] Compared to traditional materials prepared by the grafting of simple, unprotected aminosilanes, the trityl-spaced amines behaved as if they were site-isolated. Quantitative stoichiometric transformations of the amine groups were possible with the trityl-spaced material but were generally not realized with the material prepared via traditional grafting techniques.[6-8] The interesting fundamental question then becomes, how dense an array of amines can be made while still preparing sites that are chemically different from traditional, densely-loaded aminosilica materials? Certainly, as the size of the protecting group is decreased and as the amines are more closely positioned together, at some point the amines prepared by the imine-protected grafting route and the traditional unprotected grafting route should start to behave similarly. In this work, we describe our initial efforts at probing this threshold. We present here a new benzyliminosilane (benzylidene-(3-trimethoxysilanyl-

propyl)-amine), which when added to a silica surface followed by surface capping reactions provides an aminopropylsilyl-functionalized silica (benzyl-imine spaced silica) with greater amine density than previously reported spacing methods,[6] while providing some finite amount of surface spacing to help prevent amine-amine interactions that are indicative of amine clustering. Interestingly, we show that the benzyl-spaced aminosilica material has amines that are chemically different from a material that was prepared via traditional aminosilane grafting techniques, despite the fact that amine loadings are similar.

2.2 Experimental Section

Materials. The following chemicals were commercially available and used as received: redistilled benzaldehyde (Aldrich), Pluronic 123 (Aldrich), HCl (Fisher), tetraethyl orthosilicate (Aldrich), 3-aminopropyltrimethoxysilane (Aldrich), 1,1,1,3,3,3-hexamethyldisilazane (Aldrich), 0.1N perchloric acid in acetic acid (LabChem Inc.), glacial acetic acid (Fisher), methyl violet (Alfa Aesar), anhydrous toluene (Acros), anhydrous tetrahydrofuran (Aldrich) and 1-pyrenecarboxylic acid (Aldrich). Anhydrous dichloromethane, and anhydrous hexanes were obtained from a packed bed solvent purification system utilizing columns of copper oxide catalyst and alumina (hexanes) or dual alumina columns (dichloromethane).[9] Anhydrous methanol (Acros) was further dried over 4-Å molecular sieves prior to use. All air- and moisture-sensitive compounds were transferred using standard vacuum line, Schlenk, or cannula techniques under dry, deoxygenated argon or in a drybox under a deoxygenated N_2 atmosphere.

Synthesis of SBA-15.

SBA-15 was synthesized similar to literature methods.[10] To 561 g of DI H_2O, 18.0 g of EO-PO-EO block co-polymer and 99.5 g of HCl was added and stirred overnight. To the micellular solution, 39.8 g of tetraethyl orthosilicate was added and stirred for 5 minutes. The solution was stirred for 20 h at 35 ºC. To swell the pores, a temperature treatment of 80 ºC for 24 h was applied. The resulting solid was filtered with copious amounts of distilled H_2O and dried overnight at 60 ºC. The as-prepared material was calcined using the following temperature program: (1) increasing the temperature (1.2 °C/min) to 200 °C, (2) heating at 200 °C for 1 h, (3) increasing at 1.2 °C/min to 550 °C, and (4) holding at 550 °C for 6 h. Approximately 11 grams of SBA-15 was synthesized with this method. Prior to use, the SBA-15 was dried under vacuum at 200 ºC for 3 h and stored in a N_2 drybox.

Synthesis of Densely Loaded Amine-Functionalized SBA-15.

Excess 3-aminopropyltrimethoxysilane (1.0 g, 5.58 mmol) was added to 1 g of SBA-15 in anhydrous toluene. The mixture was allowed to stir for 24 h at room temperature under argon. The resulting solid was filtered, washed with toluene, dried under vacuum at 50 ^oC overnight, and then stored in a drybox. TGA showed 1.21 mmol/g material of APTMS was immobilized on the SBA-15.

Synthesis of benzylidene-(3-trimethoxysilanyl-propyl)-amine Spacer.

Benzaldehyde (0.60 g, 5.65 mmol) was refluxed with 3-aminopropyltrimethoxysilane (APTMS) (1.02 g, 5.69 mmol) in dry toluene equipped with a Dean Stark trap for 24 h. The toluene was removed in vacuo. The excess APTMS was removed under vacuum at

90 ºC overnight. NMR data: ^{1}H NMR (400 MHz, CD_3OD): δ 0.70 (2 H), 1.83 (2H), 3.57 (9 H), 3.61 (2 H), 7.40 (3 H), 7.72 (2 H), 8.27 (1 H).

Synthesis of SBA-15 Functionalized with the Benzylimine Spacer.

The benzylimine spacer (1.0 g, 3.74 mmol), was added to 2 g of SBA-15 with anhydrous toluene and stirred at room temperature under argon for 24 h. The resulting solid was filtered and washed with toluene in a drybox, dried under vacuum at 50^{o}C overnight, and then stored in a drybox.

Silanol Capping Reaction.

The capping synthesis was carried out by contacting a large excess of hexamethyldisilazane (HMDS) with the benzylimine spaced SBA-15 in anhydrous hexanes at room temperature under argon for 24 h. The resulting solid was filtered and washed with toluene and hexanes in a drybox, dried under vacuum at 50^{o}C overnight, and then stored in a drybox.

Hydrolysis.

The capped benzylimine SBA-15 (0.6 g) was added to 60 g of a 1:1:1 solution of H_2O/MeOH/HCl (38 wt %). The mixture was stirred in air at room temperature for 6 h. The solid was collected via filtration, washed with copious amounts of DI water, anhydrous methanol, and anhydrous THF, and then dried under vacuum at 50^{o}C overnight.

Second Silanol Capping.

The hydrolyzed amine-functionalized SBA-15, excess HMDS, and anhydrous hexanes were mixed and stirred at room temperature under argon for 24 h. The resulting solid was

filtered and washed with toluene and hexanes in a drybox, dried under vacuum at 50°C overnight, and then stored in a drybox.

Loading of Fluorescent Probe Molecule on Aminopropylsilyl-Functionalized SBA-15 materials.

A slight excess of 1-pyrenecarboxylic acid was added to 500 mg of densely-loaded or hydrolyzed, benzyl-spaced aminosilica in anhydrous toluene in a N_2 drybox. The solution was brought to reflux for 24 hours after the N_2 was replaced with argon. The solid was washed with copious amounts of anhydrous toluene and anhydrous THF to remove any physisorbed acid. The material was dried at 60 °C at a pressure of 6 mTorr.

Material Characterization.

The XRD patterns were collected on a PAN analytical X'Pert Pro powder X-ray diffractometer using Cu Kα radiation and a PW3011 proportional detector with a parallel plate collimator. Scanning electron microscopy (SEM) images were captured on a Hitachi S800 field emission gun (FEG) SEM. Cross-polarization magic angle spinning (CP-MAS) NMR spectra were collected on a Bruker DSX 300-MHz instrument. Samples were packed in 7-mm zirconia rotors in a nitrogen drybox and spun at 5 kHz. Typical ^{13}C CP-MAS parameters were 3000 scans, a 90° pulse length of 4 μs, and recycle times of 4 s. Typical ^{29}Si CP-MAS parameters were 5000 scans, a 90° pulse length of 5 μs, and recycle times of 5 s. FT-Raman spectra were obtained on a Bruker FRA-106. At least 1024 scans were collected for each spectrum, with a resolution of 2-4 cm^{-1}. FT-IR spectra were collected on a Bruker IFS 66v/S spectrometer with an aperture setting of 9mm and a scanning velocity of 3.0 kHz. Thermogravimetric analysis (TGA) was performed on a Netzsch STA409. Samples were heated under air from 30 to 900 °C at a rate of 10

°C/min. The organic loading was measured by determining the weight loss from 200 to 650 °C. The organic loading was determined by assuming two methoxy linkages to the surface before hydrolysis and three methoxy linkages after. For the traditional amine-functionalized SBA-15, two methoxy linkages were assumed. Nitrogen physisorption measurements were conducted on a Micromeritics ASAP 2010 at 77 K. SBA-15 samples were pretreated by heating under vacuum at 150 °C for 24 h. Organic loaded samples were pretreated by heating at 75^{o}C under vacuum for 24 hours. Non-aqueous potentiometric titrations were carried out in 30mL of glacial acetic acid with 50-300 mg of aminosilica. The aminosilica was titrated with 10-100μL aliquots of 0.1N perchloric acid in acetic acid. Fluorescence experiments were collected at Oak Ridge National Laboratories on a Jobin Yvon FluoroMax® -P spectrometer. The continuous light source was a 150-W ozone-free xenon arc-lamp. The samples were studied under vacuum with slits set to 1 nm.

2.3 Results and Discussion

The benzylimine spacer was chosen in an attempt to produce an aminosilica with an organic loading approaching those achieved using traditional synthetic methods, while preventing amine-silanol interactions. The advantage to the imine functionality is that it can be easily transformed into a primary amine. This benzyl spaced aminosilica synthesis is shown in Figure 2.2. The benzylimine silane was synthesized by a condensation reaction between benzaldehyde and 3-aminopropyltrimethoxysilane using a Dean-Stark trap. The synthesized benzylimine spacer was added to calcined SBA-15 (A). To prevent possible amine-silanol interactions in later steps, the unreacted silanols

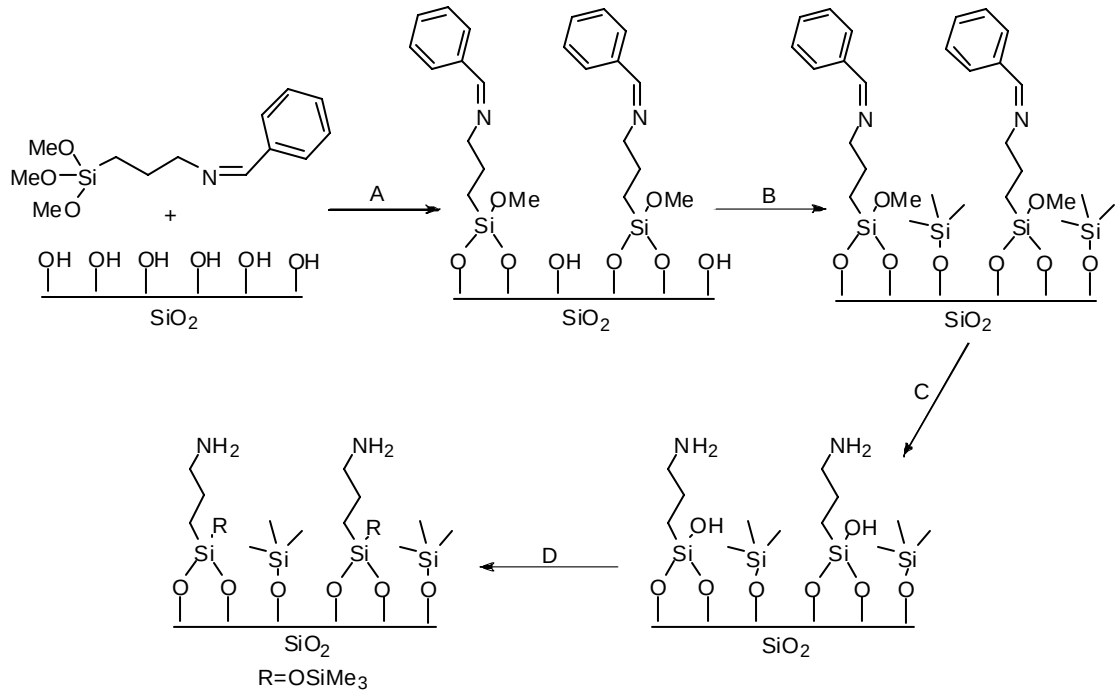

Figure 2.2. Protection/deprotection grafting method.

were capped with the well-known silylating agent HMDS (B).[11, 12] In the third step, the imine was converted to the amine by acid hydrolysis (C). Lastly, the surface was reacted with HMDS an additional time to ensure all accessible silanols were capped after the acidic solution was added (D).

The organic loading on SBA-15 was determined by thermogravimetric analysis (TGA). The organic loading of the benzylimine on SBA-15 was 0.98 mmol N=C/g material. After the hydrolysis step, the amine loading was estimated to be 0.99 mmol NH_2/g material. This is consistent with the hypothesis that the imine functionalities were completely removed from the support material. Spectroscopic evidence presented later confirms this assumption. The organic loading was determined by assuming two methoxy linkages to the surface before hydrolysis and three methoxy linkages after. As a

comparison material, traditional densely loaded aminopropylsilyl-functionalized SBA-15 gave a loading of 1.21 mmol NH_2/g material. This indicates that the benzyl-spaced aminosilica approaches the loading of traditional dense aminosilicas.

To confirm the TGA experiments, non-aqueous potentiometric titrations were performed. The imine was titrated to approximately 0.99 mmol N=C/g material (Figure 2.3A). The material was then contacted with an acid solution to hydrolyze the imine species and to remove the benzyl protecting group. A base wash was then performed with ammonium hydroxide in water to remove any excess acid after the hydrolysis step.[13] After this wash, the material was dried with heat under vacuum to remove any remaining ammonia. The hydrolyzed material was titrated to 0.95 mmol NH_2/g material (Figure 2.3B). As a comparison, titration experiments were performed right after the hydrolysis. The amines were most likely protonated by HCl in this case, leading to titration of only 50-70% of the amines.

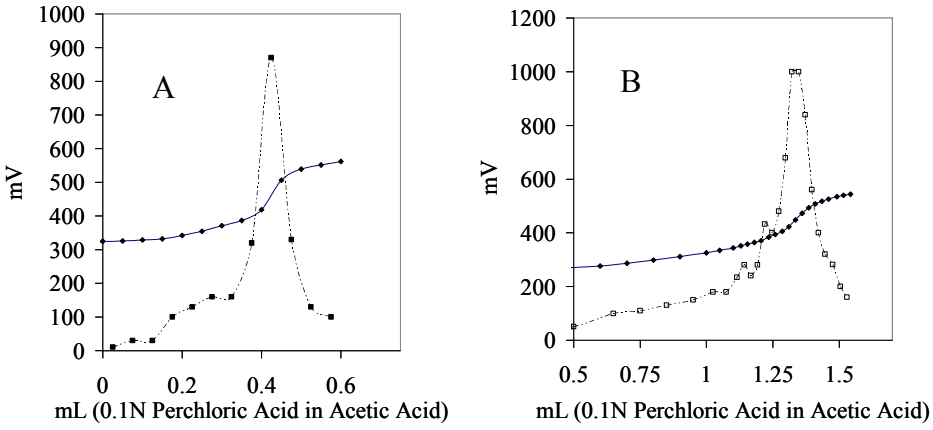

Figure 2.3. Nonaqueous potentiometric titration of benzylimine loaded on SBA-15 (A) and the material after hydrolysis and base wash (B). The derivative of the potential with respect to volume added is plotted on each graph to identify the equivalence point.

X-ray diffraction patterns were collected for the materials after various steps of functionalization. In the calcined SBA-15 material (Figure 2.4A), three well resolved peaks that correspond to the (100), (110), and (200) reflections were noted. The peaks were attributed to a well-defined 2D-hexagonal mesostructure (p6mm).[10] A d-spacing of 90 Å was determined from this material, corresponding to 104 Å for the unit cell parameter. However, as shown in Figure 2.4B, after functionalization with the benzylimine spacer, only one peak can be seen (100). The decrease of the (110) and (200) peaks is common for silanated silica frameworks.[14, 15] After the hydrolysis step, all of the peaks corresponding to a well-defined 2D-hexagonal structure reappeared. This

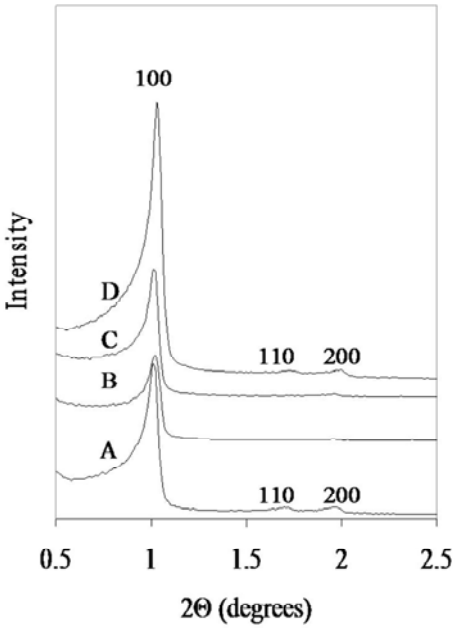

E

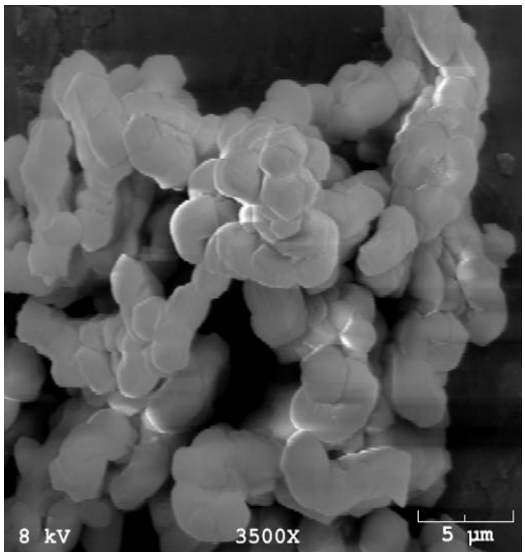

Figure 2.4. Powder X-ray diffraction patterns for the calcined SBA-15 (A), benzylimine loaded SBA-15 (B), capped benzylimine SBA-15 (C), hydrolyzed to amino-functionalized SBA-15 (D), and SEM image of calcined SBA-15 particles (E).

indicates that the hydrolysis step is not harsh enough to disrupt the order of the mesoporous silica framework. Also, it shows that the loss of the benzylimine functionalities results in a material very similar in its mesostructure to calcined SBA-15. Included in Figure 2.4E is an SEM image of the calcined SBA-15 particles used as the support material in this work. The particles have a range of sizes of approximately 1 – 5 μm in diameter.

The pore diameter and surface area of the material was tracked in each step by nitrogen physisorption (Table 2.1). The calcined SBA-15 gave a BET surface area of 930 m^2/g and a pore diameter of 65 Å determined from the BJH adsorption curve. The BET surface area presented reflects both mesopores (that are accessible to the bulky silane)

Table 2.1. N_2 physisorption data for SBA-15 after various stages of the benzylimine functionalization.

Nitrogen Physisorption Results at 77 K		
Sample	**Average pore diameter (Å)**	**BET surface area (m^2/g SiO_2)**
SBA-15	65	930
Benzylimine Patterned SBA-15	48	280
Capped Benzylimine SBA-15	48	272
Material After Hydrolysis	63	510

and micropores (that are likely not accessible), due to the SBA-15 synthesis procedure used.[16-18] After contact with the benzylimine patterning agent, the surface area and pore diameter were reduced, indicating reaction of the benzylimine spacer within the mesoporous silica material. After hydrolysis, the pore diameter returned to a similar size relative to the calcined SBA-15.

^{29}Si CP-MAS NMR spectra are shown in Figure 2.5 for the benzylimine functionalized SBA-15 (A) and the material after hydrolysis (B). The spectrum of the benzylimine functionalized SBA-15 (A) shows the Q^2, Q^3, and Q^4 silicon resonances between -90 and -110 ppm.[19] Also, three distinct peaks at -51 ppm, -60 ppm, and -66

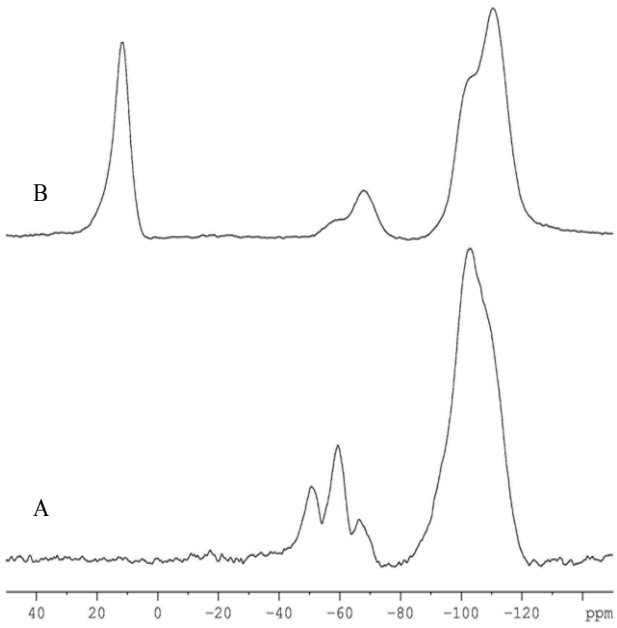

Figure 2.5. ^{29}Si CP-MAS NMR spectra for (A) benzylimine spaced SBA-15 and (B) the material after hydrolysis.

ppm correspond to the alkyl linkages to the surface by reaction of 1, 2, or 3 methoxy groups, respectively.[6, 20] Although cross-polarization experiments are not strictly quantitative, assuming all the silicon atoms in the silane cross-polarize with roughly similar efficiencies, it appears that the majority of the silanes react to the surface by two methoxy groups. This interpretation is consistent with TGA and titration results. After the hydrolysis step, mainly Q^3 and Q^4 silicon resonances are seen between -100 and -111 ppm. Also, the spectrum may be interpreted as being consistent with mainly three

methoxy groups reacting with the surface. The resonance of the trimethylsilyl groups derived from capped silanols can also be seen at 12 ppm.

Solid State ^{13}C CP-MAS spectra are shown in Figure 2.6. The functionalized material was analyzed after the addition of the benzylimine to the SBA-15 (A) and after the removal of the imine functionalities by hydrolysis (B). With the benzylimine spacer loaded on SBA-15, the spectrum shows all of the peaks expected. The aromatic carbons are located at 134 ppm and 127 ppm. The imine carbon is located at 162 ppm. After

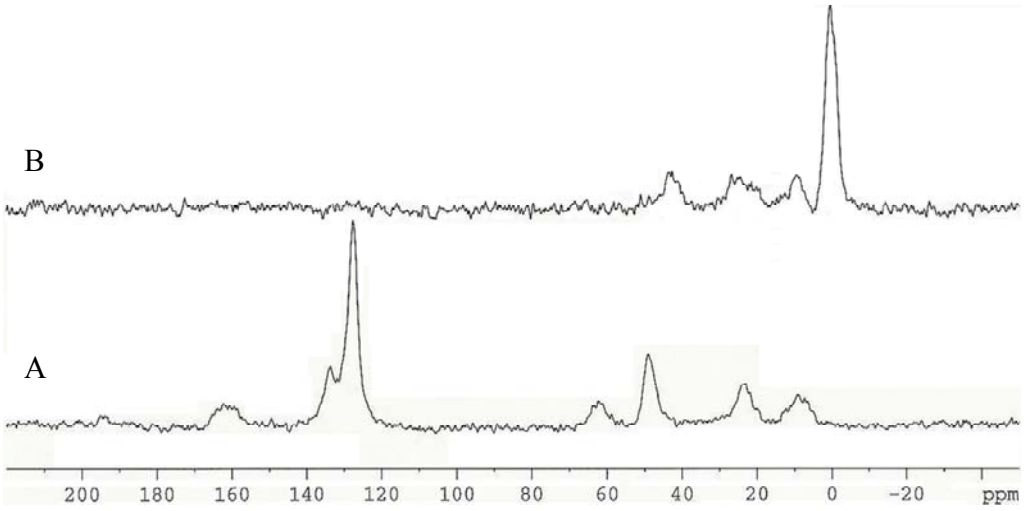

Figure 2.6. ^{13}C CP-MAS NMR spectra for (A) benzylimine spaced SBA-15 and (B) the material after hydrolysis.

hydrolysis, both the aromatic and imine carbon peaks disappeared. This indicates that the hydrolysis transformed the imines to primary amines. Also, it is noted that the carbon next to the imine shifts from 62 ppm to 43 ppm after hydrolysis. Overall, the spectrum of the deprotected aminopropylsilyl-functionalized SBA-15 after hydrolysis resembles that of aminopropylsilyl-modified silicas prepared by traditional grafting techniques.[6, 21] As

seen in the ^{13}C CP-MAS NMR spectrum, residual methoxy groups at 50 ppm are removed after hydrolysis, indicating that the silanes are bonded by mostly three linkages after hydrolysis. The very large peak at 0 ppm is the result of trimethylsilyl groups left by use of HMDS as a silanol capping agent. All the peak assignments are collected in Table 2.2.

Table 2.2. ^{13}C CP-MAS NMR chemical shifts for SBA-15 functionalized with the benzylimine moiety (A) and the same material after hydrolysis (B).

A	
Assignment	**Resonance (ppm)**
-Si - **C**H_2 -	9
-Si - CH_2 - **C**H_2 -	24
-Si - O**C**H_3	49
-CH_2 - **C**H_2 - N=	62
Aromatic carbons	129
-**C**H = N-	162
B	
Assignment	**Resonance (ppm)**
-Si - **C**H_3	0
-Si - **C**H_2 -	9
-Si - CH_2 - **C**H_2 -	27
-CH_2 - **C**H_2 - NH_2	43

As shown in Figure 2.7, FT-Raman spectroscopy was used as a complimentary technique to ^{13}C CP-MAS NMR to track the changes before (A) and after imine hydrolysis (B). The main peaks of interest are those that involve only the benzylimine spacer. For instance, the spectrum (A) has three distinct transitions corresponding to the aromatic C-H ($\nu_{\text{Aromatic C-H}} = 3100\ cm^{-1}$), C=N ($\nu_{C=N} = 1640\ cm^{-1}$), and C=C($\nu_{C=C} = 1601\ cm^{-1}$) stretches. After hydrolysis, these three bands are absent from the spectrum (B).

The only band remaining is the broad stretch from the aliphatic C-H (ν_{C-H} = 2900 cm^{-1}) that is seen in both (A) and (B). After hydrolysis, the N-H stretch is not visible in the spectrum. Nonetheless, the presence of amines has been verified by potentiometric titration (vide supra). The complete removal of the aromatic C-H bands is different from our previously reported amine spacing techniques, which show only a reduction in aromatic peak intensities rather than removal.[6] The residual aromatic C-H bands in previously reported syntheses may be a consequence of the synthetic method employed and the relative size of the organic spacers. The previously reported method[6] involved mixing a 3,3,3-triphenyl-propionaldehyde and 3-aminopropyltrimethyoxysilane in anhydrous methanol. The methanol was used to inhibit the polymerization of the silanes that could be caused by water formed in the reaction. In this work, we utilized a Dean-Stark trap to remove the water generated by the reaction. Also, the trityl group is much bulkier and less soluble than the benzyl functionality. Hence, the smaller benzyl-capped materials are expected to be more easily hydrolyzed. After hydrolysis, it is expected that the benzyl functionalities are removed from the pores more easily, resulting in a lack of aromatic C-H bands in FT-Raman experiments.

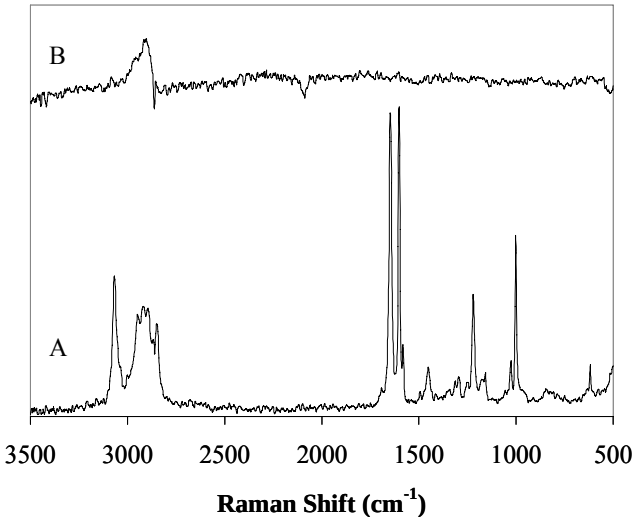

Figure 2.7. FT-Raman spectra of (A) benzylimine spaced SBA-15 and (B) the material after hydrolysis.

The proximity of the amine groups (degree of clustering) was studied by steady-state fluorescence emission experiments.[3, 22, 23] The hydrolyzed benzyl spaced SBA-15 material was contacted with 1-pyrenecarboxylic acid, carefully washed, and then dried under vacuum. To insure that the pyrene species were associated with the amine groups on the surface, bare SBA-15 was also contacted with 1-pyrenecarboxylic acid, washed and dried in the same manner. TGA data indicated that only a trace of pyrene moieties remained on the bare silica surface (< 0.04 mmol/g or ~10% of the pyrene loading on the aminosilica materials), indicating that majority of the pyrene species are associated with surface aminopropyl groups. The fluorescence spectrum of the pyrene-loaded benzyl-spaced material is shown in Figure 2.8A. Monomer emission was strongly detected by this technique. However, when performing the same experiment on densely-loaded

aminopropyl-functionalized silica, the spectrum (B) shows strong excimer emission.[3] This indicates that the benzyl spaced amines are separated far enough to prevent excimer formation. The dense material, on the other hand, has amines positioned close enough to allow for this formation (Figure 2.9 – acid-base interactions are shown although this is not conclusively known to be the means by which the amines interact with the pyrene acid). This result is somewhat surprising, as it might be surmised that the materials should be very similar in amine distribution due to their roughly similar loadings. It is suggested that this observation is a consequence of the synthetic method used, where the benzyl spacing methodology prevents the aminosilanes from being deposited on the surface in very close proximity to each other, perhaps by inhibiting the clustering of the

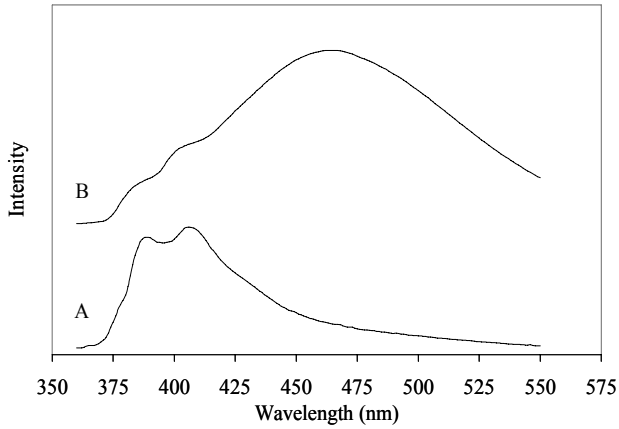

Figure 2.8. Fluorescence emission spectra of 1-pyrenecarboxylic acid loaded on (A) benzyl spaced aminosilica and (B) densely-functionalized aminosilica. The solid materials were excited at 330 nm. Arbitrary units used for the fluorescence intensity.

free amines during the grafting process. FT-IR experiments indicate that the interaction between the probe molecule and the amine scaffold may occur via an acid-base or hydrogen-bonding interaction, due to the lack of amide stretches in the spectrum of the pyrene-functionalized solid (Figure 2.10). TGA experiments on traditionally prepared aminosilica SBA-15 loaded with 1-pyrenecarboxylic acid indicated that 34% of the amine sites could be bound with the acid probe molecule (for a loading of 0.41 mmol pyrene/g silica). Similarly, the benzyl-spaced material loaded with 1-pyrenecarboxylic

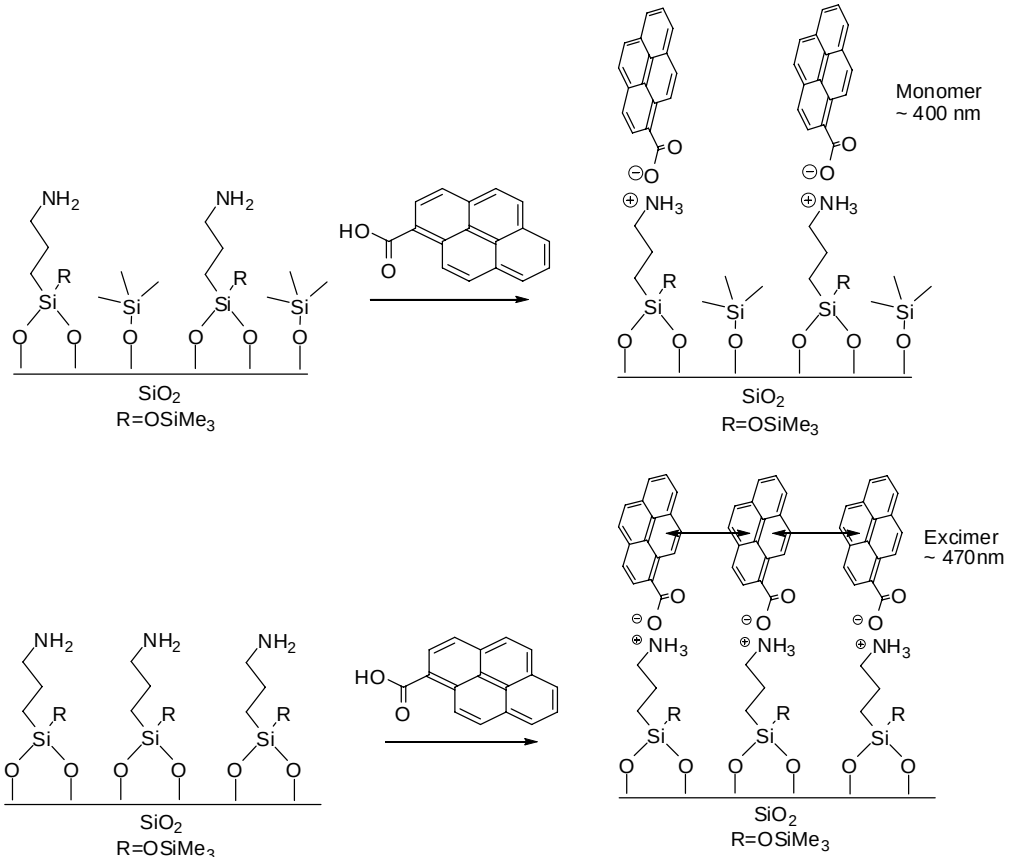

Figure 2.9. Surface reaction between PCA and either benzyl-spaced amines or traditional amines.

acid resulted in 37% amine coverage with the probe molecule (for a loading of 0.37 mmol pyrene/g silica). The TGA results indicate that the loadings of the acid probe molecule are comparable on the two materials.

The benzyl spaced aminosilica synthesized here can be used to better understand the role of isolated amines vs. amine pairs or clusters for a variety of different applications including catalysis, adsorption, and separation. For instance, as previously mentioned, our group has shown the importance of spacing the amines for an enhancement in catalytic productivity for the polymerization of ethylene using Group 4 constrained-geometry catalysts (CGCs).[7, 8, 24-26] The presented synthesis adds a new type of aminosilica material to the repertoire of materials designers, one with a relatively dense array of amines, yet with amines that are potentially spaced relative to each other. Data from fluorescence experiments imply that the amines on the surface of the benzyl-spaced aminosilica are chemically different from those on a traditional, densely-loaded

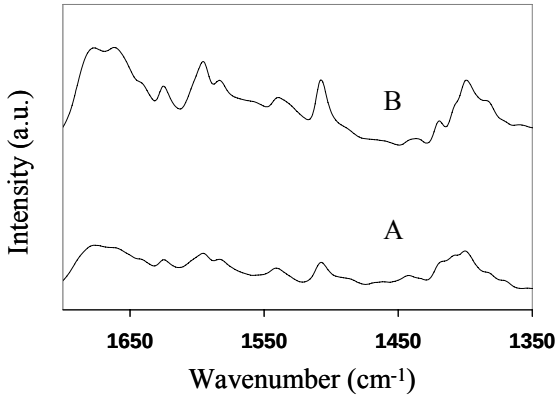

Figure 2.10. FT-IR spectra for (A) 1-pyrenecarboxylic acid and (B) 1-pyrenecarboxylic acid reacted with amine-functionalized SBA-15.

aminosilica material. Currently, the threshold between monomer and excimer formation in fluorescence characterization of a variety of differently "spaced" amine-functionalized silica materials is being probed and these results will be reported in a future publication.

2.4 Conclusions

The results presented show the synthesis of an aminopropyl-silica material with a high amine loading yet some evidence of limited amine-spacing relative to aminopropyl-silicas made via traditional grafting techniques. ^{29}Si CP-MAS NMR and N_2 physisorption data confirm functionalization within the mesopores. XRD data provide evidence that the functionalization steps leave the 2D-hexagonal mesoporous framework undisturbed. All the data together support the preparation of a well-defined aminopropyl-functionalized silica. Site-isolation was probed by fluorescence emission techniques. These results indicate that the benzyl spaced amines are positioned far enough apart as to prevent excimer formation. The degree of site-isolation in aminosilica materials continues to be a topic of study in our laboratory.

2.5 References

1. Wulff, G.; Heide, B.; Helfmeier, G., *J. Am. Chem. Soc.* **1986,** 108, 1089.

2. Wulff, G.; Heide, B.; Helfmeier, G., *React. Polym.* **1987,** 6, 299.

3. Katz, A.; Davis, M. E., *Nature* **2000,** 403, 286.

4. Bass, J. D.; Katz, A., *Chem. Mater.* **2003,** 15, 2757.

5. Bass, J. D.; Anderson, S. L.; Katz, A., *Angew. Chem. Int. Ed.* **2003,** 42, 5219.

6. McKittrick, M. W.; Jones, C. W., *Chem. Mater.* **2003,** 15, 1132.

7. McKittrick, M. W.; Jones, C. W., *J. Catal.* **2004,** 227, 186.

8. McKittrick, M. W.; Jones, C. W., *Chem. Mater.* **2005,** 17, 4758.

9. Pangborn, A. B.; Giardello, M. A.; Grubbs, R. H.; Rosen, R. K.; Timmers, F. J., *Organometallics* **1996,** 15, 1518.

10. Zhao, D.; Huo, Q.; Feng, J.; Chmelka, B. F.; Stucky, G. D., *J. Am. Chem. Soc.* **1998,** 120, 6024.

11. Anwander, R.; Gorlitzer, H. W.; Gerstberger, G.; Palm, C.; Runte, O.; Spiegler, M., *J. Chem. Soc. Dalton Trans.* **1999**, 3611.

12. Tao, T.; Maciel, G. E., *J. Am. Chem. Soc.* **2000,** 122, 3118.

13. Tsuji, K.; Jones, C. W.; Davis, M. E., *Microporous Mesoporous Mater.* **1999,** 29, 339.

14. Evans, J.; Zaki, A. B.; El-Sheikh, M. Y.; El-Safty, S. A., *J. Phys. Chem. B* **2000,** 104, 10271.

15. Yoshitake, H.; Yokoi, T.; Tatsumi, T., *Chem. Mater.* **2002,** 14, 4603.

16. Miyazawa, K.; Inagaki, S., *Chem. Commun.* **2000**, 2121.

17. Galarneau, A.; Cambon, H.; Renzo, F. D.; Fajula, F., *Langmuir* **2001,** 17, 8328.

18. Kruk, M.; Jaroniec, M.; Kim, T.-W.; Ryoo, R., *Chem. Mater.* **2003,** 15, 2815.

19. Sindorf, D. W.; Maciel, G. E., *J. Phys. Chem.* **1982,** 86, 5208.

20. Sindorf, D. W.; Maciel, G. E., *J. Am. Chem. Soc.* **1983,** 105, 3767.

21. Sudholter, E. J. R.; Huis, R.; Hays, G. R.; Alma, N. C. M., *J. Colloid Interface Sci.* **1985,** 103, 554.

22. Ivanov, I. N.; Dabestani, R.; Buchanan III, A. C.; Sigman, M. E., *J. Phys. Chem. B* **2001,** 105, 10308.

23. Thomas, A.; Polarz, S.; Antonietti, M., *J. Phys. Chem. B* **2003,** 107, 5081.

24. McKittrick, M. W.; Jones, C. W., *J. Am. Chem. Soc.* **2004,** 126, 3052.

25. Yu, K. Q.; McKittrick, M. W.; Jones, C. W., *Organometallics* **2004,** 23, 4089.

26. McKittrick, M. W.; Yu, K. Q.; Jones, C. W., *J. Mol. Catal. A* **2005,** 237, 26.

CHAPTER 3

SPACING AND SITE ISOLATION OF AMINE GROUPS IN 3-AMINOPROPYL-GRAFTED SILICA MATERIALS –THE ROLE OF PROTECTING GROUPS[†]

3.1 Introduction

The original hypothesis concerning the utility of the trityl-protected 3-aminopropylsilane grafting method was that both the protection of the amine via formation of an imine (Figure 3.1a) and the relative bulk of the trityl group lead to the effective spacing of amines on the surface via both (i) the prevention of formation of "clusters" of amine groups in hydrophobic grafting solutions (such as toluene) that can react in "packs" on the silica substrate (Figure 3.2) and (ii) physical separation of sites on the surface by the bulky trityl group (Figure 3.3).[1] Subsequently, we reported a benzyl-protected 3-aminopropyltrimethoxysilane (Figure 3.1b),[2] a molecule with very little steric bulk in the protecting group, for the creation of an aminosilica material with a higher amine loading that approached the loading of traditional densely-loaded aminopropylsilyl functionalized silicas. Curiously, attempts to probe amine-amine distances on the surface via spectroscopic methods suggested that the amine-amine spacing was different from materials prepared via traditional, unprotected grafting techniques, even though the amine

---

[†]Reproduced in part with permission from Chemistry of Materials, 2006, 18, 5022. Copyright 2006 American Chemical Society.

loadings were similar. This suggests that significant steric bulk in the protecting group is not the sole factor that leads to different surface amine site distributions compared to materials made by the traditional method of grafting unprotected 3-aminopropylsilanes onto the silica surface.

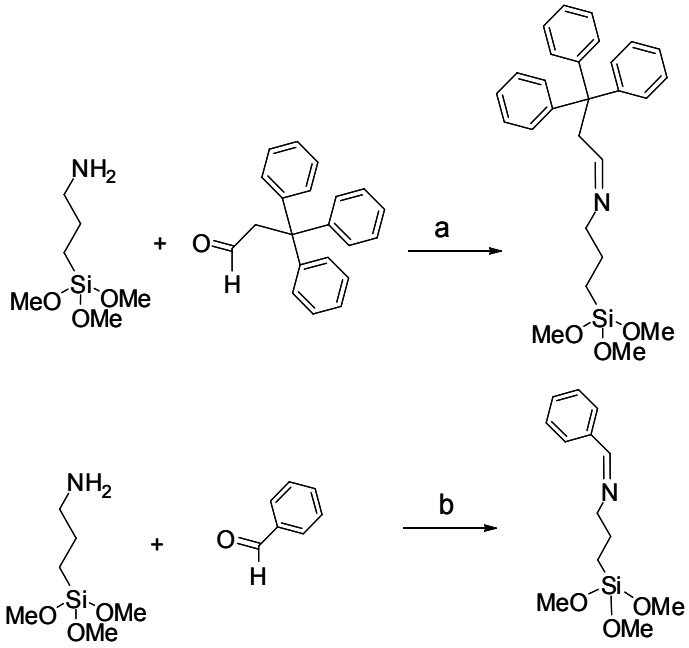

Figure 3.1. Protecting the amines with (a) trityl or (b) benzyl groups.

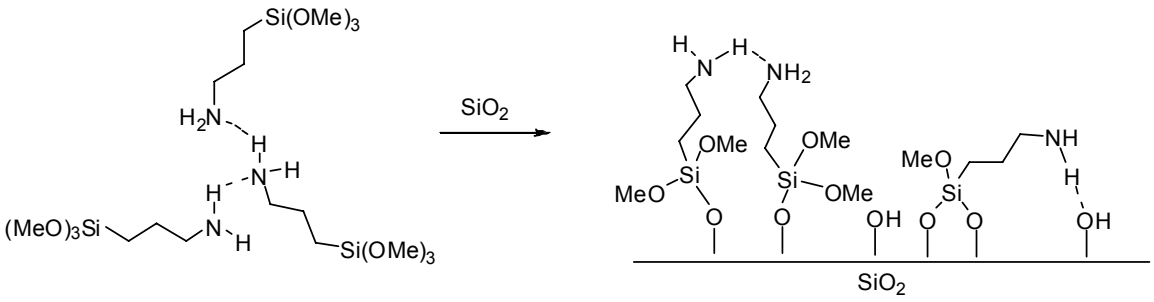

Figure 3.2. Clustering of amines in solution forming packs on surface.

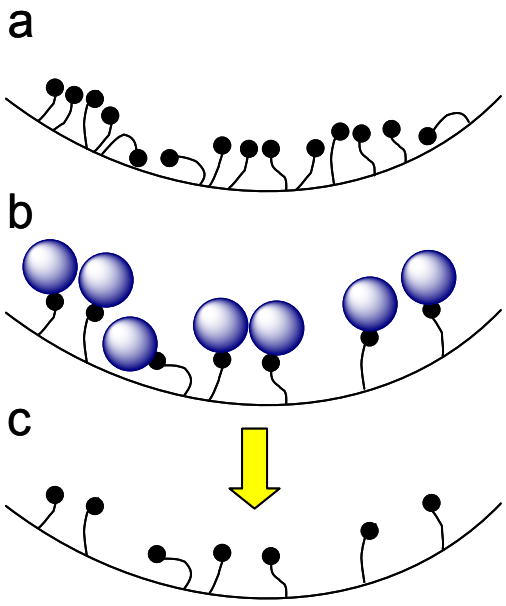

Figure 3.3. Comparing the traditional grafted APTMS silica (a) with the protection/deprotection (b, c) strategy. The protection/ deprotection method produces separation of the amine sites due to the bulky trityl protecting group.

3-aminopropylsilyl modified silica materials prepared by a protection/deprotection approach have been studied on a molecular-level in regard to catalytic activity,[3-5] adsorption properties,[6, 7] site isolation,[4, 5, 8, 9] and organic chain

mobility,[8] whereas relatively few reports have focused on the relative spacing and accessibility of amines on the surface of grafted materials with higher loadings.[10, 11] In this report, we study the mechanism of spacing using the protected 3-aminopropylsilyl silica grafting approach and employ a fluorescence analytical technique as a sensitive tool to probe the spacing, or degree of site isolation, of these important inorganic-organic hybrid materials. In particular, we use pyrene fluorescence spectroscopic data from a variety of 3-aminopropylsilyl modified silica materials to assess the degree of site-isolation of surface amines and the role of the protecting group in defining the amine surface density. Furthermore, we show that the amine-protected grafting route is a generally applicable method for the creation of 3-aminopropylsilyl modified silicas with controllable amine spacings, while dilution of unprotected 3-aminopropyl silanes during grafting results in materials with a relatively higher amount of amine clustering on the surface.

3.2 Experimental Section

Materials. The following chemicals were commercially available and used as received: redistilled benzaldehyde (Aldrich), 3,3,3-triphenylpropionic acid (Aldrich), 1.0 M $LiAlH_4$ in tetrahydrofuran (Aldrich), Pluronic 123 (Aldrich), hydrochloric acid (VWR International), anhydrous ether (Aldrich), tetraethyl orthosilicate (Aldrich), 3-aminopropyltrimethoxysilane (Aldrich), 1,1,1,3,3,3-hexamethyldisilazane (Aldrich), anhydrous tetrahydrofuran (Aldrich), anhydrous methanol (Aldrich), 1-pyrenebutyric acid (Aldrich) and 1-pyrenecarboxylic acid (Aldrich). Anhydrous toluene and anhydrous hexanes were further treated by a packed bed solvent purification system utilizing

columns of copper oxide catalyst and alumina.[12] All compounds were transferred using standard vacuum line, Schlenk, or cannula techniques under dry, deoxygenated argon or in a drybox under a deoxygenated N_2 atmosphere in order to reduce/prevent amine-CO_2 interactions.

Synthesis of SBA-15. SBA-15 was synthesized similar to literature methods.[2, 13] To 561 g of DI water, 17.9 g of EO-PO-EO block co-polymer and 99.4 g of HCl was added and stirred overnight. To the micellular solution, 39.6 g of tetraethyl orthosilicate was added and stirred for 5 minutes. The solution was stirred for 20 h at 35 ºC. To swell the pores, a temperature treatment of 80 ºC for 24 h was applied. The resulting solid was filtered with copious amounts of DI water and dried overnight at 60 ºC. The as-prepared material was calcined using the following temperature program: (1) increasing the temperature (1.2 °C/min) to 200 °C, (2) heating at 200 °C for 1 h, (3) increasing at 1.2 °C/min to 550 °C, and (4) holding at 550 °C for 6 h. Approximately 11.3 grams of SBA-15 was collected with this method. Prior to use, the SBA-15 was dried under vacuum at 200 ºC for 3 h to remove physisorbed surface water and stored in a N_2 drybox.[14-16]

Synthesis of Traditional Amine-Functionalized SBA-15 Materials. Excess 3-aminopropyltrimethoxysilane, APTMS, (1.0 g, 5.58 mmol) was added to 1 g of SBA-15 in anhydrous toluene. The mixture was allowed to stir for 24 h at room temperature under argon. The resulting solid was filtered, washed with toluene, dried under vacuum at 50 ^{o}C overnight, and then stored in a drybox. TGA showed 1.64 mmol/g SiO_2 of APTMS was immobilized on the SBA-15. Two additional aminosilica materials were synthesized by decreasing the solution concentration of APTMS to produce aminosilicas with lower loadings. For instance, to obtain an amine loading on the SBA-15 of 0.72 mmol/g SiO_2,

approximately 0.73 mmol of APTMS in 20 mL of toluene was mixed with 1 gram of SBA-15. The same procedure was used to immobilize 1.26 mmol of APTMS on 1 gram of SBA-15. Each material was then capped by contacting a large excess (2.0 g, 12.4 mmol) of 1,1,1,3,3,3-hexamethyldisilazane (HMDS) with the aminosilica in anhydrous hexanes at room temperature under argon for 24 h. The resulting solid was filtered and washed with toluene and hexanes in a drybox, dried under vacuum at 50^{o}C overnight, and then stored in a drybox.

Synthesis of Protected Aminoalkoxysilanes. To synthesize the benzyl-protected aminoalkoxysilane, we employed the same procedure as previously reported.[2] Benzaldehyde (0.60 g, 5.65 mmol) was refluxed with 3-aminopropyltrimethoxysilane (APTMS) (1.02, 5.69 mmol) in dry toluene in a 100 mL round bottom flask equipped with a Dean Stark trap for 24 h. The toluene was removed in vacuo. The excess APTMS was removed under vacuum at 90 ºC overnight. NMR data: ^{1}H NMR (400 MHz, CD_2Cl_2): δ 0.67 (2 H, m), 1.79 (2H, m), 3.57 (9 H, s), 3.60 (2 H, m), 7.40 (3 H, m), 7.72 (2 H, m), 8.27 (1 H, s).

We used a similar procedure to synthesize the trityl-deprotected aminoalkoxysilane.[1, 17] First 6.5 g (0.0215 mol) of 3,3,3-triphenylpropionic acid was reduced to the corresponding alcohol by addition of 32.5 mL of 1M $LiAlH_4$ in anhydrous THF (50 mL) overnight in an ice bath. The solvent was removed from the crude mixture via rotovap (yield ~ 4.6 g). Then, 2 g of the crude mixture containing the synthesized 3,3,3-triphenylpropanol was mixed with 3.64 g of pyridinium dichromate in 100 g of methylene chloride and stirred for 6 hours. The solvent was removed by rotovap and fresh anhydrous ether was added to dissolve the aldehyde. Lastly, the pyridinium

dichromate was removed via two separate filtrations through plugs of silica. NMR data: ^{1}H NMR (400 MHz, $CDCl_3$): δ 3.60 (2 H, d), 7.1 – 7.4 (15 H, m), 9.47 (1 H, s). The aldehyde (1.41 g, 4.92 mmol) was refluxed with APTMS (0.895 g, 4.99 mmol) in dry toluene equipped with a Dean Stark trap for 24 h. The toluene was removed in vacuo. The excess APTMS was removed under vacuum at 90 ºC overnight. NMR data: ^{1}H NMR (400 MHz, CD_3OD): δ 0.39 (2 H, t), 1.52 (2 H, m), 3.19 (2 H, t), 3.49 (9 H, s), 3.61 (2 H, m), 7.15 – 7.36 (15 H, broad), 7.43 (1 H, s).

Synthesis of SBA-15 Functionalized with Benzyl- or Trityl-Protected Aminoalkoxysilanes. The benzylimine spacer (1.0 g, 3.74 mmol) or tritylimine spacer (0.84 g, 1.88 mmol), was added to 2 g of SBA-15 with anhydrous toluene and stirred at room temperature under argon for 24 h. The resulting solid was filtered and washed with toluene in a drybox, dried under vacuum at 50^{o}C overnight, and then stored in a drybox. The capping step was carried out by contacting a large excess (2.0 g, 12.4 mmol) of HMDS with the protected aminosilica in anhydrous hexanes at room temperature under argon for 24 h. The resulting solid was filtered and washed with toluene and hexanes in a drybox, dried under vacuum at 50^{o}C overnight, and then stored in a drybox. The capped benzylimine SBA-15 (0.6 g) was added to 60 g of a 1:1:1 solution (by mass) of H_2O/MeOH/HCl(aq). The mixture was stirred in air at room temperature for 6 h. The tritylimine SBA-15 (0.5 g) was hydrolyzed with 50 g of a 2:2:1 solution (by mass) of H_2O/MeOH/HCl(aq) and stirred for 5 h. The deprotected solid was collected via filtration; washed with copious amounts of DI water, anhydrous methanol, and anhydrous THF; and then dried under vacuum at 50^{o}C overnight. The deprotected SBA-15 (0.5 g), excess HMDS (1.0 g, 6.2 mmol) and anhydrous hexanes were mixed and stirred at room

temperature under argon for 24 h. The resulting solid was filtered and washed with toluene and hexanes in a drybox, dried under vacuum at 50^{o}C overnight, and then stored in a drybox.

Loading of Fluorescent Probe Molecule on Aminopropylsilyl-Functionalized SBA-15 Materials. A three-fold excess (to amine loading) of 1-pyrenecarboxylic acid or 1-pyrenebutyric acid was added to 500 mg of traditional or deprotected-benzyl or trityl aminosilica in anhydrous toluene.[18] The reaction mixture was refluxed in anhydrous toluene for 24 hours under argon. The solid was washed with 6 x 75 mL of both toluene and THF to remove any physisorbed acid. The material was then dried at 60 ^{o}C under high vacuum for further removal of solvent.

Material Characterization. FT-Raman spectra were obtained on a Bruker FRA-106. At least 1024 scans were collected for each spectrum, with a resolution of 2-4 cm^{-1}. Thermogravimetric analysis (TGA) was performed on a Netzsch STA409. Samples were heated under a nitrogen and air stream from 30 to 900 °C at a rate of 10 °C/min. The organic loading was measured from the weight loss from 200 to 650 °C. The organic loading was determined by assuming two methoxy linkages to the surface before hydrolysis and three methoxy linkages after. For the traditional amine-functionalized SBA-15, two methoxy linkages were assumed. The loading of the fluorophore was determined by TGA from the weight loss from 200 to 750 ^{o}C. Steady-state fluorescence spectra were obtained on a Jobin Yvon Horiba FluoroMax-P spectrometer equipped with single monochrometer on both the excitation and emission sides. All emission and excitation spectra were recorded from the front face of the cell containing the solid sample and were corrected for instrumental response using the correction factors

provided by the manufacturer. Degassed solid samples for fluorescence and lifetime measurements were prepared in glass tubes equipped with a 0.1 cm quartz cell attachment and were flame-sealed under vacuum ($P \geq 1x10^{-6}$ Torr) to prevent oxygen quenching. Fluorescence lifetimes were measured by time correlated single photon counting technique on an IBH (Jobin Yvon Horiba) model 5000F instrument equipped with single monochrometer on the excitation and emission sides and a picosecond photon detection module (TBX-04). The excitation source was a Nano LED with a pulse width of 800 ps at 336 nm. Data acquisition for all the data reported on solid samples was carried out in a diffuse reflective mode. Degassed samples were subjected to 336 nm excitation pulses and the emission signals at various wavelengths (i.e. 377nm, 465 nm) were collected and averaged (i.e. 5000 counts) to obtain the decay profile. Decay analysis and the fitting routine to determine the lifetime(s) for the decay profiles were performed using the DAS6 software provided by IBH.

3.3 Results and Discussion

The interaction between amine groups immobilized on silica using a traditional grafting approach has been hypothesized to involve amine-amine hydrogen bonding – although isolated amines and silanol-complexed amines can also be present – due to "clusters" of amine groups in hydrophobic solutions (such as toluene) that can react in "packs" on the silica substrate (Chapter 1, Figure 1.10).[10] A molecular level understanding of the surface chemistry in these materials requires knowledge about the mechanism of grafting as well as methods to control the amine-amine spacing on the surface. We probe both of these issues here using pyrene fluorescence spectroscopy.

3.3.1 Functional Group Spacing by Pyrene Fluorescence Spectroscopy

Fluorescence spectroscopy has been extensively used as a tool to probe the degree of isolation or location of functional groups in heterogeneous media labeled with fluorescent probes such as pyrene.[19-35] Pyrene molecules form excimers when they can interact at a close distance via stacking.[36, 37] In contrast, isolated pyrene molecules fluoresce via a monomeric emission. For example, the distance between two fluorescing pyrene molecules in crystal form yielding an excimer has been calculated to be approximately $3 \leq r \leq 10$ Å, where r is the distance between two pyrene molecules.[37] Thus, it is hypothesized that pyrene molecules must be 1 nm or closer to form excimers, and the presence or lack of excimer formation can be used as a sensitive probe of pyrene separation. Thus, using this as a model for heterogeneous systems, one can infer separation of these pyrene groups via detection of the excimer formation. Antonietti and coworkers reported the effects of changing the silica pore size on the formation of excimers from pyrene molecules confined in the mesopores, which indicated that pore sizes of ~20 - 40 Å produce less excimers than mesoporous materials synthesized with > 40 Å pores.[38] Wang et al. reported a method by using fluorescence experiments to determine how functional groups on silica surface migrate when water is present for one month, obtaining a very small migration rate constant of ~ 10^{-20} cm^2/s with a 6 Å distance of separation for excimer formation.[39] By using the excimer formation of pyrene as a test for pyrene-pyrene distances, it is plausible to use fluorescence spectroscopy as a tool to determine the degree of separation between immobilized species on a silica substrate.

Since fluorescence spectroscopy provides an immense amount of information, we characterize various aminopropylsilyl modified silica surfaces prepared via several

techniques, including traditional grafting of unprotected 3-aminopropyltrimethoxysilane as well as grafting of a variety of differently protected 3-aminopropyltrimethoxysilanes, by using either 1-pyrenecarboxylic acid or 1-pyrenebutyric acid as a fluorescent tag. Using these two fluorophores loaded on the different aminosilica materials, we show that the relative separation of these amine groups can be easily determined by fluorescence spectroscopy and that solution "clustering" of these amine functionalities can be reduced by protecting the amines or, to a lesser extent, by dilution of unprotected 3-aminopropyltrimethoxysilane (APTMS) in solution before grafting on the silica surface.

3.3.2 Aminosilica Materials Studied

The silica support material used in this study is mesoporous SBA-15.[13] This material was chosen due to its extensively characterized unidimensional hexagonal array of mesopores.[13, 40-43] For our studies, the SBA-15 that was synthesized had a BET surface area of 960 m^2/g SiO_2 and a BJH adsorption pore diameter of 65 Å. As indicated by Thomas et al., using such materials for pyrene confinement studies is ideal due to silica's tailorable pore size as well its stability and inertness.[38]

Our group has studied two types of amine-protecting/spacing protocols using either a trityl- or benzyl-protecting group (Figure 3.4).[1, 2] First, the protected aminopropylalkoxysilane, in the form of an imine, is reacted to the silica surface under strictly anhydrous conditions to prevent oligomerization. A capping step with HMDS is then used to create a hydrophobic surface and decrease the potential for amine-silanol interactions after deprotection. The hydrolysis of the protecting group is performed in a HCl(aq)/MeOH solution. After deprotection, the surface is capped an additional time in

case the aqueous solution formed additional silanols (Figure 3.5). The samples prepared via benzyl protection are denoted **2a** and **2b**, and those prepared by trityl protection **3a** and **3b** (Table 3.1).

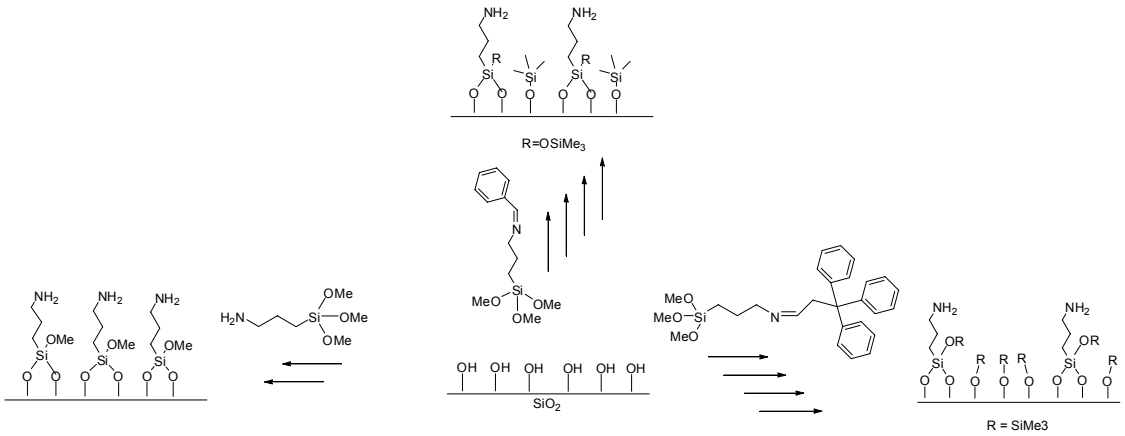

Figure 3.4. Aminosilica materials synthesized.

As the main comparison material, a traditional grafting approach was used to create aminosilicas without a protecting group. In this study, a 3.5 fold excess of APTMS was reacted with SBA-15, and then the remaining silanols were capped, creating samples **1a** and **1b**. Additional samples with different surface amine loadings were prepared by changing the concentration of APTMS in solution, assuming that all of the added silane ended up grafted on the surface. These materials had amine loadings lower than traditional aminosilica materials made with an excess of alkoxysilane. Samples **1c** and **1d** were synthesized with a loading of 1.26 mmol amine per gram of silica and

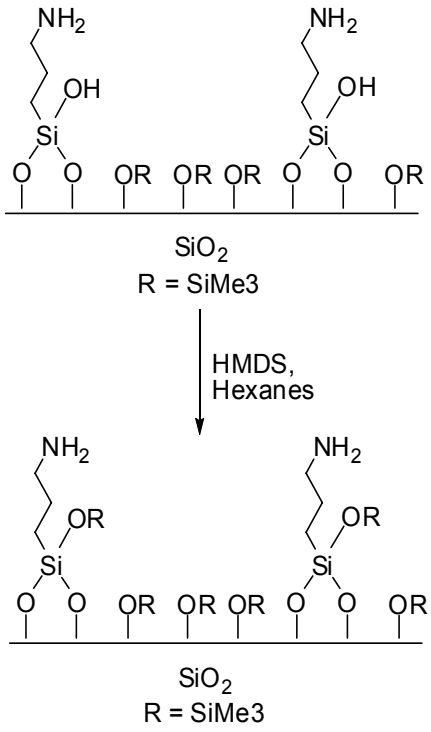

Figure 3.5. Capping residual silanols.

samples **1e** and **1f** were synthesized with a loading of 0.72 mmol amine per gram of silica. Lastly, all of these aminosilicas were contacted with either 1-pyrenecarboxylic

acid (PCA) or 1-pyrenebutyric acid (PBA) and studied with both steady-state fluorescence spectroscopy and time-resolved lifetime techniques. Pyrene was the fluorophore chosen due to its well known ability to form excimers when close enough to another pyrene molecule, as well as the literature precedent of using it in functional group spacing studies.[4, 9, 44] The carboxylic acid functionalities were used to allow for ionic or hydrogen bonding interactions between the amines on the surface and the fluorophore (Figure 3.6),[2] which is discussed in more detail in the next section. Table 3.1 lists the loadings of the amine groups on the various 3-aminopropylsilyl functionalized silica materials and the pyrene probe molecules that were loaded on these materials. Similar amine to pyrene ratios were obtained on all materials as determined from TGA experiments. Figure 3.7 shows the FT-Raman spectra of the materials before and after deprotection of the trityl (a & b) or benzyl (c & d) groups compared to traditional aminopropylsilyl functionalized silica (e).

Table 3.1 Loadings of organic groups on SBA-15 and monomer/excimer ratios.[a]

sample	protecting group	loading (mmol NH_2/g SiO_2)	probe molecule	% probe per amine site	I_{exc}/I_{mon}
1a	-------	1.64	PCA	34%	4.50
1b	-------	1.64	PBA	33%	110.4
1c	-------	1.26	PCA	27%	1.10
1d	-------	1.26	PBA	35%	3.53
1e	-------	0.72	PCA	28%	0.54
1f	-------	0.72	PBA	37%	0.89
2a	benzyl	1.35	PCA	37%	0.30
2b	benzyl	1.35	PBA	34%	1.64
3a	trityl	0.55	PCA	34%	0.20
3b	trityl	0.55	PBA	36%	0.34

[a] Loadings of protected and deprotected 3-aminopropylsilyl groups as well as loadings of PCA or PBA were determined by thermogravimetric analysis. The excimer to monomer ratio (I_{exc}/I_{mon}) was determined for each material based on the probe molecule.

In our previous report on the synthesis of benzyl-deprotected aminopropylsilyl functionalized silica materials,[2] we noticed that to obtain materials after deprotection that

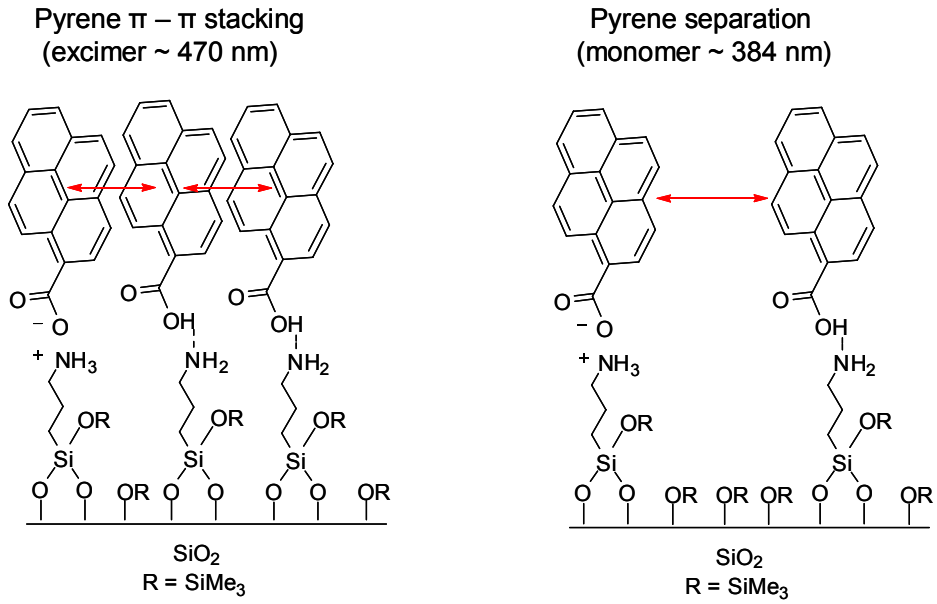

Figure 3.6. Reaction of PCA on various aminosilicas depicting π – π stacking (excimer) and monomeric emission.

completely lack any residual protecting groups [as determined spectroscopically via the removal of the aromatic C-H transition ($\nu_{C\text{-}H\ aromatic}$ = 3100 cm^{-1}) and the C=N transition ($\nu_{C=N}$ = 1601 cm^{-1})], a Dean-stark trap was needed to prevent oligomerization of the alkoxysilane groups during the synthesis of protected silane via the reaction between the aldehyde and the amine. Initially, we thought that the residual trityl groups within the pore seen in our previous report were there due to the steric bulk of the trityl group and the subsequent difficulty it might have diffusing out of the pore.[1] However, it is now hypothesized that complete removal of all the trityl groups was prevented due to inaccessibility to some sites due to the slight oligomerization of the silane during the

synthesis of the protected alkoxysilane. This hypothesis is consistent with the relatively broad ^{1}H NMR resonance observed for the tritylsilane reported previously.[1] In this work, when the tritylimine was synthesized using a Dean-stark trap to remove the water generated *in situ*, oligomerization was more likely prevented and the bulky trityl groups were easily removed from the material during deprotection, as shown by the absence of the C-H aromatic transition ($\nu_{C\text{-}H\ aromatic}$ = 3100 cm^{-1}) and the C=N transition ($\nu_{C=N}$ = 1595 cm^{-1}) (Figure 3.7b). Thus, in this work, after deprotection of the trityl- (Figure 3.7b) or benzyl- (Figure 3.7d) protected aminopropylsilyl functionalized materials, the main transitions remaining in the FT-Raman spectra are due solely to the aliphatic C-H bonds in the propyl linker ($\nu_{C\text{-}H\ aliphatic}$ = 2840 - 2990 cm^{-1}), as is seen in the traditional aminopropylsilyl functionalized silica material (Figure 3.7e).

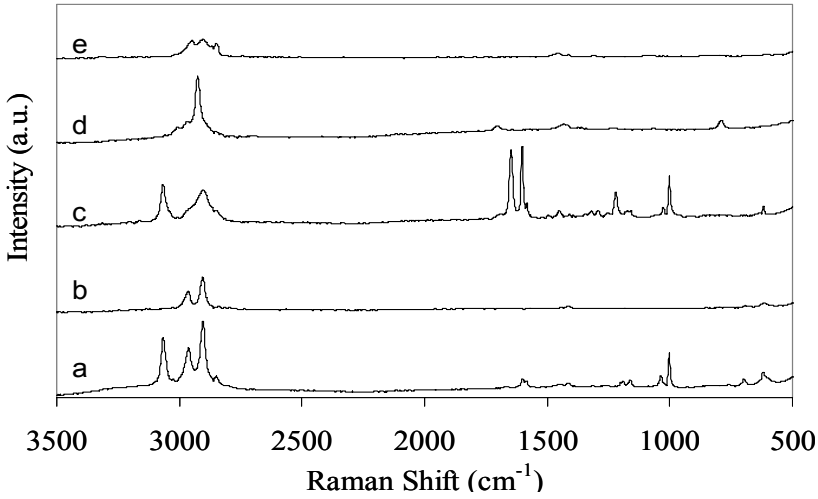

Figure 3.7. FT-Raman spectra tracking synthesis of the aminosilicas: (a) trityl-protected aminopropylsilyl SBA-15, (b) trityl-deprotected aminopropylsilyl SBA-15, (c) benzyl-protected aminopropylsilyl SBA-15, (d) benzyl-deprotected aminopropylsilyl SBA-15 and (e) traditional (unprotected) aminopropylsilyl SBA-15.

3.3.3 Steady-State Emission Experimental Results

Steady-state emission studies were performed to obtain information on the relative separation of amine groups on the surface of the differently prepared aminosilicas. The emission spectra in Figure 3.8 were obtained by exciting the aminopropylsilyl functionalized silica materials loaded with 1-pyrenecarboxylic acid (PCA) at 330nm. From the data, two distinct peaks associated with the pyrene monomer are visible at 384 nm and 405 nm in all three samples. However, it is obvious that when the traditional grafting approach was used to create the aminosilica, a very broad, intense, structureless peak at 465 nm is also present. This peak corresponds to the pyrene excimers that have formed on this aminosilica material. However, the excimer formation is much less noticeable for the benzyl-deprotected and trityl-deprotected aminosilica.

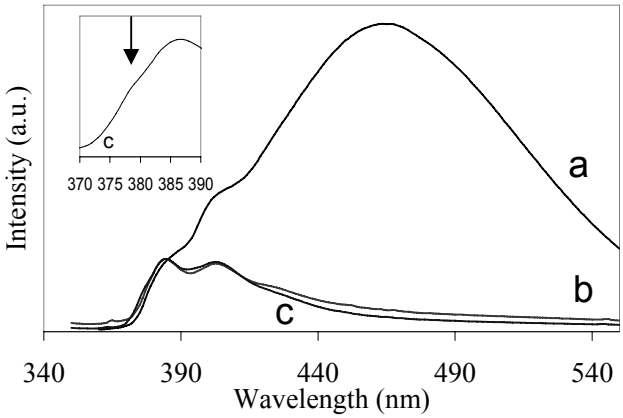

Figure 3.8. Steady-state fluorescence spectra of PCA loaded on traditional grafted **1a** (a), benzyl-deprotected **2a** (b) and trityl-deprotected **3a** (c) aminosilicas excited at 330 nm.

This observation suggests that the amine groups on the surface are distanced enough to prevent the PCA molecules from aggregating and forming excimers. Thus, the amount of excimer (and consequently the pyrene density) tracks well with amine loading. When the ratio of the excimer to monomer (I_{470}/I_{384}) is compared for the various materials, the ratio decreases in the order of: traditional (4.50) > benzyl-deprotected (0.30) > trityl-deprotected (0.20).

In our work reporting the benzyl-deprotected aminosilica synthesis, we indicated by FT-IR that the interaction between the PCA and the aminosilica was most likely an acid-base or hydrogen bonding interaction, due to the lack of amide transitions in the FT-IR spectrum with PCA on an aminosilica.[2] It is good to comment here that work by Milosavljevic and Thomas on pyrene-3-carboxylic acid further supports confirm our studies.[36, 45] As indicated in their work, PCA can be present in three different forms: anionic ($PyCOO^-$), neutral (PyCOOH) and protonated ($PyCOOH^+_2$). By changing the pH

of the solution, they were able to monitor the excitation and emission of PCA in various environments or media to determine how each species would respond. From their studies, when PCA is anionic, the maxima associated from these two groups were 376 nm, 397 nm, and 416 nm, and when PCA is neutral the maxima were 384 nm, 404 nm, and 425 nm. From our spectra, it is apparent that peaks associated with the neutral forms are present. Upon further analysis, it may be suggested that anionic forms at 377 nm are present as a small shoulder, although these peaks are very difficult to see in the traditional aminosilica, as excimer formation is quite large. This might be expected, as one would assume an equilibrium to be present between the anionic and neutral species. Nevertheless, since the protic, hydrophilic nature of the surface was changed by capping with HMDS, it is expected that the acid fluorophores are most likely interacting with the surface amine groups rather than any surface silanols. This hypothesis was tested by determining the loading of PCA on capped SBA-15. TGA experiments indicate that < 0.01 mmol PCA/g SiO_2 is physically adsorbed on the surface when no amines are present. The hydrophobicity of our sample can be inferred from the observation that the intensity of the 404 nm peak is similar to the 384 nm peak, indicating a more nonpolar environment compared to a silanol-rich, hydrophilic surface environment.[46]

To probe the role of pyrene-amine distance and pyrene flexibility, the various aminosilica materials were also loaded with 1-pyrenebutyric acid (PBA). Here, the aminosilicas were excited at 330 nm (Figure 3.9). In this case, the excimer formation increases for all of the materials, when compared to the PCA case (Figure 3.8). It is noteworthy that as the protecting group is changed, when a fluorophore with more length is used, the excimer formation appears to be a function of the bulkiness of the protecting group and thus the amine loading. For instance, if the trityl-deprotected aminopropylsilyl modified silica is compared to the benzyl-deprotected version, the fluorescent data

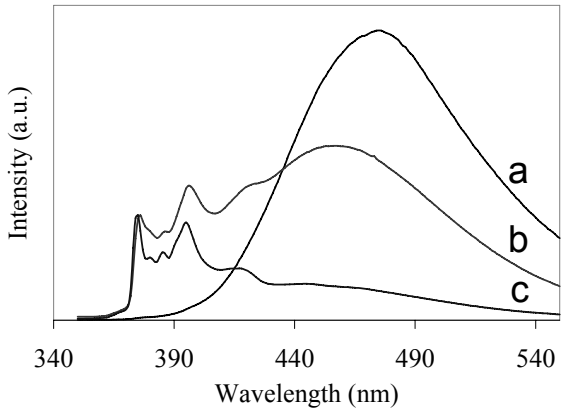

Figure 3.9. Steady-state fluorescence spectra of PBA loaded on traditional grafted **1b** (a), benzyl-deprotected **2b** (b) and trityl-deprotected **3b** (c) aminosilicas excited at 330 nm.

suggest that the amines produced with a bulkier protecting group (such as a trityl functionality) are separated sufficiently to reduce the excimers of the long chain pyrene molecules on the surface, indicating an increase in amine separation. It is also interesting to see how the traditional grafted approach shows essentially no monomeric emission but

instead shows strong excimer formation. It is proposed that the amines in this case are so close together the PBA molecules can pack very closely and form virtually all excimers, which can be seen with a red shift to 475 nm. However, when either the trityl- or benzyl-deprotected aminosilicas are examined, the excimer formation is much less compared to the traditional approach. In the case when the amines are separated by a distance of at least a trityl group, the PBA probe molecules are now relatively far away, which prevents formation of as much excimer as was observed in the benzyl-deprotected or traditional grafted aminosilicas. This can be seen when looking at the ratios of excimer (at 475 nm for traditional and 450 nm for benzyl- and trityl-deprotected) to monomer fluorescence (at 375 nm). As the amine groups are separated from closely packed (traditional) to benzyl- and trityl-deprotected aminosilicas, the ratios (I_{exc}/I_{375}) decrease from 110.4 to 1.64 and 0.34, respectively. The ratios for all samples are listed in Table 3.1.

3.3.4 Fluorescent Lifetime Analysis

Steady-state fluorescence gives much information about the separation of probe molecules by tracking the formation of excimers. However, it is also useful to understand more about how the separation of the pyrene molecules attached to the aminosilica surface affects the lifetime of the fluorophore. Shown in Figure 3.10 is the monomer decay of PCA on the various aminosilicas excited at 336 nm and monitored at 377 nm. For lifetime analyses, the data were fit using the sum of two exponentials with a third exponential component included to fit the scattered light from the instrument (Equation 1).[47] When a three exponential equation was used, the third component had a lifetime value in picoseconds. However, if solely a two exponential fit was used, a χ^2

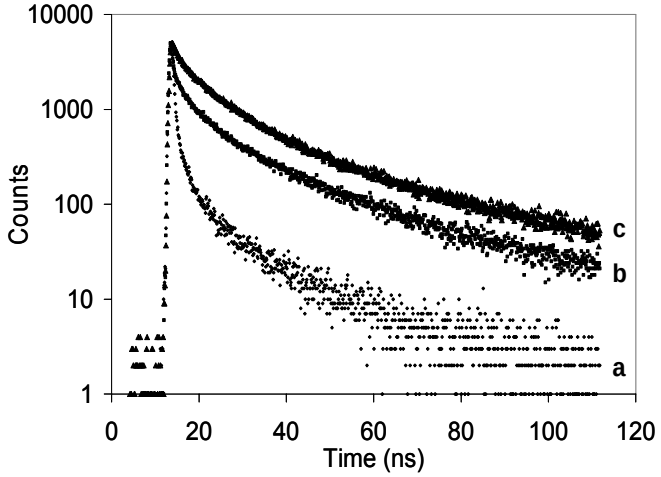

Figure 3.10. Lifetime decay curves of PCA loaded on traditional grafted **1a** (a), benzyl-deprotected **2a** (b) and trityl-deprotected **3a** (c) aminosilicas excited at 336 nm and monitored at 377 nm.

value greater than 3.0 was found. To best fit the data and use only a two exponential fit, Equation 1 was used where τ_0 was set to 0.056 ns (Equation 2). This fixes the scattered light component and allows for the other two lifetime parameters to be determined (τ_1 and τ_2).

$$I = A + A_0 \exp(-\frac{t}{\tau_0}) + A_1 \exp(-\frac{t}{\tau_1}) + A_2 \exp(-\frac{t}{\tau_2}) \quad (1)$$

$$\text{where } \tau_0 = 0.056 \ ns \quad (2)$$

When looking at the decay of the PCA in Figure 3.10, two components are seen: a short lived component and a longer lived component that is more distinct for materials **2a** and **3a**. If the traditional aminosilica was used, the resulting longer lived lifetime of the PCA monomer on the surface is calculated to be 14.8 ± 0.31 ns (**1a**, Table 3.2). However, if the benzyl- or trityl-deprotected aminosilicas were analyzed, the lifetimes of

the longer lived PCA monomer component increase to 27.7 ± 0.22 ns (**2a**) and 32.3 ± 0.22 ns (**3a**) respectively. Considering the longer lived component, the lifetime

Table 3.2. Comparing the lifetimes of PCA and PBA on various aminosilicas excited at 336nm and monitored at 377 nm (PCA) and 375 nm (PBA).

sample	fluorophore	lifetime, τ_1	lifetime, τ_2	χ^2
1a	PCA	2.0 ± 0.08 ns	14.8 ± 0.31 ns	1.25
1b	PBA	3.0 ± 0.12 ns	24.2 ± 0.58 ns	1.20
2a	PCA	5.5 ± 0.10 ns	27.7 ± 0.22 ns	1.52
2b	PBA	8.3 ± 0.24 ns	54.8 ± 0.24 ns	1.50
3a	PCA	7.3 ± 0.10 ns	32.3 ± 0.22 ns	1.65
3b	PBA	8.6 ± 0.29 ns	114.0 ± 0.80 ns	1.29

difference of PCA between the benzyl- and trityl-deprotected aminosilica is roughly 4.6 ns. Thus, the PCA molecules on the surface of either of these materials seem to be very similar. In contrast, when viewing PCA on the traditional aminosilica, the lifetime is reduced by ~13 – 17 ns. This indicates that the fluorophores in **1a** are close enough to interact and shorten the lifetime of the monomers by static quenching (excimer formation).

When the lifetimes of PBA are determined on these materials, much larger differences are observed. For instance, on the trityl-deprotected aminosilica, the lifetime of the longer lived PBA molecule is 114.0 ± 0.80 ns (**3b**, Table 3.2). This lifetime is over four times that of the PBA molecule on traditional aminosilica (**1b**, Table 3.2). This is expected as there is virtually no monomer seen in the steady-state spectrum of the PBA

loaded traditional aminosilica (Figure 3.11), allowing the excimer formation to drastically quench the monomer lifetime. The decay curves of the PBA fluorophore also show two components: a short lived component followed by a longer lived component in the "tail" of the spectrum. It is interesting to compare the "tail" of the benzyl- and trityl-deprotected aminosilicas, as it seems the benzyl-spaced amine groups produce a longer lived PBA molecule early in the decay. However, the amines spaced a distance of the trityl group produce PBA molecules that decay almost in a flatline manner. The fluorescent probes on the trityl-deprotected material are in essence spaced far enough to more than double the lifetime of the PBA probes (**3b**, Table 3.2) compared to the benzyl-spaced PBA probes (**2b**, Table 3.2).

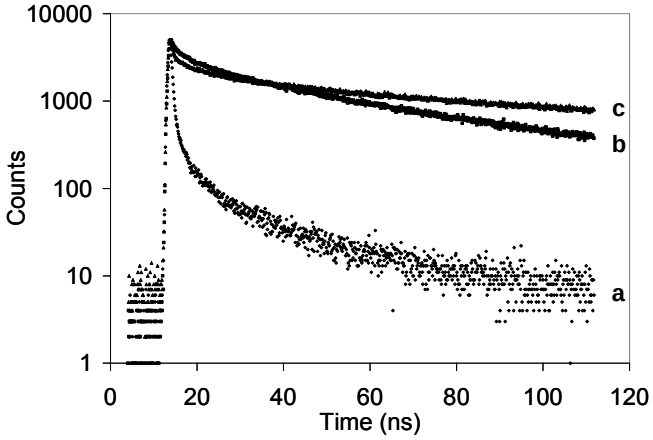

Figure 3.11. Lifetime decay curves of PBA loaded on traditional grafted **1b** (a), benzyl-deprotected **2b** (b) and trityl-deprotected **3b** (c) aminosilicas excited at 336 nm and monitored at 375 nm.

3.3.5 Changing the Amine Loading in Traditional Grafting

In the above materials, both excimer formation and lifetime track well with amine loading. This suggests the question, is total amine loading the only factor that influences fluorescence properties and hence amine density? To address this issue and to understand how "clustering" of amines in solution affects the proximity of these groups on silica, several samples were made by reducing the concentration of APTMS in toluene to obtain a specific loading on the silica, assuming all the silane was grafted onto the silica surface (materials **1c-1f**). This could be an alternative approach to producing isolated sites on a silica surface without the need for amine protection. In this approach, to obtain an amine loading on the SBA-15 of 0.72 mmol/g SiO_2, approximately 0.73 mmol of APTMS in 20 mL of toluene was mixed with 1 gram of SBA-15 (**1e** or **1f**). The same procedure was used to immobilize 1.26 mmol of APTMS on 1 gram of SBA-15 (**1c** or **1d**). These materials were compared to the material prepared by grafting in the presence of a 3.5 fold excess of 3-aminopropyltrimethoxysilane in solution, our standard or traditional grafting approach (materials **1a** and **1b**, amine loading = 1.64 mmol/g SiO_2). Under the standard conditions the excess silane should cause significant opportunities for amine-amine interactions in solution via "clustering" and these solution-assembled silane clusters may then be transferred onto the surface in "packs" of aminopropyl groups. This clustering might be reduced by both amine protection and reduction in solution amine loading. All the new materials were loaded with PCA or PBA and the fluorescence spectra were obtained.

For the PCA materials (Figure 3.12), it is obvious that as the amine loading is decreased, the excimer/monomer ratio decreases as well, indicating much more excimer

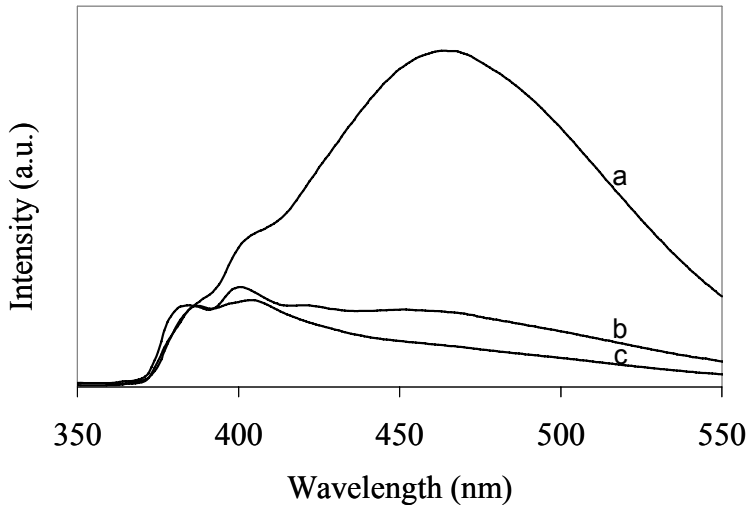

Figure 3.12. Steady-state fluorescence spectra of PCA loaded on traditional grafted aminosilicas with various amine loadings: 1.64 mmol/g SiO_2 **1a** (a), 1.26 mmol/ g SiO_2 **1c** (b) and 0.72 mmol/g SiO_2 **1e** (c) aminosilicas excited at 330 nm.

at larger amine loadings. This trend was the same as was observed using the protected synthesis. However, when reducing the amine loading in the unprotected synthesis, it was observed that the degree of excimer formation decreases less rapidly with loading than in the case of materials made via the protected synthesis. Figure 3.13a illustrates the change in the ratio I_{exc}/I_{mon} as the loading is decreased using either a protected or unprotected synthesis. From this data, it is clear that a protected synthesis results in more evenly spaced amines for a given loading, and amine "packs" on the surface have been limited. Similarly, Figure 3.13b illustrates how the lifetimes change as the amine loading is decreased using both the protected and unprotected synthesis. Again, it is clear that the two synthetic methods produce materials with different amine spacings at a given total amine loading. An interesting comparison that illustrates this point is between the 0.72

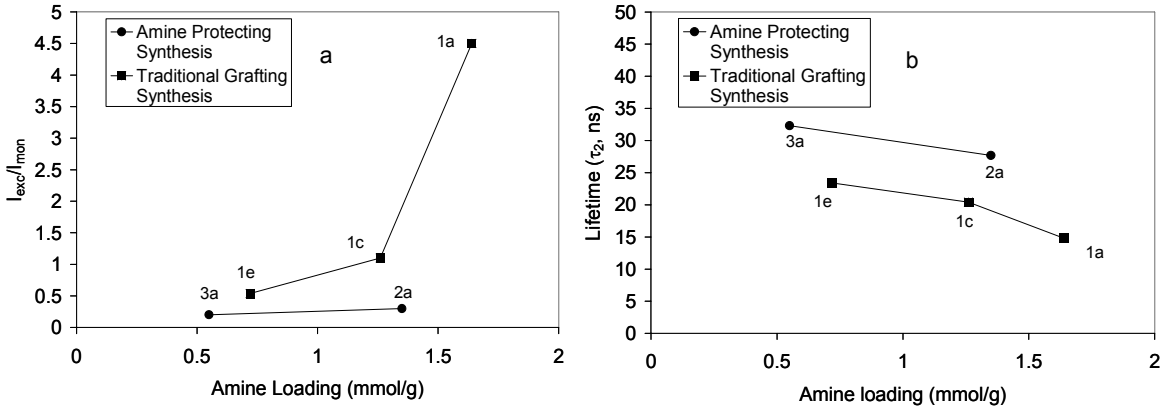

Figure 3.13. Tracking the intensity of excimer to monomer, I_{exc}/I_{mon}, of PCA (a) and the lifetime, τ_2, of PCA (b) as a function of amine loading for the protection/deprotection aminosilica synthesis versus the traditional grafting synthesis.

mmol/g SiO_2 traditional aminosilica (**1e**, Figure 3.7) loaded with PCA and benzyl-deprotected aminosilica (1.35 mmol/g SiO_2) loaded with PCA (**2a**, Figure 3.3). The ratios of the excimer to monomer (I_{exc}/I_{mon}) for these materials are 0.54 for **1e** and 0.30 for **2a**, indicating that the benzyl-deprotected aminosilica **2a** has roughly one-half the excimer present compared to the unprotected material **1e**, despite the fact that protected material has a 75% greater amine loading. These data strongly suggest that the protected synthesis produces a significantly different material from the diluted, unprotected synthesis. Hence, to prepare isolated amines, it is better to protect the amine groups before immobilization than to attempt amine separation by reducing the amine loading by dilution.

Similar results are seen when PBA was used as the fluorescent probe molecule. As the amine loading was decreased, the excimer/monomer ratio also decreased (Figure 3.14). When using the PBA probe, the amount of excimer relative to the monomer peak

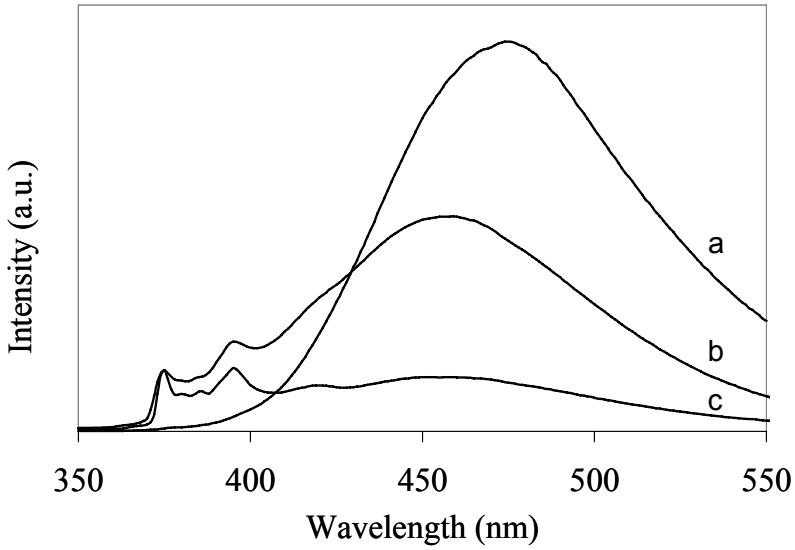

Figure 3.14. Steady-state fluorescence spectra of PBA loaded on traditional grafted aminosilicas with various amine loadings: 1.64 mmol/g SiO_2 **1b** (a), 1.26 mmol/ g SiO_2 **1d** (b) and 0.72 mmol/g SiO_2 **1f** (c) aminosilicas excited at 330 nm.

was greater than that of the PCA. This was expected since the PBA probe has a longer linker to the amine, more excimer should be seen since each probe can interact with another probe that is spaced further away.

The lifetimes of these materials are shown in Table 3.3. The results indicate that not only have the aminosilicas produced less excimer when the loading of the amines on the surface is decreased, but the lifetimes of the PCA and PBA monomers are much longer. Therefore, amine density can be reduced to some degree by limiting the concentration of amine sites in solution during the grafting process. However, due to a finite amount of amine clustering that occurs either in solution before grafting or on the

Table 3.3. Comparing the lifetimes of PCA and PBA on traditionally grafted aminosilicas excited at 336nm and monitored at 377 nm (PCA) and 375 nm (PBA).

sample	fluorophore	lifetime, τ_1	lifetime, τ_2	χ
1a	PCA	2.0 ± 0.08 ns	14.8 ± 0.31 ns	1.25
1b	PBA	3.0 ± 0.12 ns	24.2 ± 0.58 ns	1.20
1c	PCA	5.5 ± 0.23 ns	20.4 ± 0.39 ns	1.63
1d	PBA	7.3 ± 0.52 ns	28.7 ± 0.40 ns	2.58
1e	PCA	6.3 ± 0.01 ns	23.4 ± 0.01 ns	1.63
1f	PBA	7.8 ± 0.05 ns	98.5 ± 0.32 ns	1.56

surface during the grafting process, the local amine density on the surface is higher at a given overall amine loading when the unprotected grafting approach is used. Thus, this study confirms that amine clustering occurs during the unprotected grafting process. Bass and Katz have also shown that clustering can occur during protected grafting methodologies when using relatively small protecting groups.[48] The data presented here support this finding and show that the use of sterics to control surface site density can be an effective means to control final amine density on the surface, with bulky trityl groups allowing for the synthesis of the most isolated amine sites of the materials studied here.

3.4 Conclusions

Recently, we developed a simple methodology for synthesizing aminopropyl-modified silica materials with control over amine spacing.[1, 2] Using a protection/deprotection strategy with different sized protecting or "spacing" groups, we created materials with different amine loadings. Probe reaction and spectroscopic tests indicated that these new aminosilica materials were functionally different from traditional aminosilica materials with high amine loadings prepared via grafting. Our hypothesis

was that the density of amine sites was controlled by two factors. First, we hypothesized that by preventing aminosilanes from hydrogen bonding or "clustering" in solution, we could prevent these pre-grafting amine "clusters" from being transformed into clustered surface species. Thus, we used iminosilanes that could not cluster by hydrogen bonding in solution for grafting. Second, we believed we could use the steric spacing imparted by a bulky protecting group (such as a trityl group) when such species were used as spacers to position the amines on the surface a minimum distance apart. In this work, we probed the average amine-amine surface spacing of a variety of aminosilica materials and used the results to reassess our original amine-spacing hypothesis.

This study addressed the separation of amine groups functionalized on SBA-15 by reacting either PCA or PBA as fluorescent probes to the aminopropylsilyl modified silica. The data indicate the local surface amine spacing, on a length scale of 1 nm or less, can be manipulated easily by using a protected synthesis route. The combined evidence suggests that local amine-amine distance on the surface is larger on materials prepared by a protected synthesis route than materials with a similar overall amine loading prepared by an unprotected, traditional synthesis. The data suggest that both (i) prevention of amine clustering in solution or during the surface grafting process and (ii) steric spacing of amines on the surface based on the size of the protecting group influence the excellent average site isolation on functionalized 3-aminopropylsilyl silica surfaces prepared via the protection/deprotection route studied here.

3.5 References

1. McKittrick, M. W.; Jones, C. W., *Chem. Mater.* **2003,** 15, 1132.

2. Hicks, J. C.; Jones, C. W., *Langmuir* **2006,** 22, 2676.

3. Bass, J. D.; Anderson, S. L.; Katz, A., *Angew. Chem. Int. Ed.* **2003,** 42, 5219.

4. Bass, J. D.; Katz, A., *Chem. Mater.* **2003,** 15, 2757.

5. Bass, J. D.; Solovyov, A.; Pascall, A. J.; Katz, A., *J. Am. Chem. Soc.* **2006,** 128, 3737.

6. Poovarodom, S.; Bass, J. D.; Hwang, S.-J.; Katz, A., *Langmuir* **2005,** 21, 12348.

7. Wulff, G., *Chem. Rev.* **2002,** 102, 1.

8. Defreese, J. L.; Hwang, S.-J.; Parra-Vasquez, A. N. G.; Katz, A., *J. Am. Chem. Soc.* **2006,** 128, 5687.

9. Katz, A.; Davis, M. E., *Nature* **2000,** 403, 286.

10. White, L. D.; Tripp, C. P., *J. Colloid Interface Sci.* **2000,** 227, 237.

11. Kanan, S. M.; Tze, W. T. Y.; Tripp, C. P., *Langmuir* **2002,** 18, 6623.

12. Pangborn, A. B.; Giardello, M. A.; Grubbs, R. H.; Rosen, R. K.; Timmers, F. J., *Organometallics* **1996,** 15, 1518.

13. Zhao, D.; Huo, Q.; Feng, J.; Chmelka, B. F.; Stucky, G. D., *J. Am. Chem. Soc.* **1998,** 120, 6024.

14. Ek, S.; Root, A.; Peussa, M.; Niinisto, L., *Thermochim. Acta* **2001,** 379, 201.

15. Trebosc, J.; Wiench, J. W.; Huh, S.; Lin, V. S.-Y.; Pruski, M., *J. Am. Chem. Soc.* **2005,** 127, 3057.

16. Grunberg, B.; Emmler, T.; Gedat, E.; Shenderovich, I.; Findenegg, G. H.; Limbach, H.-H.; Buntkowsky, G., *Chem. Eur. J.* **2004,** 10, 5689.

17. Cha, J. S.; Chun, J. H.; Kim, J. M.; Kwon, O. O.; Kwon, S. Y.; Lee, J. C., *Bull. Korean Chem. Soc.* **1999,** 20, 400.

18. In our previous report on the synthesis of benzyl-deprotected aminosilicas,[2] we found that roughly 30 - 50% of the amine sites could not be titrated after the deprotection step unless an NH_3(aq) wash was performed. We, thus, reacted PCA with the aminosilicas after an NH_3(aq) wash to determine if the surface protonated amines affected the resulting steady-state fluorescence data. However, we did not see a significant difference in the fluorescence data with the base washed materials.

19. Bauer, R. K.; Borenstein, R.; De Mayo, P.; Okada, K.; Rafalska, M.; Ware, W. R.; Wu, K. C., *J. Am. Chem. Soc.* **1982,** 104, 4635.

20. Bauer, R. K.; De Mayo, P.; Natarajan, L. V.; Ware, W. R., *Can. J. Chem.* **1984,** 62, 1279.

21. Bauer, R. K.; De Mayo, P.; Okada, K.; Ware, W. R.; Wu, K. C., *J. Phys. Chem.* **1983,** 87, 460.

22. Bauer, R. K.; De Mayo, P.; Ware, W. R.; Wu, K. C., *J. Phys. Chem.* **1982,** 86, 3781.

23. Barbas, J. T.; Dabestani, R.; Sigman, M. E., *J. Photochem. Photobiol. A: Chem.* **1994,** 80, 103.

24. Barbas, J. T.; Sigman, M. E.; Arce, R.; Dabestani, R., *J. Photochem. Photobiol. A: Chem.* **1997,** 109, 229.

25. Barbas, J. T.; Sigman, M. E.; Dabestani, R., *Environ. Sci. Technol.* **1996,** 30, 1776.

26. Dabestani, R.; Ellis, K. J.; Sigman, M. E., *J. Photochem. Photobiol. A: Chem.* **1995,** 86, 231.

27. Dabestani, R.; Higgin, J.; Stephenson, D. M.; Ivanov, I. N.; Sigman, M. E., *J. Phys. Chem. B* **2000,** 104, 10235.

28. Dabestani, R.; Nelson, M.; Sigman, M. E., *Photochem. Photobiol.* **1996,** 64, 80.

29. Ivanov, I. N.; Dabestani, R.; Buchanan, A. C.; Sigman, M. E., *J. Phys. Chem. B* **2001,** 105, 10308.

30. Sigman, M. E.; Barbas, J. T.; Chevis, E. A.; Dabestani, R., *New J. Chem.* **1996,** 20, 243.

31. Dewar, P. J.; MacGillivray, T. F.; Crispo, S. M.; Smith-Palmer, T., *J. Colloid Interface Sci.* **2000,** 228, 253.

32. Lochmuller, C. H.; Colborn, A. S.; Hunnicutt, M. L.; Harris, J. M., *J. Am. Chem. Soc.* **1984,** 106, 4077.

33. Metivier, R.; Leray, I.; Lefevre, J.-P.; Roy-Auberger, M.; Zanier-Szydlowski, N.; Valeur, B., *Phys. Chem. Chem. Phys.* **2003,** 5, 758.

34. Metivier, R.; Leray, I.; Roy-Auberger, M.; Zanier-Szydlowski, N.; Valeur, B., *New J. Chem.* **2002,** 26, 411.

35. Pankasem, S.; Thomas, J. K., *J. Phys. Chem.* **1991,** 95, 7385.

36. Thomas, J. K., *Chem. Rev.* **2005,** 105, 1683, and references therein.

37. Winnik, F. M., *Chem. Rev.* **1993,** 93, 587, and references therein.

38. Thomas, A.; Polarz, S.; Antonietti, M., *J. Phys. Chem. B* **2003,** 107, 5081.

39. Wang, H.; Harris, J. M., *J. Am. Chem. Soc.* **1994,** 116, 5754.

40. Galarneau, A.; Cambon, H.; Renzo, F. D.; Fajula, F., *Langmuir* **2001,** 17, 8328.

41. Kruk, M.; Jaroniec, M., *Chem. Mater.* **2000,** 2, 1961.

42. Kruk, M.; Jaroniec, M.; Kim, T.-W.; Ryoo, R., *Chem. Mater.* **2003,** 15, 2815.

43. Miyazawa, K.; Inagaki, S., *Chem. Commun.* **2000**, 2121.

44. Winnik, F. M., *Chem. Rev.* **1993,** 93, 587, and references within.

45. Milosavljevic, B. H.; Thomas, J. K., *J. Phys. Chem.* **1988,** 92, 2997.

46. Kalyanasundaram, K.; Thomas, A., *J. Am. Chem. Soc.* **1977,** 99, 2039.

47. *HORIBA Jobin Yvon IBH DAS6 Fluorescence Decay Analysis Software User Guide*.

48. Bass, J. D.; Katz, A., *Chem. Mater.* **2006,** 18, 1611.

CHAPTER 4

ASSESSING SITE-ISOLATION OF AMINE GROUPS ON AMINOPROPYL-FUNCTIONALIZED SBA-15 MATERIALS VIA SPECTROSCOPIC AND REACTIVITY PROBES

4.1 Introduction

As previously discussed, many site-isolation protection/deprotection methods have been reported.[1-10] Various other methods to produce grafted, site-isolated organosilane functionalized materials have been reported.[11-14] In general, these methods involve the use of dilute mixtures of the target silane with a 'spacer' silane, and we term this approach 'cooperative dilution' in this report. For example, methods using mixtures of organoalkoxysilanes with various lengths of the alkoxy group have been reported as ways to isolate the longer chains from each other, while replacing surface Si-OH groups with the shorter silanes between the isolated species.[11, 12] More recently a method posited to produce site-isolated aminosilicas was reported whereby a mixture of methyltrimethoxysilane (MTMS) in large excess with a very dilute amount of 3-aminopropyltrimethoxysilane (APTMS) was used to synthesize new aminosilica materials (Figure 4.1). It was suggested based on FT-IR spectroscopic results that the materials synthesized with a ratio of less than 1:20 (APTMS:MTMS) had amine sites separated by a sufficient distance to prevent the H-bonding between adjacent amines

(NH_2 and NH_3^+ species). These entities were assigned to the 3000 and 2000 cm^{-1} region in the IR spectrum. Although this method was suggested to produces materials with a similar degree of amine isolation as protection/deprotection methods, no direct comparison was made between the two sets of materials.

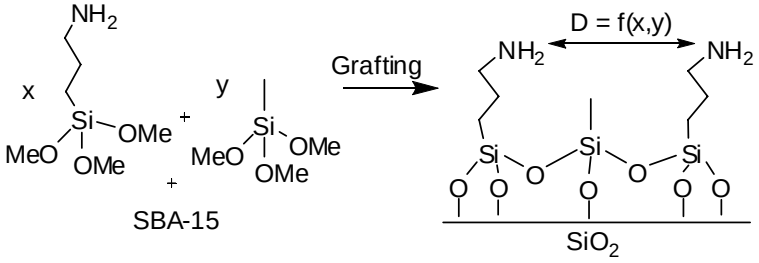

Figure 4.1. Synthesis of spaced amines via cooperative dilution.

To address this matter, this report focuses on a direct comparison of three types of aminopropylsilyl-functionalized SBA-15 silica materials: (1) control materials made via the traditional grafting of 3-aminopropyltrimethoxysilane in toluene, (2) materials made by a protection/deprotection method using benzyl- or trityl-spacers,[4, 9, 10] and (3) materials made via a cooperative dilution method where 3-aminopropyltrimethoxysilane and methyltrimethoxysilane are co-grafted on the silica surface as a silane mixture.[13] The site-isolation and accessibility of the amine groups are probed via three different methods – fluorescence spectroscopy, a stoichiometric chemical reaction, and a catalytic chemical reaction. In the first test, a fraction of each material is contacted with pyrene compounds, and the average pyrene-pyrene distances are probed via fluorescence spectroscopy. Using another fraction of each material, the reactivity and accessibility of the amines are probed via reaction with chlorodimethyl(2,3,4,5-tetramethyl-2,4-cyclopentadien-1-yl)silane ($Cp'Si(Me)_2Cl$) and chloro(cyclopenta-2,4-dienyl)dimethylsilane ($CpSi(Me)_2Cl$). Yields

in these reactions are indicative of amine accessibility. Finally, these Cp-silane functionalized solids are then metallated with tetrakis(dimethylamino)zirconium to create constrained-geometry-inspired precatalysts (CGCs). These supported organometallic complexes are then used in the catalytic polymerization of ethylene, with overall polymer yields related to site-accessibility and site-isolation. [4, 15-19]

4.2 Experimental Section

Materials. The following chemicals were commercially available and used as received: 3-aminopropyltrimethoxy silane (APTMS, Aldrich), 2,6-di-tertbutylpyridine (Acros), methyltrimethoxysilane (MTMS, Aldrich), tetrakis (dimethylamino)zirconium (Aldrich), dichlorodimethylsilane (Acros), tetraethyl orthosilicate (TEOS, Aldrich), 1,1,1,3,3,3-hexamethyldisilazane (HMDS, Aldrich), trimethylaluminum (TMA, Aldrich), triisobutylaluminum (TIBA, Aldrich), and 1-pyrenecarboxylic acid (Aldrich). Anhydrous toluene and anhydrous hexanes were treated by a packed bed solvent purification system utilizing columns of copper oxide and alumina.[20] The anhydrous toluene was further dried with Na/benzophenone and subsequently distilled. Cyclopentadiene (Cp, Aldrich) and tetramethylcyclopentadiene (Cp', Aldrich) were distilled before use. Chlorodimethyl(2,3,4,5-tetramethyl-2,4-cyclopentadien-1-yl)silane (Cp'Si(Me)$_2$Cl) and chloro(cyclopenta-2,4-dienyl)dimethylsilane (CpSi(Me)$_2$Cl) were synthesized according to previous reports using a lithium salt.[17, 21, 22] Tris(pentafluorophenyl)borane (B(Ar)$_F$, Aldrich) was purified by sublimation. All compounds were transferred using standard vacuum line, Schlenk, or cannula techniques under dry, deoxygenated argon or in a drybox under a deoxygenated nitrogen atmosphere

in order to reduce/prevent amine-CO_2 interactions. SBA-15 was synthesized similar to previously reported methods.[10, 23] Prior to use, the SBA-15 was dried under vacuum at 200 ºC for 3 h to remove physisorbed water and was stored in a nitrogen drybox.

Synthesis of Traditional Aminosilica, SBA-NH2-DF. The traditional aminosilica was synthesized using a method analogous to our previous reports.[4, 9, 10] The organic loading by thermogravimetric analysis (TGA) was found to be 1.41 mmol NH_2/g. The material was then capped with 1,1,1,3,3,3-hexamethyldisilazane (HMDS) using previously reported methods.[4, 9, 10] This approach is termed "traditional," resulting in densely-functionalized (DF) aminosilicas.

Synthesis of Patterned Benzyl Spaced Aminosilica, SBA-NH2-BI. The benzyl spaced aminosilica was synthesized in a manner analogous to our previous reports.[4, 9, 10] The organic loading by TGA was found to be 1.15 mmol NH_2/g.

Synthesis of Patterned Trityl Spaced Aminosilica, SBA-NH2-TI. The trityl spaced aminosilica was synthesized in a manner analogous to our previous reports. [2, 4, 10] The organic loading by TGA was found to be 0.53 mmol NH_2/g.

Synthesis of Cooperative Dilution Aminosilicas, SBA-NH2-CD1, SBA-NH2-CD2, SBA-NH2-CD3. These aminosilica materials were synthesized according to the reported procedures by M. Luechinger et al.[13] First, ~ 1 gram of SBA-15 was refluxed in 25 mL of water for 1 hour. Afterwards, the material was filtered and washed with 20 mL of anhydrous toluene. The "wet" material was suspended in 100 mL of anhydrous toluene and the "free" water was removed via azeotropic distillation. Then, amounts of methyltrimethoxysilane (MTMS) and 3-aminopropyltrimethoxysilane (APTMS) were added in different ratios. For instance, the materials were made with ratios of

APTMS:MTMS (while keeping the total amount of reactive silane at 19 mmol/g silica) of 1:5 (SBA-NH2-CD1), 1:15 (SBA-NH2-CD2) and 1:50 (SBA-NH2-CD3). First, the MTMS was added, followed by the APTMS. The mixture was stirred for 14 hours at room temperature, filtered, and then refluxed in 100 mL of fresh solvent for an hour. Elemental analysis showed loadings of 2.0 mmol NH_2/g (SBA-NH2-CD1), 0.86 mmol NH_2/g (SBA-NH2-CD2), and 0.33 mmol NH_2/g (SBA-NH2-CD3). The materials were then capped with HMDS to remove any additional surface silanols using previously reported methods.[4, 9, 10]

Materials for Pyrene Fluorescence Studies. Approximately 300 mg of aminosilica was dispersed in 25 mL of toluene and mixed with a three fold excess of 1-pyrenecarboxylic acid (PCA). The resulting mixture was refluxed overnight. After reaction, the unreacted PCA was washed away by filtration and rinsed with multiple toluene and THF washes. The PCA loading on the 1:5, 1:15 and 1:50 materials (SBA-NH2-CD1, SBA-NH2-CD2, SBA-NH2-CD3) was 0.35 mmol/g, 0.18 mmol/g, 0.13 mmol/g, respectively.

Reactivity Studies of the Aminosilicas with Cp'Si(Me)$_2$Cl or CpSi(Me)$_2$Cl. To any of the synthesized aminosilicas dispersed in hexanes, either Cp'Si(Me)$_2$Cl or CpSi(Me)$_2$Cl was added (in excess to amine loading) with 2,6-di-tertbutylpyridine as a proton sponge. After 24 hours of stirring in a N_2 environment at room temperature, the material was filtered and washed with hexanes. The procedure was repeated one additional time. After the second reaction and workup of the material, the Cp'Si- and CpSi-modified aminosilica was dried at 60 ^oC overnight at a pressure of 10 mTorr.

Synthesis of Tethered Constrained Geometry Catalysts (ZrCGC). A three fold excess of tetrakis(dimethylamino)zirconium (compared to amine loading) was added in

anhydrous toluene. The reaction vessel was heated to reflux for 24 hours. The resulting solid was filtered and washed in the N_2 drybox. The ligand exchange from dimethylamine to chloride ligands was accomplished by stirring Me_2SiCl_2 with the immobilized metallated CGCs overnight in toluene. The mixture was then filtered and washed in a N_2 drybox.

Material Characterization. Organic loadings were obtained by thermogravimetric analysis (TGA) on a Netzsch STA409. The organic/inorganic hybrid materials were heated under a stream of nitrogen and a stream of air from 30 to 900 °C at 10 °C/min. The organic loading was determined from the weight loss from 200 to 700 °C. Steady-state fluorescence spectra were obtained on a Jobin Yvon Horiba FluoroMax-P spectrometer. Solid samples were degassed and flame-sealed under vacuum ($P \leq 1x10^{-6}$ Torr) to prevent oxygen quenching. Emission spectra were corrected for instrumental response using correction factors provided by the manufacturer. All emission spectra were collected by exciting the fluorophore loaded materials at 330 nm. An Ocean Optics USB2000 Fiber Optic Spectrometer was used to obtain the diffuse reflectance UV–Vis spectra for the solid materials. The UV-Vis spectrometer was used in a N_2 drybox. PTFE was used as the diffuse reflectance standard.

Polymerization Studies. The ZrCGC materials were mixed with a solution of 10 mL of toluene, trimethylaluminum (TMA) or triisobutylaluminum (TIBA) (400:1 Al:Zr), and tris(pentafluorophenyl)borane (1.5:1 B:Zr) in a N_2 drybox. The resulting mixture was stirred for 30 minutes. Ethylene (Polymer Purity, 99.9%) was further purified through an in-line oxygen and water purifier (Matheson Oxygen Absorbing Purifier Model 6410 with cartridge 641-01). The ethylene was added to the reactor at 60 psig for 10 minutes.

The polymerization was quenched by releasing the ethylene pressure, followed by addition of acidic ethanol to induce polymer precipitation. The polymer was filtered and stored in an oven at 60 ^{o}C until all solvent was removed.[24]

4.3 Results and Discussion

The materials presented in this report were synthesized using three different routes: (1) direct grafting of unprotected aminopropylalkoxysilanes with the silica surface (control material), (2) protection/deprotection of the amine via an imine[4, 9, 10], and (3) cooperative dilution of amines via grafting dilute quantities of unprotected aminopropylalkoxysilanes mixed with methylalkoxysilanes[13]. The materials are listed in Table 4.1, along with their amine loadings.

The protection/deprotection strategy is thought to achieve site-isolation by reducing the possibility of amine-amine interactions in solution and amine-silanol interactions on the surface.[25, 26] In addition, it allows for separation of the amine groups on the surface by changing the size of the protecting group (i.e. trityl- vs. benzyl spacers).[4, 9, 10] The cooperative dilution technique focuses on dilution of the 3-aminopropyltrimethoxysilane (APTMS) in solvent with large quantities of methyltrimethoxysilane (MTMS). The use of a slightly "wet" surface is suggested to be crucial, as the water acts as a catalyst for the reaction between the alkoxysilanes and the surface silanols.[11-13] Also, the amine can catalyze the reaction of the silanes to the silica surface by activating the silanols.[13, 25, 26] The traditional method was used to create a control material with a high loading of amine sites. The traditional aminosilica was

synthesized in a one-step reaction between the silica surface and APTMS in a nitrogen drybox using toluene as solvent.

The synthesis of "site-isolated" amines via the protection/deprotection method occurs in five steps.[27] Firstly, 3-aminopropyltrimethoxysilane is protected by addition of either 3,3,3-triphenylpropanal or benzaldehyde. Secondly, the protected alkoxysilane is mixed with silica to form the tethered organic/inorganic hybrid material. A capping step with 1,1,1,3,3,3-hexamethyldisilazane (HMDS) is performed afterwards in order to prevent amine-silanol interactions in later steps. The deprotection occurs by cleaving the imine with an acidic H_2O/MeOH solution. A final capping step with HMDS is performed after deprotection to cap any silanols produced during the deprotection step. The resulting materials ideally have amine groups separated on average by the size of the protecting group.[4, 9, 10] The organic loadings of the materials synthesized are listed in Table 4.1.

Table 4.1. Materials synthesized and organic loadings.

Material	Synthesis Method	Ratio of APTMS:MTMS	mmol NH_2/g
SBA-NH2-DF	Traditional	Pure APTMS	1.41[a]
SBA-NH2-BI	Benzyl Protected	------	1.15[a]
SBA-NH2-TI	Trityl Protected	------	0.53[a]
SBA-NH2-CD1	Cooperative Dilution	1:5	2.00[a,b]
SBA-NH2-CD2	Cooperative Dilution	1:15	0.86[a,b]
SBA-NH2-CD3	Cooperative Dilution	1:50	0.33[a,b]

[a] Determined by TGA

[b] Determined by Elemental Analysis

The cooperative dilution method first begins with producing as many silanols on the surface as possible. The silica is refluxed in H_2O for one hour and filtered. Secondly, toluene is added to the wet silica and an azeotropic distillation removes "free" water from the solution. After distillation, the resulting silica material is slightly wet, in order to increase the organic loading and catalyze the reaction of the alkoxysilane with the surface silanol. Next, the slightly "wet" silica is suspended in toluene and different ratios of APTMS:MTMS are added (Table 4.1). After 14 hours at 25 ^{o}C, the materials are filtered and fresh solvent is added and allowed to react for an additional hour at 110 ^{o}C. The solid aminosilica is then collected and dried of solvent.

Each of the syntheses was tracked using nitrogen physisorption (Table 4.2). The materials show a substantial loss in the BET surface area after reaction of the organoalkoxysilanes with the silica surface due to micropore filling or blocking. Also, the BJH pore diameter decreases after organoalkoxysilane grafting. Upon examination of the data, it is apparent that the materials synthesized by cooperative dilution produce a greater decrease in surface area and pore diameter than those synthesized by the protection/deprotection method. It is possible that the surface water catalyzes the reaction of the organoalkoxysilane to the surface while oligomerizing the organoalkoxysilanes within the mesopores whereby they grow off the surface.[25] Thus, this type of surface reaction appears to produce vertical chains of organosilanes extending outward in the pore space. However, aminosilicas prepared by protection/deprotection have porosity changes that are similar to the directly grafted traditional aminosilica control material. It is possible that the presence of water on the surface affects the grafting process enough to create multiple layers of methylsilyl- and aminopropylsilyl

groups on the surface. The lack of moisture present in the traditional and protection/deprotection approaches reduces the possibility of forming multiple layers, producing complete or patchy monolayers of the organic groups on the pore surface.[25]

The first of three methods used to assess amine isolation and accessibility was steady-state fluorescence of pyrene groups adsorbed onto the aminosilica materials.[10] Figure 4.2 shows the steady state fluorescence spectra of 1-pyrenecarboxylic acid (PCA) loaded onto the amines (using cooperative dilution). The results of the PCA study are very similar to the fluorescence results obtained by the protection/deprotection method.[10] Fluorescence spectroscopy was used because of its ability to determine the degree of separation between probe molecules on surfaces.[3, 9, 10, 28-45] The utility of fluorescence

Table 4.2. Nitrogen physisorption of materials synthesized.

Entry	Material	Surface Area (m^2/g)	Pore Diameter (Å)
1	SBA-NH2-DF	380	49
2	SBA-NH2-BI	440	55
3	SBA-NH2-TI	470	58
4	SBA-NH2-CD1	180	34
5	SBA-NH2-CD2	270	44
6	SBA-NH2-CD3	335	54
7	SBA-15	961	66

spectroscopy stems from different types of fluorescence of probe molecules that occur depending on their proximity to another probe molecule. For instance, when two pyrene molecules are in close proximity in the excited state ($3 \geq r \leq 10$ Å), the pyrene groups can transfer energy and stabilize the excited state, producing a broad structureless fluorescence pattern (excimer, ~ 470nm).[46] However, if the pyrene groups are separated far enough ($r \geq 10$ Å), the resulting fluorescence pattern becomes more structured

(multiple peaks associated to the specific pyrene molecule) and located at higher energies (monomer, ~ 377 nm).[46] In our previous report, we found that as the average distance between the amine groups is increased, the ratio of the excimer to monomer (I_{470}/I_{384}) decreases.[10] For instance, as previously reported, when the traditional, benzyl spaced, and trityl spaced aminosilicas are loaded with PCA, the I_{470}/I_{384} ratio decreases from 4.50 to 0.30 to 0.20, respectively (Figure 4.3).[10] This indicates that less excimer is present when the amines are forced apart from each other due to synthesis using a protecting group. The protecting groups separate the amines far enough apart that the pyrene groups cannot transfer energy to each other when excited, resulting in a reduced excimer emission (~ 470 nm) and an increased monomer emission (~ 377 nm). Both the benzyl spaced and trityl spaced aminosilicas loaded with PCA produced an order of magnitude

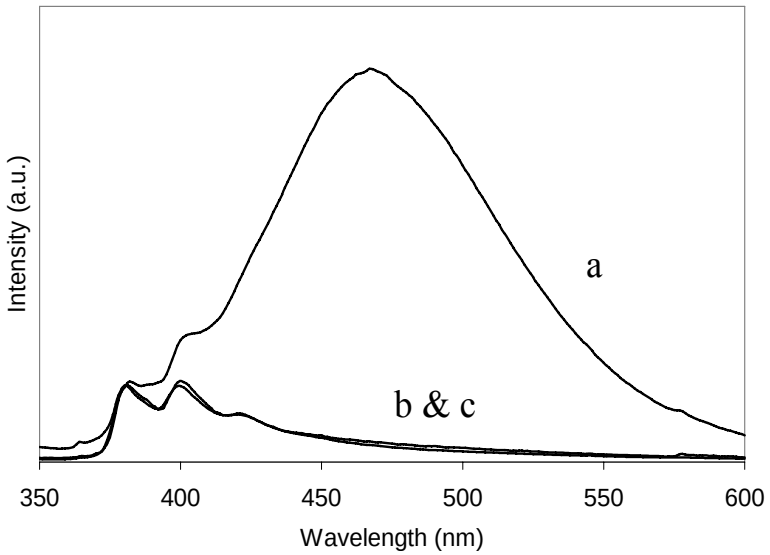

Figure 4.1. Fluorescence spectra of 1-pyrenecarboxylic acid loaded on SBA-NH2-CD1 (a), SBA-NH2-CD2 (b), and SBA-NH2-CD3 (c).

less excimer than PCA on traditional (dense) 3-aminopropyltrimethoxysilane grafted SBA-15. When fluorescence spectroscopy is applied to 1-pyrenecarboxylic acid reacted with the cooperative dilution aminosilicas, the results mimic that of the protection/deprotection method. For instance, when the APTMS:MTMS is changed from 1:5, 1:15, and 1:50, the I_{470}/I_{384} ratio decreases from 5.16 (Figure 4.2a) to 0.26 (Figure 4.2b) to 0.21 (Figure 4.2c), respectively. These results suggest that the cooperative dilution method is successful in separating the amine groups compared to using

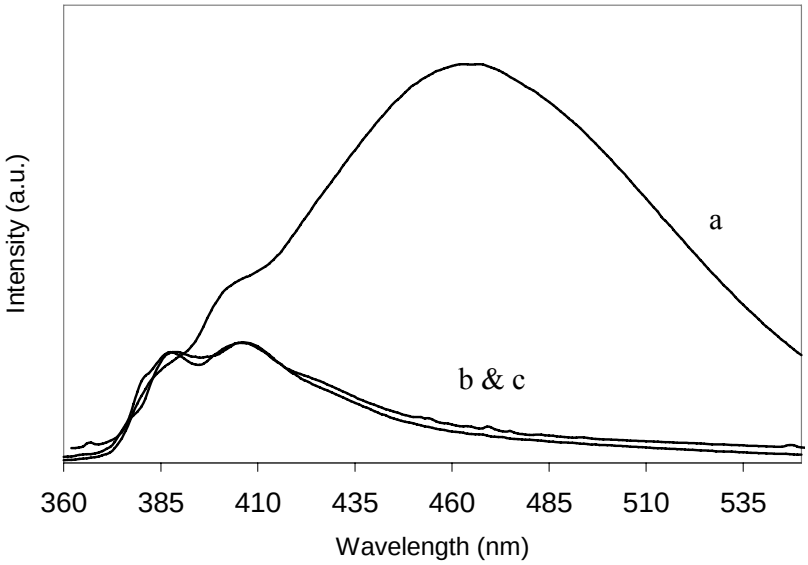

Figure 4.3. Fluorescence spectra of 1-pyrenecarboxylic acid loaded on SBA-NH2-DF (a), SBA-NH2-BI (b), and SBA-NH2-TI (c).[10]

unprotected, pure 3-aminopropyltrimethoxysilane. As stated above, PCA loaded on the cooperative dilution aminosilicas behaved similarly to the traditional, benzyl spaced and trityl spaced aminosilicas loaded with PCA. The fluorescence spectra appear to

corroborate the results obtained by FT-IR, which were previously interpreted to give evidence of similarity between cooperative dilution materials and protection/deprotection materials.[13]

However, there is a critical set of data that complicate this analysis. In all our previous work, we achieved PCA/N loadings of ~0.35. Indeed, for the traditional, benzyl spaced and trityl spaced aminosilicas, the PCA/N loading was 0.34, 0.37, and 0.34, respectively.[10] In contrast, in this study comparing the cooperative dilution aminosilicas, the pyrene/N loading was determined as 0.17, 0.21, and 0.38 for SBA-NH2-CD1, SBA-NH2-CD2, and SBA-NH2-CD3, respectively. The most critical comparison between the protection/deprotection and cooperative dilution methods is between SBA-NH2-TI and SBA-NH2-CD3, as these have the lowest amine loadings. In this case, PCA/N ratios are similar and I_{470}/I_{384} ratios are similar, suggesting that these materials have similar degrees of site isolation, as probed by this technique. However, the combination of drastically different porosity results and different degrees of amine reactivity with PCA suggested that something made the CD and TI materials quite different.

The second approach used to study the accessibility and isolation of the amines was via stoichiometric reaction probes. Either $CpSi(Me)_2Cl$ or $Cp'Si(Me)_2Cl$ was reacted with the aminosilicas to determine how many amines react with the chlorosilanes (Figure 4.4). These reactions were chosen because they have previously been reported as probe reactions for the determination of accessible surface amine sites and they produce precursors needed for the next reactions (vide infra).[4, 22, 47, 48] A proton sponge (2,6-di-isobutylpyridine) was added to scavenge the HCl produced from the reaction of the

chlorosilane and the amine groups. The loadings of the amines and degree of amine

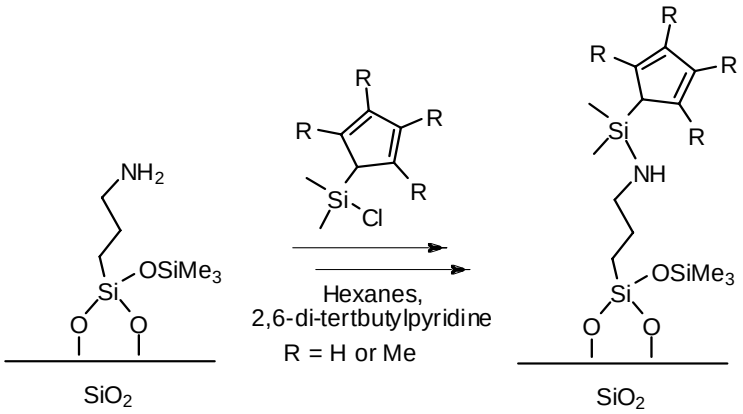

Figure 4.4. Reactivity studies with $Cp'Si(Me)_2Cl$ and $CpSi(Me)_2Cl$.

conversion by the chlorosilanes are shown in Table 4.3 and Table 4.4. It is apparent that the reactivity of the amines with the chlorosilanes is more favorable when the

Table 4.3. Reactivity studies using $CpSi(Me)_2Cl$.

Material	mmol NH_2/g	mmol CpSi/g[a]	% (mmol CpSi/ mmol NH_2)
SBA-NH2-DF	1.41	0.52	37%
SBA-NH2-BI	1.15	0.90	78%
SBA-NH2-TI	0.53	0.53	100%
SBA-NH2-CD1	2.00	0.60	30%
SBA-NH2-CD2	0.86	0.45	52%
SBA-NH2-CD3	0.33	0.17	52%

[a] Determined by TGA.

protection/deprotection method is used. After reaction of the $CpSi(Me)_2Cl$ with the trityl spaced aminosilica, quantitative conversion of the amine to the corresponding amidosilyl group was obtained (Table 4.3). However, the cooperative dilution methods converted only about 50% of the amines with $CpSi(Me)_2Cl$ (Table 4.3), which is similar to the

Table 4.4. Reactivity studies using $Cp'Si(Me)_2Cl$.

Material	mmol NH_2/g	mmol Cp'Si/g[a]	% (mmol Cp'Si/ mmol NH_2)
SBA-NH2-DF	1.41	0.41	29%
SBA-NH2-BI	1.15	0.73	63%
SBA-NH2-TI	0.53	0.41	77%
SBA-NH2-CD1	2.00	0.35	18%
SBA-NH2-CD2	0.86	0.35	41%
SBA-NH2-CD3	0.33	0.12	36%

[a] Determined by TGA.

loadings obtained from the traditional aminosilica (SBA-NH2-DF). The conversion of $Cp'Si(Me)_2Cl$ with the aminosilicas was slightly lower, but yielded a similar trend to the $CpSi(Me)_2Cl$ reactivity (Table 4.4). In these studies, the chlorosilanes reacted with approximately 76% of the trityl spaced amines (SBA-NH2-TI). Also, about 64% of the benzyl spaced amines were converted to the amidosilyl functional groups (SBA-NH2-BI). Again, the aminosilicas produced by the cooperative dilution method were less accessible for reaction with the $Cp'Si(Me_2)Cl$ groups (~40%). These materials reacted similarly to the traditional aminosilica (~30%, SBA-NH2-DF). As seen previously in the fluorescence spectra, the cooperative dilution method produced isolated aminosilica

materials based on analysis by that technique (SBA-NH2-CD2 and SBA-NH2-CD3). However, in both reactivity of PCA and reactivity of either $CpSi(Me)_2Cl$ or $Cp'Si(Me)_2Cl$, the cooperative dilution aminosilicas behaved very similarly to the traditional, unprotected 3-aminopropylsilyl-grafted aminosilica (SBA-NH2-DF). This result strongly suggests that a mixed dilution of silanes may separate amines randomly across the surface, but the resulting amine functionalities have limited reactivity/accessibility. This may be due to the pore-filling grafting methodology utilized in this synthesis technique.

After the aminosilicas were reacted with the Cp'SiMeCl groups, tetrakis(dimethylamino)zirconium was added to form a tethered constrained-geometry-inspired precatalyst (Figure 4.5). Subsequently, Me_2SiCl_2 was added to exchange the dimethylamine ligands with the more stable chloride ligands. Figure 4.6 shows the UV-Vis spectra of the materials after metallation and ligand exchange for the each of the

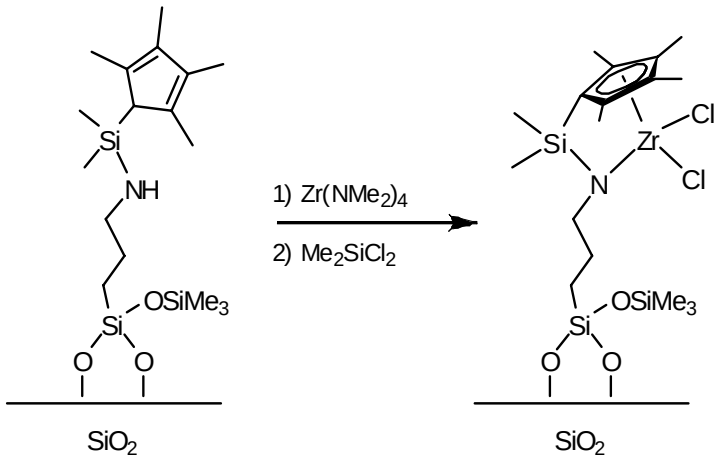

Figure 4.5. Formation of ZrCGCs using surface amines.

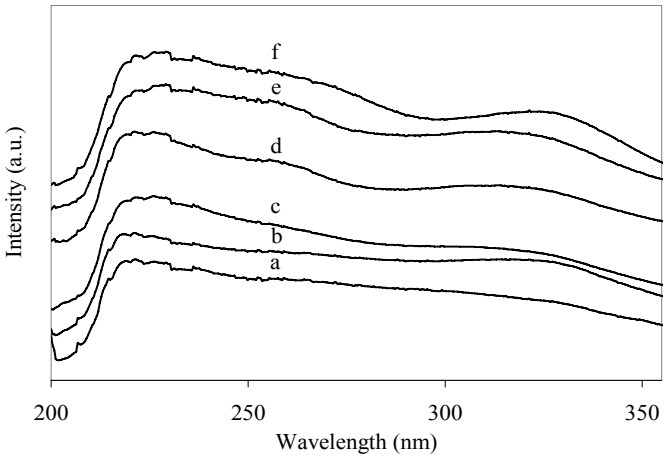

Figure 4.6. Diffuse reflectance UV-Vis spectra of the ZrCGCs on the various aminosilicas: a) SBA-NH2-CD1, b) SBA-NH2-CD2, c) SBA-NH2-CD3, d) SBA-NH2-TI, e) SBA-NH2-BI, f) SBA-NH2-DF.

zirconium-treated aminosilica materials. In each spectrum, the ligand to metal charge transfer between the Cp' ring and the Zr metal center is seen at ~320 nm. This indicates that the formation of a surface bound constrained-geometry catalyst is likely for each material.[16] In all cases, materials with a higher amount of Cp'Si(Me)$_2$ groups resulted in higher amounts of zirconium loading, due to the favorable interaction between Zr and Cp' ligands.

The polymerization of ethylene was studied for each of these materials to determine if the isolation techniques increased the catalyst productivity. We have shown in the past that when the amine sites are spaced from each other using a protection/deprotection method, a more active olefin polymerization catalyst is produced.[15-19] The polymerization of ethylene was studied at room temperature with 60 psig of ethylene pressure. Each ZrCGC material was activated by either TMA/B(Ar)$_F$ or TIBA/B(Ar)$_F$ in a N_2 drybox. After 30 minutes of activation, the reactor was removed from the drybox. Subsequently, ethylene was introduced and the polymerization was

continued for 10 minutes. The productivities of the ZrCGC materials are reported in Table 4.5. The productivities show similar trends as the stoichiometric Cp-silane reactivity studies. The highest productivity per metal atom was determined for the trityl-spaced ZrCGC with TIBA as the aluminum source (Table 4.5, SBA-NH2-TI). The second highest productivity was determined for the benzyl-spaced ZrCGC with the same aluminum source (SBA-NH2-BI). When considering the cooperative dilution materials, lower productivities were determined for these samples compared to the protection/deprotection materials. Also, it is very difficult to differentiate samples SBA-NH2-CD2 (Cp'ZrCGC on 1:15 APTMS:MTMS) and SBA-NH2-CD3 (Cp'ZrCGC on 1:50 APTMS:MTMS) for the polymerization of ethylene. In each case (either TMA or TIBA), the productivities for both materials were virtually the same. For instance,

ethylene polymerization productivities for ZrCGCs activated by TMA/$B(Ar)_F$ (SBA-NH2-CD2 and SBA-NH2-CD3) were calculated to 2.8 and 3.0 kg PE/(molZr hr), respectively. For TIBA/$B(Ar)_F$ experiments, the productivities were 4.5 and 5.7 kg PE/(molZr hr), respectively. Compared to the benzyl and trityl spaced ZrCGCs (10.2 and 12.6 kg PE(molZr hr)), the cooperative dilution method did not isolate the ZrCGCs was well as the protection/deprotection methods. We hypothesize that the main reason for the decreased reactivity and productivities found with the cooperative dilution method involves the lack of control over the separation of the amines on the molecular level, as this method relies on statistical probabilities of spacing amine groups using methyl partitions. In the toluene solution, although dilute, we suggest the amines can cluster through hydrogen bonding and react in packs on the surface.[10, 25, 26] With the cooperative

Table 4.5. ZrCGC productivities of Cp'Si$(Me)_2$-loaded aminosilicas for synthesis of poly(ethylene).[a]

Material	mmol Zr/ g material[b]	Aluminum Source[c]	Productivity (kg PE/(molZrhr)
SBA-NH2-DF	0.58	TMA	~0
SBA-NH2-DF	0.58	TIBA	2.6
SBA-NH2-BI	0.95	TMA	4.2
SBA-NH2-BI	0.95	TIBA	10.2
SBA-NH2-TI	0.58	TMA	6.3
SBA-NH2-TI	0.58	TIBA	12.6
SBA-NH2-CD1	0.34	TMA	~0
SBA-NH2-CD1	0.34	TIBA	4.4
SBA-NH2-CD2	0.37	TMA	2.8
SBA-NH2-CD2	0.37	TIBA	4.5
SBA-NH2-CD3	0.32	TMA	3.0
SBA-NH2-CD3	0.32	TIBA	5.7

[a] Polymerization time =10 minutes, B:Zr = 1.5:1, Ethylene Pressure = 60 psig, Room Temperature [b] Determined by EA. [c] TMA = trimethylaluminm, TIBA = triisobutylaluminum, Zr:Al 1:400.

dilution method, the methyltrimethoxysilane also plays a role as a diluent. On average, the reacted aminopropyl groups will be separated from one another – as shown with the fluorescence spectroscopy. However, surface clusters have most likely been reduced by dilution, but perhaps not prevented. This is seen in reactivity studies of Cp'Si$(Me)_2$Cl and CpSi$(Me)_2$Cl, as the mixed silane dilution method produces an aminosilica similar to a traditional, unprotected aminopropylsilyl-functionalized aminosilica in these reactions. Also, although the slightly "wet" surface creates a high loading of organic groups, the water can play a role in creating surface bound oligomers[25], which behave similarly to amine clusters, as sterics (or amine-amine separation) would govern amine reactivity/accessibility. With the protection/deprotection strategy, the amines cannot hydrogen bond together, reducing clustering. Also, the protecting group provides steric bulk which spaces the amine groups apart. Therefore, the reactivity of the amines produced with the protection/deprotection method should be more reactive, due to enhanced site-isolation.

4.4 Conclusions

Site-isolation and accessibility of grafted aminopropylsilyl-functionalized silica materials were studied for materials synthesized by an amine protection/deprotection method and a cooperative dilution method. These materials were compared to traditional, densely-loaded aminosilica control samples. Reactivity studies of Cp'Si$(Me)_2$Cl and CpSi$(Me)_2$Cl with the surface bound amines show that amines that are protected before functionalization and deprotected in a latter step are more accessible (reactive) than amines grafted by a mixed solution of MTMS and APTMS. After formation of tethered

zirconium CGCs, the resulting productivities for poly(ethylene) formation indicate that catalysts built off of trityl- and benzyl-spaced aminosilicas are more active than those built off traditional unprotected and surface diluted aminosilicas. These results indicate that multi-step amine protection/deprotection silica grafting methods create materials with reactivity and spacing advantages that unprotected, one-step grafting methods lack.

4.5 References

1. Wulff, G.; Heide, B.; Helfmeier, G., *J. Am. Chem. Soc.* **1986,** 108, 1089.

2. Zaitsev, V. N.; Skopenko, V. V.; Kholin, Y. V.; Konskaya, N. D.; Mernyi, S. A., *Zh. Obshch. Khim.* **1995,** 65, 529.

3. Katz, A.; Davis, M. E., *Nature* **2000,** 403, 286.

4. McKittrick, M. W.; Jones, C. W., *Chem. Mater.* **2003,** 15, 1132.

5. Bass, J. D.; Anderson, S. L.; Katz, A., *Angew. Chem. Int. Ed.* **2003,** 42, 5219.

6. Bass, J. D.; Katz, A., *Chem. Mater.* **2003,** 15, 2757.

7. Bass, J. D.; Katz, A., *Chem. Mater.* **2006,** 18, 1611.

8. Bass, J. D.; Solovyov, A.; Pascall, A. J.; Katz, A., *J. Am. Chem. Soc.* **2006,** 128, 3737.

9. Hicks, J. C.; Jones, C. W., *Langmuir* **2006,** 22, 2676.

10. Hicks, J. C.; Dabestani, R.; Buchanan III, A. C.; Jones, C. W., *Chem. Mater.* **2006,** 18, 5022.

11. Wirth, M. J.; Fatunmbi, H. O., *Anal. Chem.* **1993,** 65, 822.

12. Wirth, M. J.; Fairbank, R. W. P.; Fatunmbi, H. O., *Science* **1997,** 275, 44.

13. Luechinger, M.; Prins, R.; Pirngruber, G. D., *Micropor. Mesopor. Mater.* **2005,** 85, 111.

14. Sharma, K. K.; Asefa, T., *Angew. Chem. Int. Ed.* **2007,** 46, 2879.

15. McKittrick, M. W.; Jones, C. W., *J. Catal.* **2004,** 227, 186.

16. Yu, K. Q.; McKittrick, M. W.; Jones, C. W., *Organometallics* **2004,** 23, 4089.

17. McKittrick, M. W.; Jones, C. W., *J. Am. Chem. Soc.* **2004,** 126, 3052.

18. McKittrick, M. W.; Jones, C. W., *Chem. Mater.* **2005,** 17, 4758.

19. McKittrick, M. W.; Yu, K. Q.; Jones, C. W., *J. Mol. Catal. A* **2005,** 237, 26.

20. Pangborn, A. B.; Giardello, M. A.; Grubbs, R. H.; Rosen, R. K.; Timmers, F. J., *Organometallics* **1996,** 15, 1518.

21. Hiermeier, J.; Kohler, F. H.; Muller, G., *Organometallics* **1991,** 10, 1787.

22. Juvaste, H.; Pakkanen, T. T.; Iiskola, E. I., *Organometallics* **2000,** 19, 4834.

23. Zhao, D.; Huo, Q.; Feng, J.; Chmelka, B. F.; Stucky, G. D., *J. Am. Chem. Soc.* **1998,** 120, 6024.

24. Hicks, J. C.; Mullis, B. A.; Jones, C. W., *J. Am. Chem. Soc.* **2007,** 129, 8426.

25. White, L. D.; Tripp, C. P., *J. Colloid Interface Sci.* **2000,** 227, 237.

26. Kanan, S. M.; Tze, W. T. Y.; Tripp, C. P., *Langmuir* **2002,** 18, 6623.

27. It should not be assumed that amines are isolated simply because a protection/deprotection strategy was used. The material resulting from the use of a protection/deprotection method strongly depends on the protecting group (benzyl or trityl), the synthetic method (imine, carbamate, etc.), the environment (anhydrous, wet, hydroxylated surface, solvent, temperature), and other similar factors. In our case, we use room temperature reactions, protection of amines with imines, anhydrous silica surfaces and solvents, and a nonprotic toluene medium. Indeed, this work shows that the materials prepared here have varying degrees of isolation depending on the length scale of interest.

28. Bauer, R. K.; Borenstein, R.; De Mayo, P.; Okada, K.; Rafalska, M.; Ware, W. R.; Wu, K. C., *J. Am. Chem. Soc.* **1982,** 104, 4635.

29. Bauer, R. K.; De Mayo, P.; Ware, W. R.; Wu, K. C., *J. Phys. Chem.* **1982,** 86, 3781.

30. Bauer, R. K.; De Mayo, P.; Okada, K.; Ware, W. R.; Wu, K. C., *J. Phys. Chem.* **1983,** 87, 460.

31. Bauer, R. K.; De Mayo, P.; Natarajan, L. V.; Ware, W. R., *Can. J. Chem.* **1984,** 62, 1279.

32. Lochmuller, C. H.; Colborn, A. S.; Hunnicutt, M. L.; Harris, J. M., *J. Am. Chem. Soc.* **1984,** 106, 4077.

33. Pankasem, S.; Thomas, J. K., *J. Phys. Chem.* **1991,** 95, 7385.

34. Barbas, J. T.; Dabestani, R.; Sigman, M. E., *J. Photochem. Photobiol. A: Chem.* **1994,** 80, 103.

35. Wang, H.; Harris, J. M., *J. Am. Chem. Soc.* **1994,** 116, 5754.

36. Dabestani, R.; Ellis, K. J.; Sigman, M. E., *J. Photochem. Photobiol. A: Chem.* **1995,** 86, 231.

37. Barbas, J. T.; Sigman, M. E.; Dabestani, R., *Environ. Sci. Technol.* **1996,** 30, 1776.

38. Dabestani, R.; Nelson, M.; Sigman, M. E., *Photochem. Photobiol.* **1996,** 64, 80.

39. Sigman, M. E.; Barbas, J. T.; Chevis, E. A.; Dabestani, R., *New J. Chem.* **1996,** 20, 243.

40. Barbas, J. T.; Sigman, M. E.; Arce, R.; Dabestani, R., *J. Photochem. Photobiol. A: Chem.* **1997,** 109, 229.

41. Dabestani, R.; Higgin, J.; Stephenson, D. M.; Ivanov, I. N.; Sigman, M. E., *J. Phys. Chem. B* **2000,** 104, 10235.

42. Dewar, P. J.; MacGillivray, T. F.; Crispo, S. M.; Smith-Palmer, T., *J. Colloid Interface Sci.* **2000,** 228, 253.

43. Ivanov, I. N.; Dabestani, R.; Buchanan III, A. C.; Sigman, M. E., *J. Phys. Chem. B* **2001,** 105, 10308.

44. Metivier, R.; Leray, I.; Roy-Auberger, M.; Zanier-Szydlowski, N.; Valeur, B., *New J. Chem.* **2002,** 26, 411.

45. Metivier, R.; Leray, I.; Lefevre, J.-P.; Roy-Auberger, M.; Zanier-Szydlowski, N.; Valeur, B., *Phys. Chem. Chem. Phys.* **2003,** 5, 758.

46. Winnik, F. M., *Chem. Rev.* **1993,** 93, 587, and references therein.

47. Juvaste, H.; Iiskola, E. I.; Pakkanen, T. T., *J. Mol. Catal. A* **1999,** 150, 1.

48. Timonen, S.; Pakkanen, T. T.; Iiskola, E. I., *Journal of Organometallic Chemistry* **1999,** 582, 273.

CHAPTER 5

SULFONIC ACID FUNCTIONALIZED SBA-15 SILICA AS A MAO-FREE COCATALYST/SUPPORT FOR ETHYLENE POLYMERIZATION[†]

5.1 Introduction

In typical olefin polymerization reactions using supported single-site catalysts, methylaluminoxane (MAO) is adsorbed on a silica support and the combination is used as the supported cocatalyst.[1] To this supported activator, homogeneous single-site precatalysts can be added to produce different polymer products, as influenced by the symmetry of the catalyst, the monomer supplied, etc. Generally, when heterogeneous olefin polymerization catalysts are used in slurry reactions, metal leaching from methylaluminoxane occurs.[2, 3] As a method to prevent reactor fouling and metal leaching problems, silica-tethered olefin polymerization precatalysts have been synthesized in recent years.[2-12] Unfortunately, these materials are impractical and limited by their design – a support with a fixed precatalyst and external cocatalyst requires many different supported precatalysts to obtain a versatile array of polymer products.

Inorganic solids have also been utilized as MAO-free solid activator/supports.[13, 14] Marks and coworkers pioneered much of the work in sulfated metal oxides (SMOs) as support/activators for olefin polymerizations due to their very high Brønsted acidity.[15-18]

[†]Reproduced in part with permission from J. Am. Chem. Soc., 2007, 129, 8426. Copyright 2007 American Chemical Society.

Unlike traditional, Lewis acidic cocatalysts based on MAO or boranes, SMOs have received attention because of their very high Brønsted acidity. Marks and coworkers showed that by a metal-carbon protonolysis, an active olefin polymerization catalyst can be prepared. The solid acids are useful as combined support/activators, fulfilling two requirements of a typical polymerization recipe (precatalyst/cocatalyst/support). The most effective examples are derived from relatively expensive metal oxides such as zirconia or tin oxide.[18] Organic/inorganic hybrids based on organic sulfonic acid functionalized silicas have been utilized for more than a decade in non-polymerization applications requiring a Brønsted acid.[19-24] For example, recently, Alvaro et. al. reported a procedure to support a fluorinated organic sulfonic acid through a sultone ring-opening reaction between surface silanols and a fluorinated acid precursor (Figure 5.1).[25, 26] The

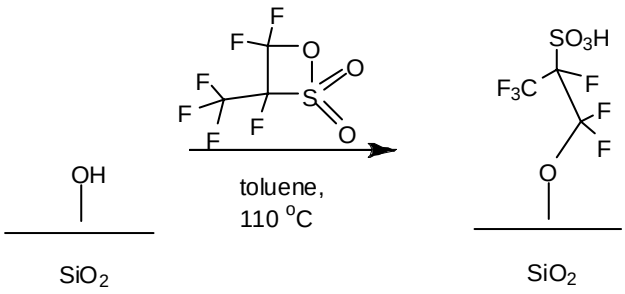

Figure 5.1. "Nafion"-like mesoporous silica.

work by Alvaro showed that the "Nafion"-like functionalized mesoporous silica could catalyze carboxylic acid esterification and Friedel–Crafts acylation reactions. Harmer and coworkers also reported the use of a tethered perfluoralkylsulfonic acid on mesoporous silica materials capable of Friedel-Crafts acylation of anisole.[23] However, there are no reports of organic/inorganic hybrid cocatalyst/supports for olefin polymerization, where

the organic functionality plays a critical role in the catalysis. We present here the first use of an organic/inorganic hybrid material as an effective combination cocatalyst/support for activation of various zirconocenes for production of poly(ethylene) in the presence of small amounts of alkylaluminum.

5.2 Experimental Section

Materials. The following chemicals were commercially available and used as received: poly(ethylene glycol)-block-poly(propylene glycol)-block-poly(ethylene glycol) (Aldrich), HCl (Fisher), tetraethyl orthosilicate (TEOS, Aldrich), anhydrous toluene (Acros), 1,2,2-trifluoro-2-hydroxy-1-(trifluoromethyl)ethanesulfonic acid beta-sultone (SynQuest Labs.), 3-mercaptopropyltrimethoxysilane (Aldrich), trimethylaluminum (TMA, Aldrich), triisobutylaluminum (TIBA, Aldrich), bis(cyclopentadienyl)dimethylzirconium(IV) (Aldrich), bis(pentamethylcyclopentadienyl)dimethylzirconium(IV) (Aldrich), ethylene (Polymer Purity, 99.9%, Matheson), 10% methylaluminoxane solution in toluene (MAO, Aldrich) and anhydrous methanol (Aldrich). The anhydrous toluene was further dried by distillation over Na/benzophenone. All air- and moisture-sensitive compounds were transferred using standard vacuum line, Schlenk, or cannula techniques under dry, deoxygenated argon or in a drybox under a deoxygenated nitrogen atmosphere.

Synthesis of SBA-15. In a given experiment, 12.0 g of poly(ethylene glycol)-block-poly(propylene glycol)-block-poly(ethylene glycol), 369 g of D.I. water, and 67 g of concentrated HCl were added together in a flask and stirred for at least three hours. Then 26.4 g of TEOS were added to the surfactant solution and stirred for 3 minutes. The

mixture was then stirred in an oven at 35 ^{o}C for 20 h. The solution was then removed from the stirrer and heated in the oven at 80 ^{o}C for 24 h. The solution was removed from the oven and cooled with D.I. water. This solution was filtered and washed with D.I. water and allowed to dry in an oven at 60 ^{o}C overnight. The material was then calcined by heating at 1.2 ^{o}C/min to a temperature of 250 ^{o}C. This temperature was held for an hour. Then it was heated again at 1.2 ^{o}C/min to 550 ^{o}C and held for 6 h. The resulting material was dried at 200 ^{o}C and 10 mTorr overnight.

Synthesis of Fluorinated Sulfonic Acid Functionalized SBA-15 Cocatalyst (SBA-FSO_3H). Approximately, 1.10 g of 1,2,2-trifluoro-2-hydroxy-1-(trifluoromethyl)ethanesulfonic acid beta-sultone was added to a mixture of 1g of SBA-15 in 40 mL of anhydrous toluene in a pressure vessel in a N_2 drybox. The reaction was allowed to proceed for 20 h at 110 ^{o}C. Upon completion, the resulting sulfonic acid functionalized solid was filtered and washed with anhydrous toluene. The solid was dried for 24 h at a temperature of 140 ^{o}C and pressure of 10 mTorr before use.

Synthesis of 3-Mercaptopropyltrimethoxysilane Functionalized SBA-15 (SBA-MPTMS). Approximately, 1.03 g of 3-mercaptopropyltrimethoxysilane was added to 1.14 g of SBA-15 in 30 g of anhydrous toluene in a nitrogen drybox. The mixture was refluxed overnight under argon. The thiol-functionalized SBA-15 was filtered and washed with toluene in a nitrogen drybox. The solid was dried at 140 ^{o}C and 10 mTorr overnight.

Synthesis of MAO-Modified SBA-15. MAO-modified SBA-15 was synthesized by first mixing 4.375 g of MAO solution (10% in toluene) with 1 g of SBA-15 (or SBA-FSO_3H).

The mixture was stirred for one hour. The solvent was removed under vacuum (10 mTorr). The resulting solid was stored and used in a nitrogen drybox.

Synthesis of 3,3,3-triphenylpropan-1-ol. The trityl alcohol was synthesized similarly to a previous report.[1] ^{13}C NMR (400 MHz, $CDCl_3$): δ 43.21 (-*C*H_2-CPh_3), 60.97 (HO-*C*H_2-CH_2-), 126 – 129 (3 peaks, Ph carbons), 147.0 (1 peak, -CH_2-*C*Ph_3). ^{1}H NMR (400 MHz, $CDCl_3$): δ 2.93 (2 H, t), 3.49 (2 H, t) and 7.20-7.35 (15 H, m).

Synthesis of 1,1,1,2,3,3-hexafluoro-3-(3,3,3-triphenylpropoxy)-propane-2-sulfonic acid (Trityl sulfonic acid). Approximately 1 equivalent of 3,3,3-triphenylpropan-1-ol was mixed with 1 equivalent of 1,2,2-trifluoro-2-hydroxy-1-trifluoromethylethane sulfonic acid beta-sultone in $CDCl_3$. ^{13}C NMR (400 MHz, $CDCl_3$): δ 38.16 (-*C*H_2-CPh_3), 68.81 (-O-*C*H_2-CH_2-), 126 – 129 (3 peaks, Ph carbons), 145.8 (1 peak, -CH_2-*C*Ph_3), the fluorinated carbons were not visible in the ^{13}C NMR. ^{1}H NMR (400 MHz, $CDCl_3$): δ 3.10 (2 H, m), 4.30 (2 H, m) and 7.20-7.35 (15 H, m). ^{19}F (400 MHz, $CDCl_3$, relative to C_6F_6): δ -0.20 (1 F), 1.73 (2 F), and 88.35 (3 F).

Polymerization Procedure. The SBA-FSO_3H was mixed with 15 mL of toluene, trimethylaluminum (TMA) and the metallocene precatalyst (Cp_2ZrMe_2 or $Cp^*_2ZrMe_2$) in a nitrogen drybox. The resulting mixture was stirred for 20 minutes in a water bath at room temperature. Ethylene (Polymer Purity, 99.9%) was further purified through an in-line oxygen and water purifier (Matheson Oxygen Absorbing Purifier Model 6410 with cartridge 641-01). The ethylene was added to the reactor at 60 psig for the specified amount of time (10 minutes). The polymerization was quenched by releasing ethylene pressure, followed by addition of acidic ethanol to allow the polymer to precipitate. The polymer was filtered and stored in an oven at 60 ^{o}C until residual solvent was removed.

Material Characterization. Thermogravimetric Analysis (TGA) and Differential Scanning Calorimetry (DSC) were performed on a Netzsch STA409. The organic loading was measured by determining the weight loss from 175 to 650 ^{o}C. Polymer melting points were determined by two heating cycles from 30 to 160 ^{o}C at 2 ^{o}/min under N_2. The melting point was taken from the second heating cycle. The XRD patterns were collected on a PAN analytical X'Pert Pro powder X-ray diffractometer using Cu Kα radiation and a PW3011 proportional detector with a parallel plate collimator. A Phi model SCA 1600 X-ray photoelectron spectrometer was used to determine surface composition of the silica substrate before and after addition of the sulfonic acid precursor. The instrument uses a monochromatic Al Kα source (1486.7 eV) and a spherical capacitor analyzer (SCA) operating at 187.85 eV pass energy. FT-IR spectra were collected on a Bruker IFS 66v/S spectrometer with an aperture setting of 8mm and a scanning velocity of 3.0 kHz. Silica materials were mixed with KBr in a nitrogen drybox to form pellets. The pellets were set in a nitrogen filled cell equipped with KBr windows for analysis. The polymerization reactor employed in this study was a 3 oz high pressure glass reactor from Andrews Glass Company.

5.3 Results and Discussion

A fluorinated sultone precursor reported by Alvaro et al. was tethered to SBA-15 by heating the mixture in toluene at 110 ^{o}C overnight (Figure 5.1).[25, 26] The SBA-15 material was synthesized with an average BJH pore diameter of 65 Å and BET surface area of 960 m^2/g (Table 5.1).[27-29] The BET surface area presented reflects both mesopores (that are accessible to the acid precursor) and micropores (that are likely not

accessible), due to the SBA-15 synthesis procedure used.[30-32] After reaction with the sultone precursor, the pore diameter and surface area decreased to 62 Å and 370 m^2/g, respectively. The sultone ring-opened to form a sulfonic acid via reaction with the surface silanols on SBA-15.[25, 26] Thermogravimetric analysis was used to determine the organic loading on the SBA-15. The weight loss from combustion indicates that the loading is approximately 1.62 mmol FSO_3H/g material. This supported sulfonic acid is the Brønsted acidic support used here.

Table 5.1. Nitrogen physisorption data of the SBA-15 before and after functionalization.

Nitrogen Physisorption Results at 77 K			
Sample	**Average pore diameter (Å)**	**BET surface area (m^2/g SiO_2)**	**Pore Volume (cm^3/g SiO_2)**
SBA-15	65	960	0.98
SBA-FSO_3H	62	370	0.57

X-ray diffraction patterns were collected for the material before and after functionalization. In the calcined SBA-15 material (Figure 5.2A), three well resolved peaks that correspond to the (100), (110), and (200) reflections are present. The peaks are attributed to a well-defined 2D-hexagonal mesostructure (p6mm).[27] A *d*-spacing of 87 Å was determined from this material, corresponding to 100 Å for the unit cell parameter. As shown in Figure 5.2B, after functionalization with the fluorinated sulfonic acid precursor, all of the peaks corresponding to a well-defined 2D-hexagonal structure remain present. This indicates that the ring-opening of the acid precursor to form an

immobilized fluorinated sulfonic acid functionality did not disrupt the order of the mesoporous silica framework.[25, 28, 33, 34]

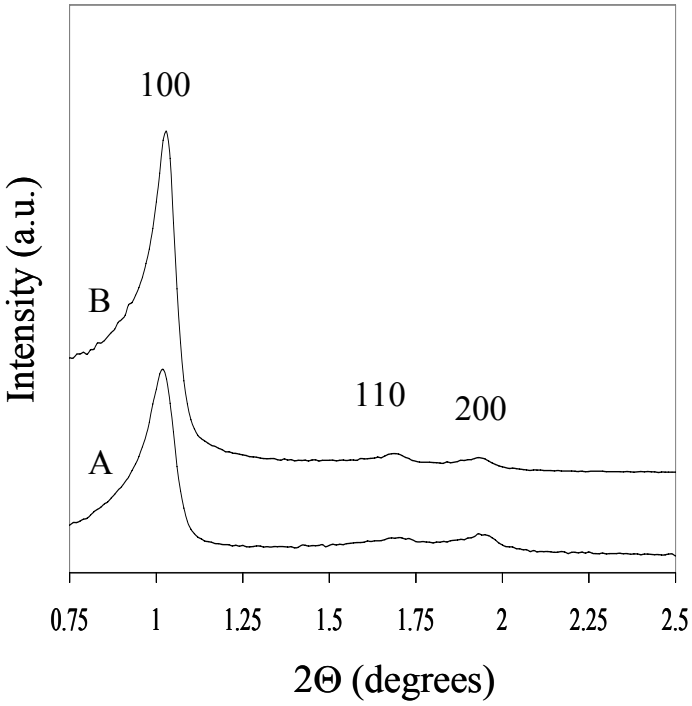

Figure 5.2. Powder X-ray diffraction patterns for the calcined SBA-15 (A) and fluorinated sulfonic acid functionalized SBA-15 (B).

X-ray photoelectron spectroscopy experiments were used to determine if a fluorinated species are present on the silica surface after functionalization. As represented in Figure 5.3, the calcined SBA-15 (A) lacks a F(1s) peak. However, after the fluorinated acid precursor is added (B), the spectrum shows a peak at 688.0 eV, which is assigned to the C-F bond in the molecule. Figure 5.4 shows the S(2p) region before (A) and after (B) functionalization of the SBA-15. Figure 5.4B shows the presence of a S(2p) peak at 169.4 eV, which is similar to the S(2p) peak of propane-sulfonic acid seen at 169 eV.[21] This indicates that the cyclic sulfonic acid precursor most likely reacts with the surface of the SBA-15 to form a sulfonic acid group.

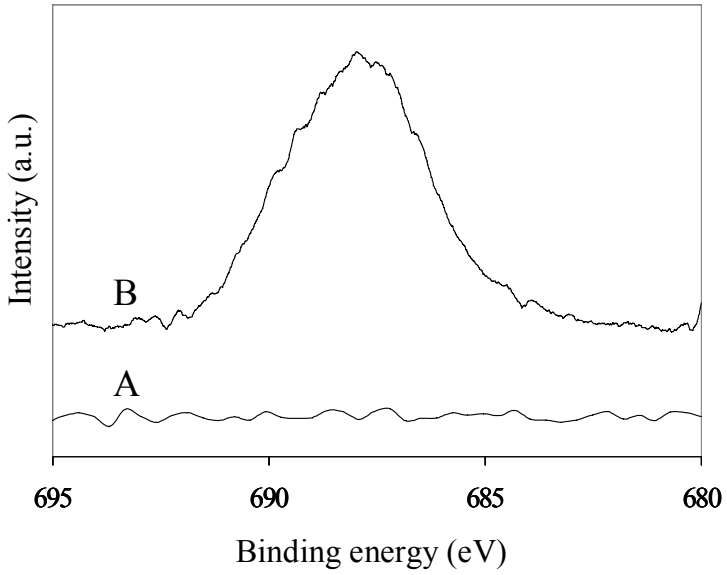

Figure 5.3. F(1s) region shown with calcined SBA-15 (A) and the fluorinated sulfonic acid functionalized SBA-15 (B).

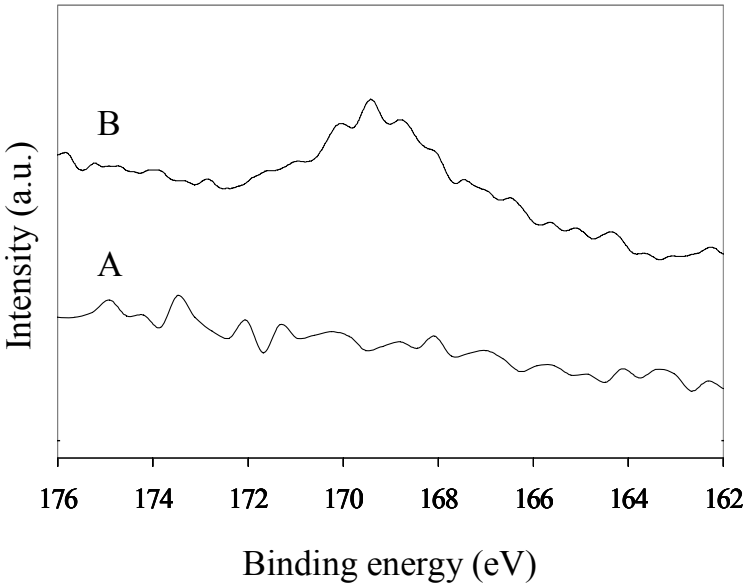

Figure 5.4. S(2p) region shown with calcined SBA-15 (A) and the fluorinated sulfonic acid functionalized SBA-15 (B).

The polymerization of ethylene was studied using bis(cyclopentadienyl)dimethylzirconium (Cp_2ZrMe_2) or bis (pentamethylcyclopentadienyl)dimethylzirconium ($Cp^*_2ZrMe_2$) as the metallocene precatalyst. It is necessary to add trimethylaluminum (TMA) in order for the polymerization to proceed.[13] When the zirconocene and SBA-FSO_3H were mixed without addition of TMA, polymerization was not observed. As shown in Table 5.2, the productivities of Cp_2ZrMe_2 are higher with a Zr:Al ratio of 1:400 than 1:700. However,

Table 5.2. Polymerization of ethylene at room temperature.

Entry	Catalyst	Cocatalyst	Al source	Zr:Al	Zr:SBA-FSO_3H	T_m (^oC)	Productivity (kgPE/molZrhr)
1	Cp_2ZrMe_2	SBA-FSO_3H	TMA	1:700	1:35	138.1	300
2	Cp_2ZrMe_2	SBA-FSO_3H	TMA	1:400	1:35	138.5	385
3	Cp_2ZrMe_2	SBA-FSO_3H	TMA	1:700	1:20	138	135
4	Cp_2ZrMe_2	SBA-FSO_3H	TMA	1:400	1:20	139.5	200
5	Cp_2ZrMe_2	SBA-FSO_3H	TIBA	1:700	1:35	-----	-----
6	Cp_2ZrMe_2	SBA-FSO_3H	TIBA	1:400	1:20	-----	-----
7	$Cp^*_2ZrMe_2$	SBA-FSO_3H	TMA	1:700	1:35	141.6	850
8	$Cp^*_2ZrMe_2$	SBA-FSO_3H	TMA	1:400	1:35	143.8	750
9	$Cp^*_2ZrMe_2$	SBA-FSO_3H	TMA	1:125	1:10	140.6	180
10	$Cp^*_2ZrMe_2$	SBA-FSO_3H	TMA	1:50	1:10	140.7	110
11	$Cp^*_2ZrMe_2$	SBA-FSO_3H	TMA	1:50	1:5	140.3	55
12	$Cp^*_2ZrMe_2$	SBA-FSO_3H	TMA	1:25	1:5	139.2	50
13	$Cp^*_2ZrMe_2$	MAO	MAO	1:125	-----	133.9	1600
14	$Cp^*_2ZrMe_2$	SBA-MAO	MAO	1:125	-----	136.5	1730
15	$Cp^*_2ZrMe_2$	SBA-FSO_3H/MAO	MAO	1:125	-----	134.1	1900

ratios of as little as 1:35 and 1:20 of Zr:SBA-FSO_3H are sufficient to activate the metallocene, yielding productivities up to 385 kg PE/mol Zr ·h. When similar experiments were performed using triisobutylaluminum (TIBA), polymer was not collected. As a control, the supported sulfonic acid with TMA was tested in the absence of the metallocene, and it was inactive. Using $Cp^*_2ZrMe_2$ as the precatalyst, the productivities were much higher compared to the Cp_2ZrMe_2 analogue. In fact, productivities approaching 1000 kg PE/mol Zr ·h were observed (Table 5.2).

In addition, in all cases, reactor fouling was not observed with the SBA-FSO_3H/TMA cocatalyst (Figure 5.5), whereas it was observed in the control experiments that utilized supported or unsupported MAO (Figures 5.6 and 5.7). The polymerization of ethylene using $Cp^*_2ZrMe_2$ activated by SBA-FSO_3H/TMA is shown in Figure 5.5. Before the addition of ethylene, the precatalyst was activated in toluene with SBA-FSO_3H/TMA for 30 minutes (Figure 5.5A). After ethylene was added to the reactor and 10 minutes of reaction, the polymerization was quenched, producing a poly(ethylene) suspension (Figure 5.5B and 5.5C). Using the SBA-FSO_3H/TMA cocatalyst, the reactor fouling was not observed. However, Figure 5.6 and Figure 5.7 are digital pictures of reactor fouling when homogeneous MAO (5.6) or silica supported MAO (5.7) is used as a cocatalyst to activate $Cp^*_2ZrMe_2$. Figures 5.6A and 5.7A show the reactor containing toluene, $Cp^*_2ZrMe_2$ and MAO or silica supported MAO, respectively. After addition of ethylene and 10 minutes of reaction, the polymerization was quenched by releasing the

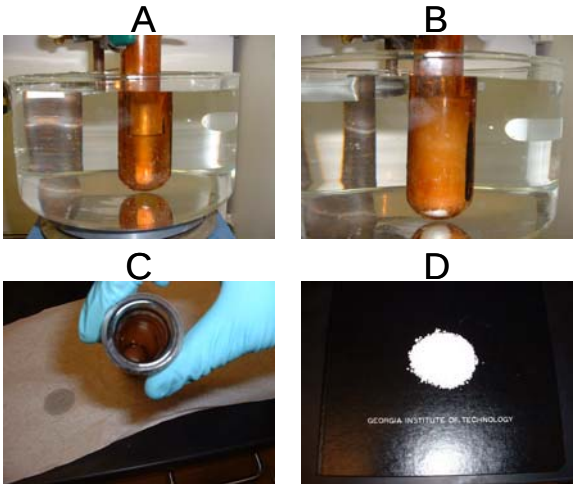

Figure 5.5. Pictures depicting ethylene polymerization with SBA-FSO_3H/TMA and $Cp_2^*ZrMe_2$: (A) mixture of SBA-FSO_3H/TMA, $Cp_2^*ZrMe_2$ and toluene, (B) polymer formed after quenching (10 min) – polymer suspension, (C) view down the reactor – polymer suspension, (D) polymer collected after filtration.

pressure of ethylene and adding acidic ethanol (Figure 5.6B or 5.7B). In this step, the polymer has coated the walls of the reactor (fouling). Figures 5.6C and 5.7C show reactor fouling by looking down the top of the reactor. The poly(ethylene) produced coated the walls of the reactor, making it very difficult to clean the reactor and re-run the experiment. This phenomenon is unwanted in industrial polymerization reactions, as reactor clean-up requires a significant amount of time and money.

To elucidate if the activation was a consequence of the regular mesoporous support, SBA-15, an additional material was synthesized using an amorphous commercial silica material (MS-3030 from PQ Corp.). With this support/activator, the polymerization of ethylene was studied with $Cp^*_2ZrMe_2$ at room temperature [1:20 $Zr:FSO_3H$, 1:400 Zr:Al]. A catalytic productivity of 413 kg PE/mol Zr ·hr was observed. When compared to MS-3030/MAO (Zr:Al of 1:400), a productivity of 1510 kg PE/mol Zr ·hr was achieved, showing that the new organic/inorganic hybrid activator/supports can give activities [best case ~850 kg PE/mol Zr ·hr] on the order of MAO/silica.

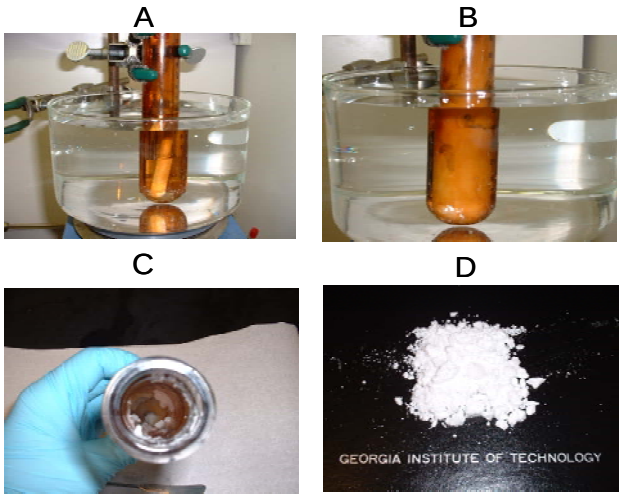

Figure 5.6. Reactor fouling during with homogeneous MAO and Cp_2*ZrMe_2: (A) mixture of Cp_2*ZrMe_2, MAO-modified SBA-15 and toluene, (B) polymer formed after quenching (10 min) – reactor fouling, (C) view down the reactor – reactor fouling, (D) polymer collected after filtration.

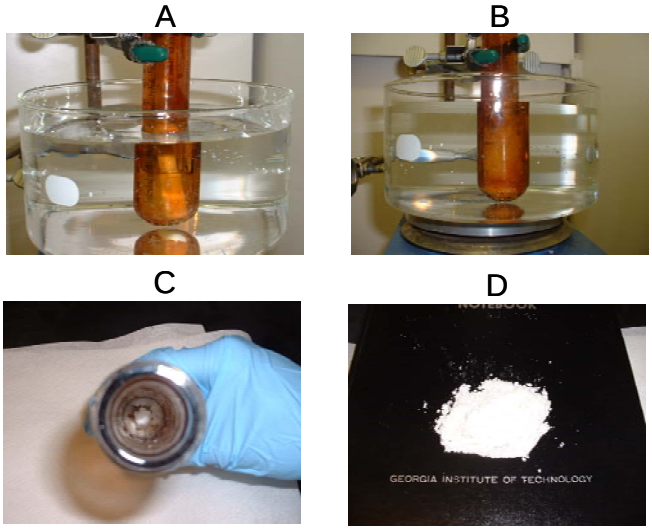

Figure 5.7. Reactor fouling during with MAO-modified SBA-15 and Cp_2*ZrMe_2: (A) mixture of Cp_2*ZrMe_2, MAO-modified SBA-15 and toluene, (B) polymer formed after quenching (10 min) – reactor fouling, (C) view down the reactor – reactor fouling, (D) polymer collected after filtration.

Three mechanisms of activation by the supported sulfonic acid were considered. In all cases, one role of the TMA is the *in situ* capping of the surface silanols to prevent Zr-O-Si metal deactivation on the silica surface. The three mechanisms are (i) *in situ* production of MAO from traces of water on the silica support, (ii) direct metallocene activation by the sulfonic acid, or (iii) activation by a combined adduct of the Brønsted acid and TMA. Each of these possible mechanisms was investigated experimentally. As reported by Scott and coworkers, the addition of TMA caps surface silanol groups by forming a bis-aluminum bridge on the Si-OH surface groups, evolving methane.[35] Loss of silanols in our work is supported by our FTIR experiments using SBA-FSO_3H/TMA, as the residual OH stretching band from the surface silanols was absent after addition of the sulfonic acid precursor and TMA to the support (Figure 5.8). TMA addition to silica

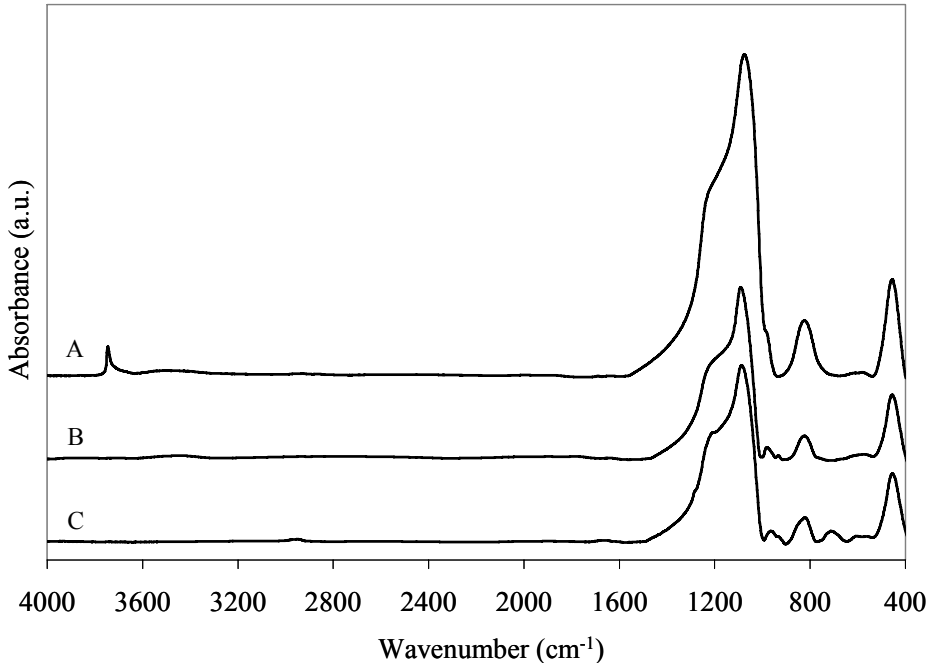

Figure 5.8. FT-IR of the SBA-15 (A), SBA-FSO_3H (B) and SBA-FSO_3H/TMA (C). The spectra show the removal of surface silanols after addition of the sulfonic acid precursor and TMA

could produce MAO *in situ* if there was sufficient water present on the support. However, our materials were rigorously dried. In addition, simply capping silanols on bare SBA-15 with TMA in the absence of sulfonic acids did not produce a solid that would activate the metallocene. To further investigate the possibility of *in situ* MAO formation, a hydrated mercaptopropyl- functionalized SBA-15 control material (SBA-MPTMS) was mixed with TMA and $Cp^*_2ZrMe_2$. This weakly acidic cocatalyst did not produce any poly(ethylene) either. Thus, *in situ* MAO formation was ruled out as an activation mechanism. Mechanism (ii) for metallocene activation, direct activation of the metallocene by protonation by the Brønsted acid, was deemed unlikely, as well. First, no polymerization was observed under any conditions in the absence of alkyl aluminum. In addition, order of reagent addition is found to be important, with active catalysts formed only when alkyl aluminums are added to the acidic support *before* addition of the metallocene. We further investigated the possibility for activation of the metallocene by the sulfonic acid alone or a combined adduct of the sulfonic acid and the alkylaluminum using small molecule analogues in solution. Figure 5.9 shows reactivity studies with an unsupported small molecule fluorinated sulfonic acid (1,1,1,2,3,3-hexafluoro-3-(3,3,3-triphenylpropoxy)propane-2-sulfonic acid or trityl sulfonic acid). All studies were conducted under dilute conditions to minimize temperature changes due to reaction exotherms. First, two equivalents of the trityl sulfonic acid were mixed with one equivalent of $Cp^*_2ZrMe_2$. An exothermic reaction occurred, producing a volatile gas. The gas evolved was inferred to be methane by the absence of Zr-*Me* resonances in the ^{13}C NMR (Table 5.3). When one equivalent of trityl sulfonic acid was added to two equivalents of $Cp^*_2ZrMe_2$, an upfield shift in the remaining Zr-*Me* resonance was

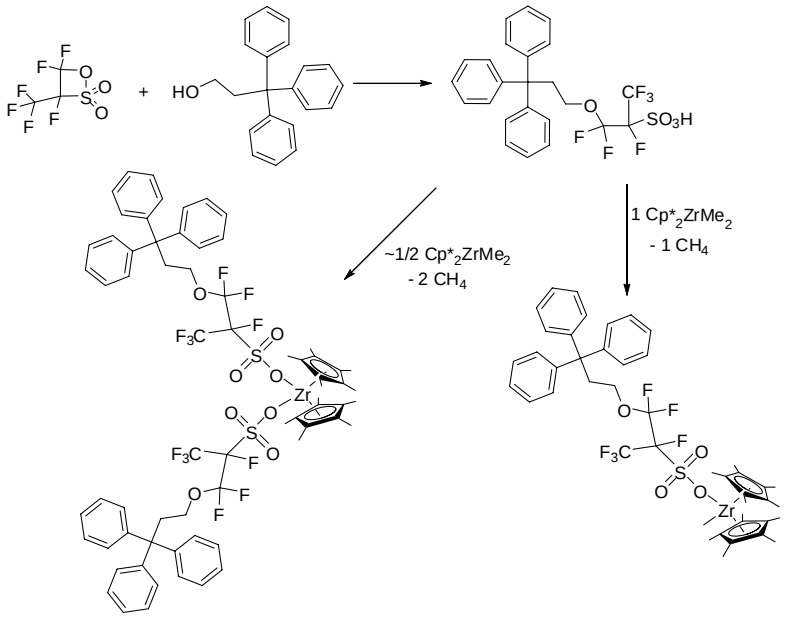

Figure 5.9. Reactivity studies using a small molecule, soluble sulfonic acid analogue. All soluble sulfonic acid adducts are inactive under the conditions studied, even in the presence of TMA.

observed (Table 5.3). This is very common for μ-oxo complexes, which are inactive olefin polymerization catalysts.[2] Subsequently, the homogeneous trityl sulfonic acid was mixed with either Cp_2ZrMe_2 or $Cp^*_2ZrMe_2$ in toluene to determine if poly(ethylene)

Table 5.3. Solution ^{13}C NMR studies on the activation of $Cp^*_2ZrMe_2$ with homogeneous sulfonic acids.

Solution 13C NMR				
Sample	δ (Zr-***C***H_3)	δ (Zr-***Cp***)	δ (Zr-Cp***C***H_3)	
$Cp^*_2ZrMe_2$	35.7	117.2	11.7	
$Cp^*_2ZrMe^+$ Trityl-O-FSO_3^-	31.41	118.96	11.2	1:1 SO_3:Zr
$Cp^*_2ZrMe^+$ Trityl-O-FSO_3^-	Removed	118.95	10.7	2:1 SO_3:Zr

could be produced in the absence of TMA. Poly(ethylene) was not made, and it was inferred that the direct coordination of the sulfonic acid to the metal center prevents the insertion of ethylene. Similarly, the silica supported sulfonic acid could not activate the precatalyst in the absence of TMA. When TMA was added to the trityl sulfonic acid, an exothermic reaction ensued. When the combination was tested for the activation of $Cp^*_2ZrMe_2$ for ethylene polymerization, again no polymer was collected. This contrasts the high activity observed when using the silica supported sulfonic acid in combination TMA. In summary, these results suggest three components are needed to activate the precatalyst – a solid surface, perhaps representing simply steric constraints (e.g. silica in this case), the fluorinated acid, and trimethylaluminum. Thus, our initial evidence suggests activation via metallocene interaction with a combined Brønsted acid – trimethylaluminum adduct (mechanism iii). Figure 5.10 depicts a hypothetical activated cation-anion pair. A structure for the sulfonic acid/TMA adduct that is suggested to form the non-coordinating anion might be derived from suggested TMA-silica structures

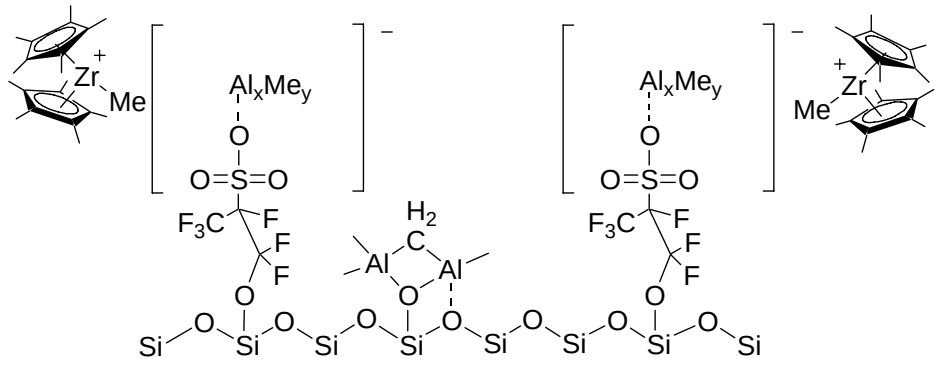

Figure 5.10. Hypothetical activated catalyst.

proposed by Scott and coworkers[35] or Maciel and coworkers[36].

To elucidate the location of the active catalyst, simple filtration studies were performed. For instance, a mixture of SBA-FSO_3H, TMA, toluene, and Cp_2ZrMe_2 or $Cp^*_2ZrMe_2$ was stirred for 30 minutes and subsequently filtered in a drybox. The filtrate was tested for polymerization activity and found to be inactive. Thus, the active catalyst likely remains coordinated to the support material.[37] Thus, it is proposed that the reaction of TMA and the SBA-FSO_3H surface creates a surface-tethered species that can activate the metallocene, creating a weakly-coordinating anion and an active metallocenium cation.

5.4 Conclusions

We thus report a method to produce active supported zirconocenes on a perfluoroalkanesulfonic acid functionalized silica support. It is necessary, however, to add trimethylaluminum to cap the surface silanols, and react with the surface Brønsted acid groups to form a site capable of activating the precatalyst. The results indicate the active catalyst is coordinated to the surface rather than in solution. The productivities are on the order of those observed with MAO-modified silica, but the materials have the advantage of preventing reactor fouling by limiting leaching of active species.

5.5 References

1. Chien, J. C. W.; He, D., *J. Polym. Sci., A: Polym. Chem.* **1991,** 29, 1603.

2. Hlatky, G. G., *Chem. Rev.* **2000,** 100, 1347.

3. Severn, J. R.; Chadwick, J. C.; Duchateau, R.; Friederichs, N., *Chem. Rev.* **2005,** 105, 4073.

4. Soga, K.; Kim, H. J.; Shiono, T., *Macromol. Chem. Phys.* **1994,** 195, 3347.

5. Chen, E. Y.-X.; Marks, T. J., *Chem. Rev.* **2000,** 100, 1391.

6. Tian, J.; Soo-Ko, Y.; Metcalfe, R.; Feng, Y. D.; Collins, S., *Macromolecules* **2001,** 34, 3120.

7. Cheng, X.; Lofthus, O. W.; Deck, P. A., *J. Mol. Cat. A* **2004,** 212, 121.

8. McKittrick, M. W.; Jones, C. W., *J. Am. Chem. Soc.* **2004,** 126, 3052.

9. Yu, K. Q.; McKittrick, M. W.; Jones, C. W., *Organometallics* **2004,** 23, 4089.

10. McKittrick, M. W.; Jones, C. W., *J. Catal.* **2004,** 227, 186.

11. McKittrick, M. W.; Jones, C. W., *Chem. Mater.* **2005,** 17, 4758.

12. McKittrick, M. W.; Yu, K. Q.; Jones, C. W., *J. Mol. Catal. A* **2005,** 237, 26.

13. Garces, J. M.; Sun, T., *Catal. Commun.* **2003,** 4, 97.

14. Lee, K.-S.; Oh, C.-G.; Yim, J.-H.; Ihm, S.-K., *J. Mol. Catal. A* **2000,** 159, 301.

15. Ahn, H.; Marks, T. J., *J. Am. Chem. Soc.* **1998,** 120, 13533.

16. Ahn, H.; Nicholas, C. P.; Marks, T. J., *Organometallics* **2002,** 21, 1788.

17. Nicholas, C. P.; Ahn, H.; Marks, T. J., *J. Am. Chem. Soc.* **2003,** 125, 4325.

18. Nicholas, C. P.; Marks, T. J., *Langmuir* **2004,** 20, 9456.

19. Corma, A., *Chem. Rev.* **1995,** 1995, 559.

20. Rhijn, W. M. V.; Vos, D. E. D.; Sels, B. F.; Bossaert, W. D.; Jacobs, P. A., *Chem. Commun.* **1998**, 317.

21. Shen, J. G. C.; Herman, R. G.; Klier, K., *J. Phys. Chem. B* **2002,** 106, 9975.

22. Melero, J. A.; van Grieken, R.; Morales, G., *Chem. Rev.* **2006,** 106, 3790.

23. Macquarrie, D. J.; Tavener, S. J.; Harmer, M. A., *Chem. Commun.* **2005**, 2363.

24. Wilson, B. C.; Jones, C. W., *Macromolecules* **2004,** 37, 9709.

25. Alvaro, M.; Corma, A.; Das, D.; Fornes, V.; Garcia, H., *Chem. Commun.* **2004**, 956.

26. Alvaro, M.; Corma, A.; Das, D.; Fornes, V.; Garcia, H., *J. Catal.* **2005,** 231, 48.

27. Zhao, D.; Huo, Q.; Feng, J.; Chmelka, B. F.; Stucky, G. D., *J. Am. Chem. Soc.* **1998,** 120, 6024.

28. Hicks, J. C.; Jones, C. W., *Langmuir* **2006,** 22, 2676.

29. Hicks, J. C.; Dabestani, R.; Buchanan III, A. C.; Jones, C. W., *Chem. Mater.* **2006,** 18, 5022.

30. Galarneau, A.; Cambon, H.; Renzo, F. D.; Fajula, F., *Langmuir* **2001,** 17, 8328.

31. Kruk, M.; Jaroniec, M.; Kim, T.-W.; Ryoo, R., *Chem. Mater.* **2003,** 15, 2815.

32. Miyazawa, K.; Inagaki, S., *Chem. Commun.* **2000**, 2121.

33. Evans, J.; Zaki, A. B.; El-Sheikh, M. Y.; El-Safty, S. A., *J. Phys. Chem. B* **2000,** 104, 10271.

34. Yoshitake, H.; Yokoi, T.; Tatsumi, T., *Chem. Mater.* **2002,** 14, 4603.

35. Scott, S. L.; Church, T. L.; Nguyen, D. H.; Mader, E. A.; Moran, J., *Top. Catal.* **2005,** 34, 109.

36. Li, J. H.; DiVerdi, J. A.; Maciel, G. E., *J. Am. Chem. Soc.* **2006,** 128, 17093.

37. The supported fluorinated acid does leach in the presence of water or alcohols. The leaching experiment described here does not rule out leaching of some inactive species.

CHAPTER 6

HYPERBRANCHED AMINOSILICAS CAPABLE OF CAPTURING CO_2 REVERSIBLY

6.1 Introduction

Due to the increase in CO_2 concentration in the atmosphere, contemporary research has focused on ways to stop or reverse this trend. There have been multiple suggestions to tackle this issue: (1) consume lower amounts of fossil fuels, (2) use renewable energy sources (such as wind, nuclear energy, biomass), (3) plant more trees and vegetation to consume the CO_2, and (4) capture CO_2 before it is released from the source. Of these options, CO_2 capture has received much attention due to the ability to reduce the emissions from concentrated sources such as energy producing power plants. A current, well-known technology for amine separations is absorption by aqueous amines. Aqueous amines were first reported as a method to capture CO_2 in 1961.[1] However, although aqueous amines have been used, these solutions are energy intensive and expensive when used for large volumes of gas (such as flue gas). This is primarily due to the high heat capacity of water, which is problematic during the desorption steps. To alleviate the problems associated with the aqueous amine technology, many types of amine-modified solid materials have been reported (e.g. polymers[2-5], amine-tethered silica materials[6-18], amines impregnated into porous silicas[19-23], etc.) as possible adsorbents for CO_2 capture from flue gas streams. However, many of these materials either suffer from low CO_2 capacities, or lack of stability from physisorbing the amine groups onto the support. Therefore, it would be advantageous to synthesize an

organic/inorganic hybrid amine-tethered silica material with high amine loadings (> 6 mmol/g) capable of reversibly binding CO_2 rather than using physisorbed, impregnated adsorbents that may be unstable after many recycles. This chapter focuses on this goal, describing the synthesis of a covalently tethered hyperbranched aminosilica (HAS) material[24] capable of binding CO_2 reversibly from simulated flue gas.

6.2 Experimental Section

Materials. The following chemicals were commercially available and used as received: Pluronic 123 (Aldrich), HCl (Fisher), 3-aminopropyltrimethoxysilane (APTMS, Aldrich), tetraethyl orthosilicate (TEOS, Aldrich), glacial acetic acid (Fisher), anhydrous toluene (Acros), sodium hydroxide pellets (VWR), N-(3-(trimethoxysilyl)propyl)ethane-1,2-diamine (AEAPTMS, Aldrich), methanol (Aldrich), 2-chloroethylamine hydrochloride (Aldrich), and polyethyeneimine (PEI, Aldrich). Anhydrous toluene and anhydrous hexanes were further treated by a packed bed solvent purification system utilizing columns of copper oxide catalyst and alumina.[25]

Synthesis of SBA-15 Support. Approximately 12.0 g of Pluronic 123 was weighed and added to a 1000 mL Erlenmeyer flask. To the polymer, 369 g of deionized (D.I.) water and 67 g of HCl was added. This solution was stirred for about 3 hours (or until the polymer dissolved). Once the Pluronic 123 dissolved, 26.4 g of TEOS was added and stirred for 3 minutes. The solution was stirred in the oven for 20 hours at 35 ^{o}C. A white precipitate was formed during this time period. At this point, the solution was not stirred and heated to 80 ^{o}C for 24 hours. The solution was quenched by adding ~ 400 mL of D.I. water. The precipitate was filtered and washed with D.I. water. The white solid was

dried in the sample oven overnight. The calcination performed involved heating at 1.2 °C/min to 200 °C and held for 1 hour. Finally, the last ramp was done at 1.2 °C/min to 550 °C and held for 6 hours. The calcined SBA was subsequently dried at 200 °C under vacuum for 3 hours.[26-29]

Synthesis of Aziridine. Aziridine was synthesized in a manner similar to reported procedures with minor changes.[30] A solution of 135 g of D.I. H_2O and 23.14 g of NaOH was prepared. To this solution, 23.60 g of 2-chloroethylamine hydrochloride was added and heated to 50°C for 2 hours. The product was then distilled at 530 mmHg. The amount of product collected was 6.99 g (80% yield). The aziridine was immediately cooled to 0°C. ^{1}H NMR (400 MHz, D_2O) δ 1.56 (s). ^{13}C NMR (400 MHz, $CDCl_3$): δ 18.1.

Reaction of Aziridine with SBA-15 (SBA-HA). The reaction of aziridine with silica was performed similarly to previous reports.[31] The hyperbranched aminosilica (HAS) was synthesized by adding 2.04 g of aziridine to 1.10 g SBA-15 in anhydrous toluene. A small amount of glacial acetic acid (20 mg) was added to catalyze the reaction with the SBA-15 surface. The mixture was stirred overnight at 110 °C in a glass pressure vessel. The resulting solid was filtered and washed with copious amounts of toluene then dried at 50 °C under high vacuum. The loading of the material was determined by TGA as 8.45 mmol N/g.[32]

Synthesis of Traditional Aminosilica (SBA-NH_2). Excess 3-aminopropyltrimethoxysilane, APTMS, (2.0 g) was added to 2 g of SBA-15 in anhydrous toluene. The mixture was allowed to stir for 24 h at room temperature under argon. The resulting solid (SBA-NH_2) was filtered, washed with toluene, dried under vacuum at 50

^{o}C overnight, and then stored in a drybox. The organic loading of the material was determined by TGA as 1.20 mmol N/g.

Synthesis of Diamine-Functionalized Silica (SBA-Diamine). Excess N-(3-(trimethoxysilyl)propyl)ethane-1,2-diamine, APAETMS, (1.0 g) was added to 1 g of SBA-15 in anhydrous toluene. The mixture was allowed to stir for 24 h at room temperature under argon. The resulting solid (SBA-NH-NH_2) was filtered, washed with toluene, dried under vacuum at 50 ^{o}C overnight, and then stored in a drybox. The organic loading of the material was determined by TGA as 2.40 mmol N/g.

Synthesis of PEI-Impregnated SBA-15 (SBA/PEI). This material was synthesized similarly to literature procedures using SBA-15 rather than MCM-41.[19, 20] The desired amount of PEI to create a material with 50 wt % PEI was dissolved in methanol and stirred for 15 minutes. Subsequently, 1 gram of SBA-15 was added and stirred for an additional 30 minutes. The methanol was removed under vacuum. The resulting SBA/PEI was dried for 16 hours at 70 ^{o}C and 10 mTorr.

Characterization Methods. Cross-polarization magic angle spinning (CP-MAS) NMR spectra were collected on a Bruker DSX 300-MHz instrument. Approximately 300 mg of the sample was packed in a 7-mm zirconia rotor and spun at 5 kHz. Typical ^{13}C CP-MAS parameters were 3000 scans, a 90° pulse length of 4 μs, and recycle times of 4 s. Typical ^{29}Si CP-MAS parameters were 5000 scans, a 90° pulse length of 5 μs, and recycle times of 5 s. FT-Raman spectra were obtained on a Bruker FRA-106 with a resolution of 2-4 cm^{-1}. At least 512 scans were collected. Thermogravimetric analysis (TGA) was performed on a Netzsch STA409. Samples were heated under air and nitrogen from 30 to 900° C at a rate of 10° C/min. The organic loading was determined

from the weight loss between 200 to 700° C. Nitrogen physisorption measurements were conducted on a Micromeritics ASAP 2010 at 77 K. The SBA-15 sample was pretreated by heating under vacuum at 200 °C for 24 h. The HAS sample was pretreated by heating at 100^{o} C under vacuum for 24 hours. CO_2 adsorption experiments were performed with a Pfeiffer Vacuum QMS 200 Prisma Quadrupole Mass Spectrometer for residual gas analysis in ultra high vacuum.

Adsorption Capacity Measurements in a Cahn Balance. CO_2 uptake experiments were conducted using a microbalance assembly consisting of a Cahn TG-131 Thermogravimetric Analyzer (TGA) at National Energy Technology Laboratory (NETL). Gas compositions were created in blending high purity gases using mass flow controllers (Brooks model 5850E controller and Brooks model 5878 instrument readout). Carbon dioxide (CO_2) of stock grade (99.9%) was supplied via gas cylinder and pressure regulator, while a house supply of nitrogen was utilized. The gas stream was humidified using a sparger vessel filled entirely with deionized water. Gas relative humidity was verified using a Vaisala HMP-36 humidity/temperature probe and a Vaisala HMI-32 instrument readout. A moisture-laden gas stream was heat-traced with electric heating tapes controlled by variable autotransformers (Variac). Each heated section along the path had one heating tape with one thermocouple mounted on the external surface. Electric power to each tape was manually govern by a Variac setting to achieve temperature readout in excess of the dew point to prevent condensation. A circulating bath of ethylene glycol/water was used to provide fine temperature control of the gas mixture prior to the gas entering the reactor assembly. For a typical experiment, 15 mg of sample was charged into a quartz cylindrical sample pan and heated under N_2 from

ambient temperature to 105^{o} C. This was done to drive-off any pre-adsorbed water and/or CO_2. Sample temperature within the reactor assembly was measured and controlled with a type K thermocouple placed just below the suspended sample pan. After reaching constant weight, the temperature was cooled to respective adsorption temperature, in our case 40^{o} C. The sample was then introduced to a humidified N_2 stream (until again constant weight of the sample was achieved) followed by a stream consisting of humidified CO_2. The gain in sample weight corresponds to the sorption of both CO_2 and H_2O. The final stages within the experiment were conducted under a dry CO_2 stream and dry N_2 stream respectively. Lastly, CO_2 was desorbed from the surface of the sorbent under dry nitrogen. Total gas flow rate was held constant throughout experiment at 200 cc/min.

Adsorption Capacity Measurements in a Fixed Bed Flow System. CO_2 capture capacities were determined by analysis via Mass Spectrometry (MS). A Pfeiffer Vacuum QMS 200 Prisma Quadrupole Mass Spectrometer for residual gas analysis in ultra high vacuum was selected for the analyses of all simulated flue gas experiments. In a typical experiment, approximately 70 – 100 mg of the sorbent was dispersed in 200 – 300 mg of sieved sand (250 – 425 micron). The dispersed sorbent was placed in a pyrex tubular reactor (1/4 in O.D.) and was pretreated with pure argon with a flow rate of 20 ml/min. The temperature was maintained at 130 ^{o}C under atmospheric pressure for three hours. During this pretreatment period, the reaction gas consisting of 10% Carbon Dioxide/Argon was humidified (~ 1.6 % water) and directed to the mass spectrometer to form the baseline carbon dioxide concentration required for these tests. The gas flow was maintained at 20 ml/min with a temperature of either 25 or 75 ^{o}C at atmospheric pressure.

Then the reaction gas stream was switched to the reactor and the amount of carbon dioxide captured by the sorbent was tracked by the mass spectrometer. After approximately 200 minutes the gas stream was switched back to the pretreatment conditions and the reactor temperature was increased to 130 ^{o}C for three hours to desorb the CO_2 from the sorbent.

6.3 Results and Discussion

The synthesis of the hyperbranched aminosilica sorbent occurred via a one-step reaction between aziridine and the silica surface (Figure 6.1).[31] As previously reported on silica wafers, the surface silanols reacted with the strained aziridine molecule and polymerized these groups off of the surface.[31] The material was referred to as a

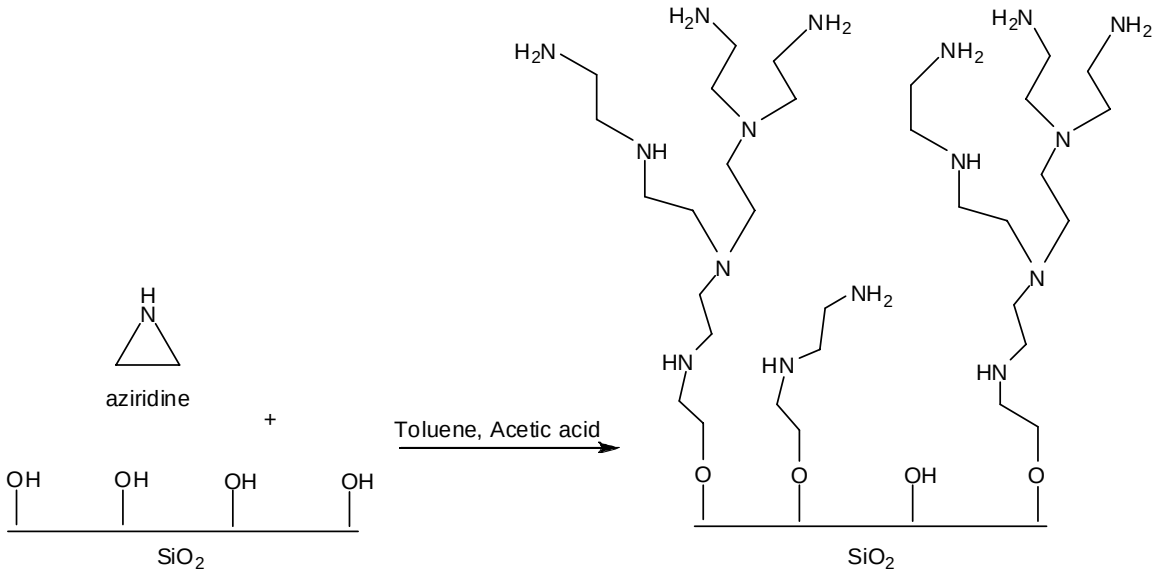

Figure 6.1. Synthesis of hyperbranched aminosilica.

hyperbranched aminosilica because the polymerization of aziridine has typically resulted in a mixture of primary, secondary and tertiary amines. Due to the low surface area, hyperbranched aminosilica materials constructed off of silica wafers are impractical CO_2 capture sorbents. However, the formation of hyperbranched aminosilicas on high surface area mesoporous silica materials[24, 33] can potentially lead to high amine loaded materials capable of reversibly binding CO_2 with substantial capacities (> 2 mmol CO_2/g). The aziridine monomer was added to SBA-15 dispersed in a toluene solution with catalytic amounts of acetic acid and heated to 110 ^oC in a glass pressure reaction vessel. The resulting material (SBA-HA) was washed with toluene to remove any physisorbed aziridine from the surface. The organic loading of the grafted hyperbranched aminosilica was determined via thermogravimetric analysis (TGA) as 8.45 mmol N/g material (Figure 6.1). As noticed from TGA (Figure 6.2), the organic groups decomposed at 200 ^oC, which is ~ 40 ^oC higher than pure PEI.[20]

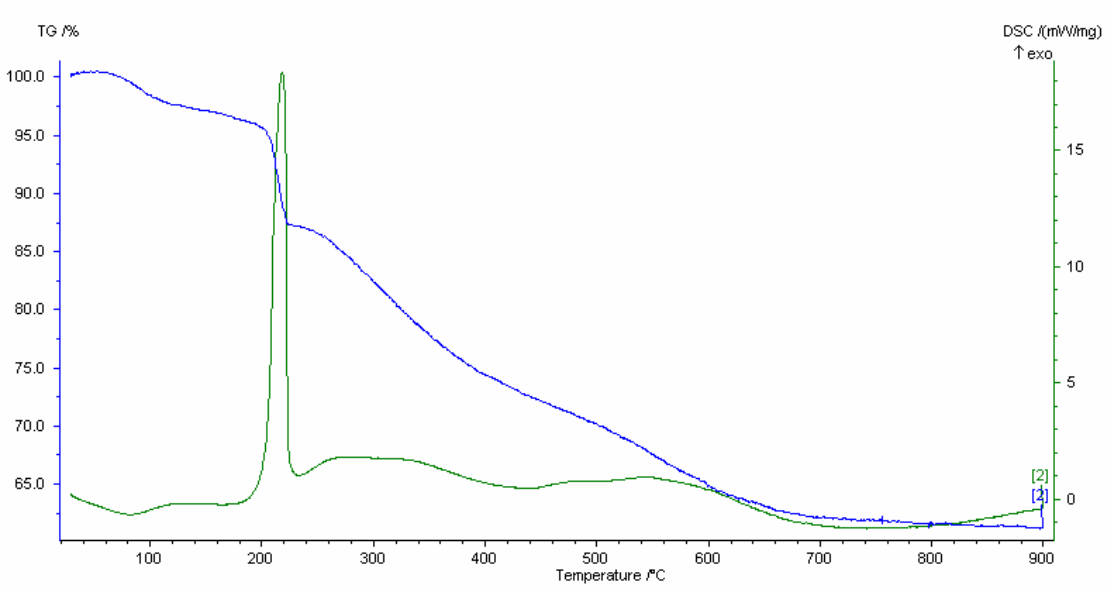

Figure 6.2 TGA of SBA-HA.

The support material and amine-modified material were characterized with nitrogen physisorption (Table 6.1). As determined from the physisorption results, the SBA-HA material showed a substantial loss in the Brunauer-Emmet-Teller (BET) surface area after polymerization of aziridine with the silica surface due to micropore filling or blocking and mesopore filling (Table 6.1).[34-36] This is seen by the decrease in BET surface area (from 932 to 169 m^2/g). Also, the Bopp-Jancso-Heinzinger (BJH) pore diameter decreased after grafting of the aziridine molecules (decreased from 65 to 45 Å), indicating reaction within the mesoporous network.

Table 6.1. Nitrogen physisorption and TGA results.

sample	BJH average pore diameter (Å)	BET surface area (m^2/g)	organic loading (mmol/g)
SBA-15	65	932	-----
SBA-HA	45	169	8.45

The FT-Raman spectrum of the hyperbranched aminosilica sorbent showed two distinct peaks associated with the formation of a hyperbranched aminosilica (Figure 6.3). The C-H aliphatic transition was seen between 3000 – 2750 cm^{-1}, while the CH_2 transition was seen at 1457 cm^{-1}, indicating the addition of organic groups on the silica surface.

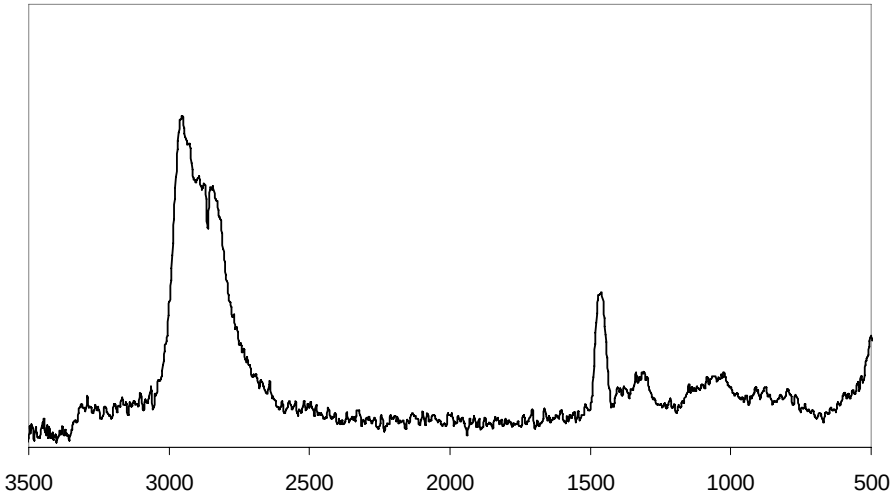

Figure 6.3. FT-Raman spectroscopy of SBA-HA.

Solid state ^{13}C CP-MAS spectroscopy showed the presence of a broad peak between 20 and 70 ppm (Figure 6.4). The broad peak included carbon resonances from the different types of carbons present in the hyperbranched aminosilica material (Figure 6.1). For instance, a broad peak was expected since multiple types of CH_2 groups were present in the material, which overlapped each other between the 30 – 60 ppm (Si-O-*C*H_2-, Si-O-CH_2-*C*H_2-NH_2, Si-O-CH_2-CH_2-NH-*C*H_2-, Si-O-CH_2-CH_2-N-(CH_2-)*C*H_2-,

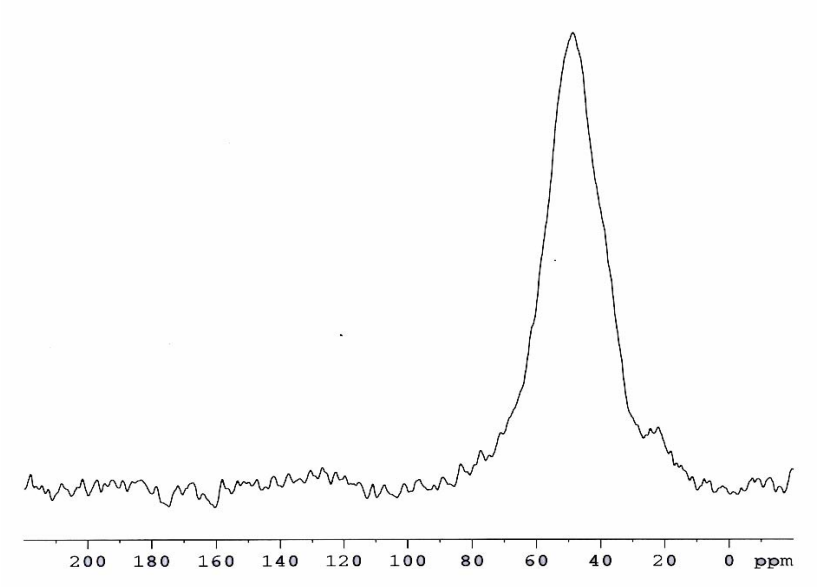

Figure 6.4. Solid state CP MAS ^{13}C NMR of SBA-HA.

etc.). It is clear that surface modification occurred with the aziridine molecule and the surface, resulting in a broad peak from the surface polymerization in the ^{13}C spectrum.[37]

Two experimental protocols to determine the sorption capacity of CO_2 were performed: (1) use of a TGA equipped with a Cahn balance (performed at the National Energy Technology Laboratory, NETL) and (2) use of a fixed bed flow system connected to a mass spectrometer (at GaTech). Due to the nature of the experiment, TGA/Cahn balance experiments routinely yield lower capacities than fixed bed, flow processes. This phenomenon is expected because most TGAs contain a small pan for the sorbent with a gas stream flowing over one side of the pan, creating gas-sample contacting problems. TGA results showed CO_2 capacities of 2.2 mmol CO_2/g sorbent at 25 ^oC in pure humidified CO_2 (Figure 6.5). In these experiments, humidified CO_2 was flowed over a sample of the hyperbranched aminosilica. Subsequently, the CO_2 was desorbed from the surface, and an additional capacity was determined. The TGA study was performed as an initial test to determine how applicable these hyperbranched aminosilicas would be as CO_2 sorbents.

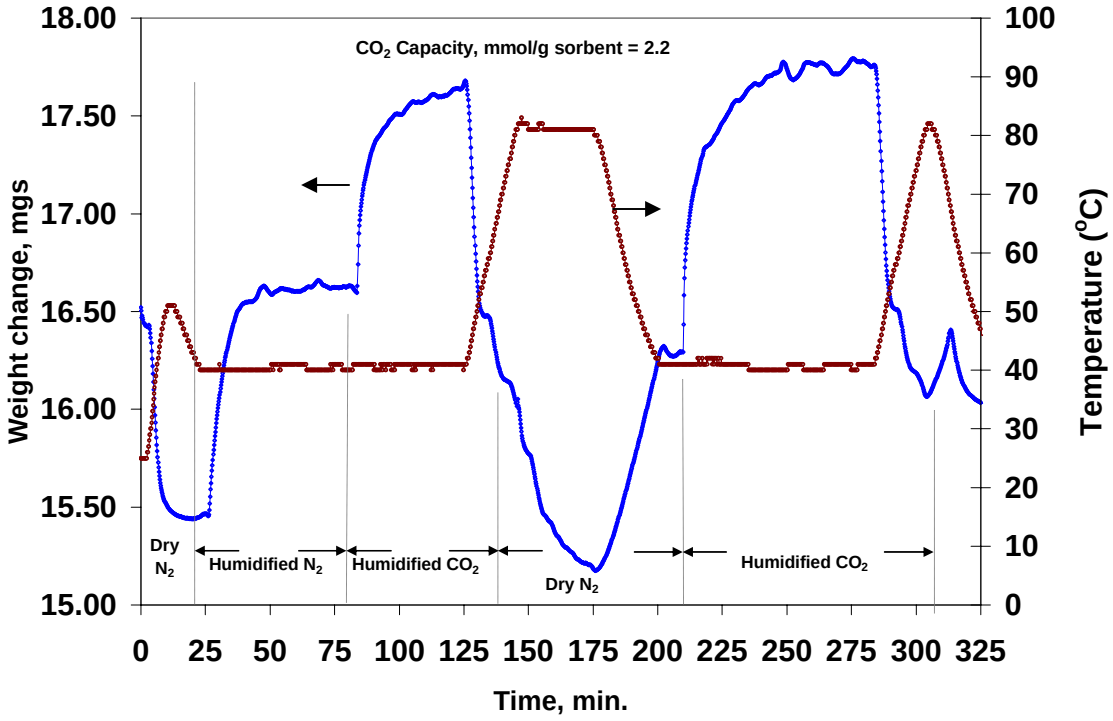

Figure 6.5. TGA analysis of CO_2 capture with a hyperbranched aminosilica. The arrows indicate which axis to use.

Similar studies were performed in a fixed-bed flow reactor system (Figure 6.6). For a given experiment, the aminosilica was dispersed in sieved sand[38] (250 – 425 micron) and placed in a pyrex tube located in a furnace. Pure argon was passed through the system at a flow rate of 20 mL/min while the adsorbent was heated to 130 ^{o}C. After at least three hours, the aminosilica was activated and ready for analysis. Subsequently, the argon flow was stopped and 20 mL/min of 10 % CO_2/Ar was supplied to the system. The system was designed to allow for humid (~ 1.6 % water) or dry flow of the 10 % CO_2/Ar stream. The mass spectrometer was connected to the exit of the adsorbent

column to analyze the effluent gas. From this analysis, the amount of CO_2 adsorbed onto the aminosilica sorbent was calculated.

As previously mentioned, fixed bed flow systems have typically generated higher CO_2 capacities compared to TGA experiments. In our flow system, the reason for this

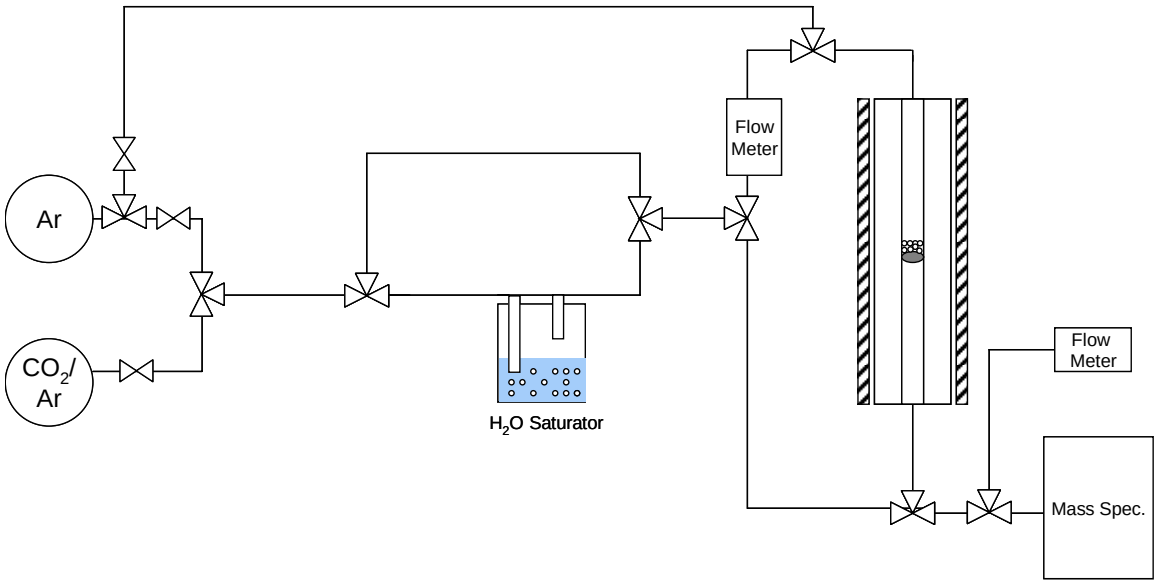

Figure 6.6. Diagram of the fixed bed flow system.

difference in capacities was dilution of the 10 % CO_2/Ar with the stagnant Ar remaining in the tubing when the gases were switched in the fixed bed flow system, which caused an overestimation of the adsorption capacity if this dilution was not taken into account via blank experiments. When the argon line was switched to the 10 % CO_2/Ar stream, the difference in concentration between the two sides created a gradient which caused dilution of the gases. This result indicated that a background must be subtracted from the adsorption data in order to generate quantitative results. For instance, a control was

performed in which pure Ar (flowrate of 20 mL/min) was passed through the tubing and adsorption column containing sand and unmodified SBA-15. Subsequently, the gas was switched to 10 % CO_2/Ar and the response was analyzed (Figure 6.6). The dilution of the 10 % CO_2/Ar in the stagnant Ar was then quantified and referred to as a background (Figure 6.7).

After the system was calibrated, the SBA-HA material was analyzed at 75 ^oC and a 10 % CO_2/Ar flow rate of 20 mL/min. In these studies, approximately 70 mg of the hyperbranched aminosilica was tested in the fixed bed flow system. The adsorption of CO_2 on the aminosilica was determined by monitoring the effluent gas with the mass spectrometer. After 200 minutes, the gas was switched to pure argon and the CO_2 was

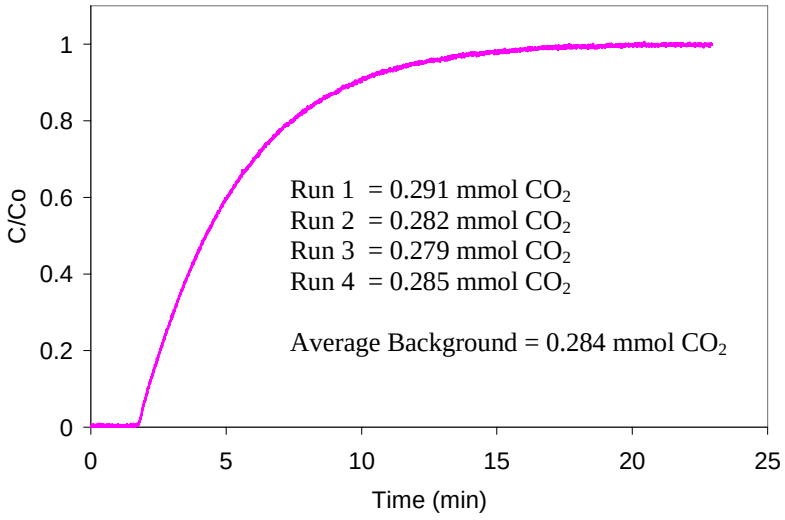

Figure 6.7. Background response of CO_2 concentration due to dilution.

desorbed from the surface at 130 ^{o}C for at least 3 hours. The material was then analyzed again (Table 6.2). As shown in Table 6.2, the SBA-HA material captured CO_2 reversibly (up to 11 experiments) with an average capacity of 5.45 mmol CO_2/g aziridine (1.98 mmol CO_2/g sorbent).[39] During these 11 cycles, the CO_2 adsorption capacity did not change much, ranging between 1.9 and 2.1 mmol CO_2/g. This indicated that the desorption step (130 ^{o}C for 3 hours in Ar) removed the CO_2 from the surface allowing for the material to be recycled. These materials were stable at temperatures up to 130 ^{o}C for multiple cycles. However, for flue gas applications, the hyperbranched aminosilica materials demonstrated promising CO_2 adsorption properties.

Table 6.2. Recycling SBA-HA at 75 ^{o}C with a flow rate of 10 % CO_2/Ar.

Run	Capacity (mmol CO_2/g material)	Capacity (mmol CO_2/g aziridine)	CO_2/N
1	1.89	5.20	0.22
2	1.96	5.39	0.23
3	1.98	5.45	0.23
4	2.02	5.56	0.24
5	1.96	5.39	0.23
6	2.12	5.83	0.25
7	1.89	5.20	0.22
8	1.98	5.45	0.23
9	1.96	5.39	0.23
10	2.00	5.50	0.24
11	2.02	5.56	0.24
High	2.12	5.83	0.25
Min	1.89	5.2	0.22
Average	1.98 ± 0.06	5.45 ± 0.17	0.23 ± 0.008

Additionally, the SBA-HA material was compared to some of the best literature reported materials. For instance, a traditionally functionalized (SBA-NH_2) and a diamine-functionalized (SBA-Diamine) aminosilica were synthesized with amine loadings of 1.2 mmol/g and 2.4 mmol/g, respectively. These materials were synthesized by reacting either 3-aminopropyltrimethoxysilane or N-(3-(trimethoxysilyl)propyl)ethane-1,2-diamine with the SBA-15. When analyzed in the fixed bed flow system, these materials produced CO_2 capacities of approximately 10 % (SBA-NH_2) and 20 % (SBA-Diamine) that of the SBA-HA material at 25 ^{o}C (Table 6.3). The high loading of amines on the hyperbranched aminosilica (SBA-HA) compared to

the SBA-NH_2 and SBA-Diamine materials allowed for a CO_2 capacity of 3.11 mmol CO_2/g, which is the basis for the data in Table 6.3.

An additional material was synthesized via impregnation of PEI[19-22] into SBA-15. The SBA/PEI material was analyzed in the flow system as capturing CO_2 approximately 70 % as well as the SBA-HA material. Similar to previous reports,[19-22] the capacities of the SBA/PEI materials increased at a higher temperature, possibly due to swelling of the polyethyleneimine within the porous support. One possibility for the lower capacity with the SBA/PEI materials was the texture of the material. When the PEI was impregnated in the SBA-15, the resulting material was very "sticky" due to the addition of the high molecular weight polymer (MW 750,000). The difficulty with the SBA/PEI material was the inability to disperse this sticky material evenly in the sieved sand. If the SBA/PEI

Table 6.3. Comparing amine-modified silica sorbents at 25 ^oC.

Material	Temperature (^oC)	mmol N/g	Capacity/Capacity HAS
SBA-HA	25	8.45	1.00
SBA-HA	75	8.45	0.68
SBA/PEI	25	11.6[a]	0.64
SBA/PEI	75	11.6[a]	0.69
SBA-Diamine	25	2.4	0.23
SBA-NH_2	25	1.2	0.13

[a] Loading: 50 wt % or 6.7E-4 mmol PEI/g material.

material was added to the adsorption column without the sand, the material clogged the column creating a significant decrease in the volumetric flow rate and a very large pressure drop. Therefore, the use of the impregnated silica material as a sorbent in a

flow system may cause additional concerns. However, the SBA-15 material remained powder-like after addition of the aziridine (SBA-HA). This material dispersed well in the sand and captured CO_2 with higher capacities compared to other known amine-based solid sorbents (Table 6.3).[40]

6.4. Conclusions

The hyperbranched aminosilica was synthesized in a one step reaction between SBA-15 and aziridine. The resulting material was capable of adsorbing CO_2 reversibly with capacities of 3.11 mmol CO_2/g material at 25 ^oC. The advantage of this sorbent over previously reported sorbents was its large CO_2 capacity. The material was recycled by desorbing the CO_2 from the surface at 130 ^oC for 3 hours. A very small change in capacity was determined after the desorption step, indicating that the CO_2 was removed from the surface. Furthermore, the organic groups on the surface were stable to temperature ranges between 25-130 ^oC, due to the covalent attachment between the surface and the polyamine groups. Currently, this hyperbranched aminosilica is one of the best reported CO_2 capture materials in the open literature.

6.5 References

1. Astarita, G., *Chem. Eng. Sci.* **1961,** 16, 202.

2. Chen, Z.; Chanda, M., *J. Polym. Mater.* **2002,** 19, 381.

3. Diaf, A.; Beckman, E., *React. & Funct. Polym.* **1995,** 27, 45.

4. Diaf, A.; Garcia, J.; Beckman, E., *J. Appl. Polym. Sci.* **1994,** 53, 857.

5. Tang, J.; Tang, H.; Sun, W.; Radosz, M.; Shen, Y., *J. Poly. Sci. Poly. Chem.* **2005,** 43, 5477.

6. Tsuda, T.; Tsuyoshi, F., *J. Chem. Soc. Chem. Commun.* **1992**, 1659.

7. Leal, O.; Bolivar, C.; Ovalles, C.; Garcia, J. J.; Espidel, Y., *Inorganica Chemica Acta* **1995,** 240, 183.

8. Gray, M. L.; Soong, Y.; Champagne, K. J.; Pennline, H. W.; Baltrus, J.; Stevens Jr., R. W.; Khatri, R.; Chuang, S. S. C., *Int. J. Environ. Techol. Manage.* **2004,** 4, 82.

9. Gray, M. L.; Soong, Y.; Champagne, K. J.; Pennline, H. W.; Baltrus, J.; Stevens Jr., R. W.; Khatri, R.; Chuang, S. S. C.; Filburn, T., *Fuel Proc. Technol.* **2005,** 86, 1449.

10. Khatri, R. A.; Chuang, S. S. C.; Soong, Y.; Gray, M., *Energy & Fuels* **2006,** 20, 1514.

11. Kim, S.; Ida, J.; Guliants, V. V.; Lin, J. Y. S., *J. Phys. Chem. B* **2005,** 109, 6287.

12. Knowles, G. P.; Graham, J. V.; Delaney, S. W.; Chaffee, A. L., *Fuel Proc. Technol.* **2005,** 2005, 1435.

13. Chang, A. C. C.; Chuang, S. S. C.; Gray, M.; Soong, Y., *Energy & Fuels* **2003,** 17, 468.

14. Zheng, F.; Tran, D. N.; Busche, B. J.; Fryxell, G. E.; Addlemann, R. S.; Zemanian, T. S.; Aardahl, C. L., *Ind. Eng. Chem. Res.* **2005,** 44, 3099.

15. Khatri, R. A.; Chuang, S. S. C.; Soong, Y.; Gray, M., *Ind. Eng. Chem. Res.* **2005,** 44, 3702.

16. Harlick, P. J. E.; Sayari, A., *Ind. Eng. Chem. Res.* **2007,** 46, 446.

17. Harlick, P. J. E.; Sayari, A., *Ind. Eng. Chem. Res.* **2006,** 45, 3248.

18. Knowles, G. P.; Delaney, S. W.; Chaffee, A. L., *Ind. Eng. Chem. Res.* **2006,** 45, 2626.

19. Xu, X.; Song, C.; Andresen, J. M.; Miller, B. G.; Scaroni, A. W., *Micropor. Mesopor. Mater.* **2003,** 62, 29.

20. Xu, X.; Song, C.; Andresen, J. M.; Miller, B. G.; Scaroni, A. W., *Energy & Fuels* **2002,** 16, 1463.

21. Xu, X.; Song, C.; Miller, B. G.; Scaroni, A. W., *Ind. Eng. Chem. Res.* **2005,** 44, 8113.

22. Xu, X.; Song, C.; Miller, B. G.; Scaroni, A. W., *Fuel Proc. Technol.* **2005,** 86, 1457.

23. Yue, M. B.; Chun, Y.; Cao, Y.; Dong, X.; Zhu, J. H., *Adv. Funct. Mater.* **2006,** 16, 1717.

24. Rosenholm, J. M.; Penninkangas, A.; Linden, M., *Chem. Commun.* **2006**, 3909.

25. Pangborn, A. B.; Giardello, M. A.; Grubbs, R. H.; Rosen, R. K.; Timmers, F. J., *Organometallics* **1996,** 15, 1518.

26. Hicks, J. C.; Dabestani, R.; Buchanan III, A. C.; Jones, C. W., *Chem. Mater.* **2006,** 18, 5022.

27. Hicks, J. C.; Jones, C. W., *Langmuir* **2006,** 22, 2676.

28. Hicks, J. C.; Mullis, B. A.; Jones, C. W., *J. Am. Chem. Soc.* **2007,** 129, 8426.

29. Zhao, D.; Huo, Q.; Feng, J.; Chmelka, B. F.; Stucky, G. D., *J. Am. Chem. Soc.* **1998,** 120, 6024.

30. Wystrach, V. P.; Kaiser, D. W.; Schaefer, F. C., *J. Am. Chem. Soc.* **1955,** 77, 5915.

31. Kim, H. J.; Moon, J. H.; Park, J. W., *J. Colloid Interface Sci.* **2000,** 227, 247.

32. This synthesis has been performed multiple times. However, the amine loadings depend on multiple factors: quantities of SBA-15, quantities of aziridine, temperature, time, etc.

33. We developed a method based on the work by Kim et al. to functionalize SBA-15 with a high amine loading by polymerizing aziridine off of the surface. The priority date of our patent ("Structures for Capturing CO_2, Methods of Making the Structures, and Methods of Capturing CO_2" filed on 12/12/06) is July 14, 2005. Soon after our initial studies, a method using SBA-15 as the support was reported (Rosenholm et al.).

34. Galarneau, A.; Cambon, H.; Renzo, F. D.; Fajula, F., *Langmuir* **2001,** 17, 8328.

35. Kruk, M.; Jaroniec, M.; Kim, T.-W.; Ryoo, R., *Chem. Mater.* **2003,** 15, 2815.

36. Miyazawa, K.; Inagaki, S., *Chem. Commun.* **2000**, 2121.

37. Currently, we have no proof that hypberbranched amines are present on the surface or the amounts primary, secondary and tertiary amines. This is an ongoing project in the Jones group.

38. The particle sizes of SBA-15 are very small and created a large pressure drop when packed in the adsorption column. Therefore, two methods were attempted to prevent the pressure drop: (1) formation of modified-silica pellets and sieving to a specific particle size, or (2) dispersing the modified-silica particles into sieved sand or another packing material. The silica pellet method was not used because the formation of the pellet decreased the surface area of the mesoporous particles, resulting in lower calculated CO_2 capacities. .

39. These experiments were stopped after 200 minutes. If the exeriments were allowed 250 minutes, capacities of 2.4 mmol CO_2/g or 6.6 mmol CO_2/g aziridine would be determined.

40. It should be noted that the data obtained from this fixed bed flow system produced CO_2 capacities lower than reported values using a flow system. It is highly likely that the cause of this issue pertains to the background substraction.

CHAPTER 7

SUMMARY AND FUTURE WORK

7.1 Summary

The major goals of this thesis were to create, characterize the structure, and use new organic/inorganic hybrid material in engineering applications, including specifically:

1. Creating a site-isolated aminosilica material with higher amine loadings than previously reported isolation methods
2. Using spectroscopic, reactivity, and catalytic (olefin polymerization precatalysts) probes to determine isolation of amine groups on these organic/inorganic hybrid materials
3. Synthesizing an organic/inorganic hybrid material capable of activating Group 4 olefin polymerization precatalysts.
4. Synthesizing an organic/inorganic hybrid material with ultra-high amine loading that is capable of reversibly capturing CO_2 in a simulated flue gas stream.

Generally, the easiest way to synthesize an aminosilica material is the reaction of 3-aminopropyltrimethyoxysilane with a silica surface, producing a material with fairly high loadings (~1-3 mmol N/g).[1, 2] Although simple, the resulting material contains a mixture of amine sites on the surface (amine-amine interactions, amine-silanol interactions, and isolated amines).[1, 2] The most successful attempts to reduce these interactions have involved the use of protection/deprotection methods – protecting the amine before

reaction with the surface and deprotecting in subsequent steps.[3-12] However, these methods usually result in materials that are deficient in amine loading (~0.1-0.5 mmol N/g), due to dilution of the protected silane or the bulkiness of the protecting group (3,3,3-triphenylpropyl- groups).[3-12] This work involved the synthesis of an aminosilica via the protection/deprotection method, which created a material with an amine loading approaching traditional methods while preventing amine-amine and amine-silanol interactions. These results indicated that loadings of ~ 1.0 mmol N/g can be obtained (compared to ~ 1.2 mmol N/g for traditional aminosilica material), while creating a material that resembles under some conditions (using fluorescence spectroscopy) materials created with bulky protecting groups (trityl protecting groups).[13]

One of the main disadvantages of the protection/deprotection method is the multi-step grafting approach used to create the materials (five steps). It has been proposed that dilution of the unprotected aminosilane on the surface could produce spaced amine sites on the surface, while controlling the distance of separation with the concentration of the amine on the surface. Multiple materials created via dilution were compared with our protection/deprotection materials (benzyl- and trityl- spaced aminosilicas) using fluorescence spectroscopy.[14] In these studies, a fluorescent tag (1-pyrenecarboxylic acid or 1-pyrenebutyric acid) was loaded on the aminosilicas and the fluorescence of the tag was studied with fluorescence spectroscopy. The results indicated that protection/deprotection methods produce spaced amine groups on the silica surface, with amine spacing governed by the size of the protecting group. However, although the dilution method produced aminosilicas that showed signs of amine separation, the resulting materials did not appear to be as spaced as the protection/deprotection

aminosilicas with similar loadings. In fact, materials produced by protection/deprotection methods are suggested to have amine sites spaced further apart on the surface with amine loadings twice that of the dilution methods.

Recently, a method to produce spaced amines by using a mixed silane grafting method (cooperative dilution) was reported, claiming isolation similar to protection/deprotection methods.[15] Spectroscopic and reactivity probes were used to determine the average degree of separation, and the accessibility of aminopropyl groups on silica materials prepared using different silane grafting approaches: (1) the traditional grafting of 3-aminopropyltrimethoxysilane in toluene, (2) a protection/deprotection method using benzyl- or trityl-spacer groups, and (3) a cooperative dilution method where 3-aminopropyltrimethoxysilane and methyltrimethoxysilane are co-condensed on the silica surface as a silane mixture.[16] The site-isolation and accessibility of the amine groups were probed via three methods: (a) evaluation of pyrene groups adsorbed onto the solids using fluorescence spectroscopy, (b) the reactions of chlorodimethyl(2,3,4,5-tetramethyl-2,4-cyclopentadien-1-yl)silane ($Cp'Si(Me)_2Cl$) and chloro(cyclopenta-2,4-dienyl)dimethylsilane ($CpSi(Me)_2Cl$) with the tethered amine sites, and (c) comparison of the reactivity of zirconium constrained-geometry-inspired catalysts (CGCs) prepared using the $Cp'Si(Me)_2$-modified aminosilicas in the catalytic polymerization of ethylene to produce poly(ethylene). The spectroscopic probe of site-isolation suggested that both the protection/deprotection method and the cooperative dilution method yielded similarly isolated amine sites that are markedly more isolated than sites on traditional aminosilica. In contrast, both reactivity probes

showed that the protection/deprotection strategy lead to more uniformly accessible amine groups. It is proposed that the reactivity probes are more sensitive tests for accessibility and site-isolation in this case.

Additionally, a hyperbranched aminosilica capable of capturing carbon dioxide from simulated flue gas streams was created. This material was synthesized in a one step reaction between aziridine and a silica surface to produce the organic/inorganic hybrid aminosilica material. A CO_2 capture system was designed and built using a mass spectrometer for in situ effluent gas analysis. The results indicated that this material was capable of capturing CO_2 with capacities ~ 30% higher than some of the best reported aminosilica CO_2 capture materials.

Lastly, the first organic/inorganic hybrid cocatalyst used to activate Group 4 olefin polymerization precatalysts for the polymerization of olefins was synthesized.[17] Silica tethered perfluoroalkanesulfonic acids in combination with trimethylaluminum (TMA) activated metallocenes for the polymerization of ethylene. Various control experiments indicated that the *in situ* formation of known cocatalysts such as MAO was not likely. It is proposed that the interaction between the alkylaluminum and the supported perfluoroalkanesulfonic acid created a site that can activate the zirconocene precatalyst to form the polymerization catalyst. The resulting material operated as a combined activator/support for single-site olefin polymerization.

7.2 Recommendations for Future Work

7.2.1 Development of New Site-Isolated Aminosilicas

One of the key advantages to the protection/deprotection method of isolating amine groups on silica surfaces involves the ability to change the protecting groups to control the distance between amine sites. Currently, we can control the amine separation or amine density on the surface by using either a benzyl- or a trityl-spacer.[7, 13, 14] However, it would be advantageous to use new protecting groups to develop new materials with different amine spacers. For instance, to increase the distance between amine sites, tris(perfluorophenyl)propanal could be used to form an imine with 3-aminopropyltrimethoxysilane. The perfluorophenyl- groups will produce a material with increased amine spacing because the F substituents are larger in size compared to the H substituents on a triphenylpropanal protecting group. Also, rather than using an imine as the cleavable protection linkage, a carbamate can be formed to protect the amine.[6, 8, 9] For instance, 3-aminopropyltrimethoxysilane can be reacted with tert-butyl chloroformate to form a tert-butyl carbamate protecting group. This group can be cleaved by thermolysis, leaving a primary amine. The various spaced aminosilicas could be used as a library for any application when the amine spacing and the distance between groups on the support are critical for the success of the project (e.g. supported olefin polymerization precatalysts, efficiency when binding heavy metals, bifunctional catalysis, etc.).

7.2.2 Potential Applications for Site-Isolated Aminosilicas

In theory, spaced aminosilicas continue to be studied because the creation of well-defined materials would provide better amine efficiency via site-isolation and molecular-level understanding of phenomena occurring on or at the surface. Understanding these

phenomena could potentially provide important information about the surface bound species, leading to the creation of novel materials.

Using Spaced Amines as Scaffolds for Heterogeneous Olefin Polymerization Cocatalysts

Homogeneous metallocenes are able to produce polyolefins with high molecular weights, narrow polydispersities (~2), and controlled tacticities.[18, 19] Although supported catalysts comprised of a metallocene precatalyst and a cocatalyst or activator are needed industrially for polyolefin production, very little is known fundamentally about supported catalysts due to the complexity of the surface species formed. In particular, single active-site homogeneous organometallic complexes become multi-sited when immobilized on surfaces. These multi-sited catalysts generally produce polyolefins with low molecular weights, broader polydispersities, and less controlled polymer tacticities.

An active metallocene polymerization catalyst requires the inclusion of a cocatalyst. The activity of the catalyst increases dramatically when partially hydrolyzed trimethylaluminum (MAO or methylaluminoxane) is added as the cocatalyst.[20] The use of MAO, however, has many drawbacks. MAO is extremely expensive, and has been shown to cause significant leaching of immobilized active catalysts when used in toluene solution. Also, when the catalysts are immobilized on a silica surface, the resulting material is poorly-defined and difficult to study due to the large excess of MAO present (~ 1000:1 Al:Metal). To alleviate these and other problems, new molecular boron cocatalysts have been developed. These boron cocatalysts can be immobilized on the support material. Afterwards, the metallocene can be added to the support material and

activated by the boron complex on the surface, producing a potentially more well-defined supported catalytic species.

Immobilization of molecular boron-based cocatalysts on a site-isolated amine scaffold[5, 7, 13, 14] allows for preparation of a new catalytic material with well-defined, isolated active sites that are more suited for molecular-level characterization. Addition of homogeneous organometallic precatalysts will then give a new catalytic material for polymerization of various olefins (e.g. ethylene, propylene, styrene). By altering site density, catalyst structure, and boron cocatalyst structure, their effects on the catalyst's polymerization activity can be determined. If a well-defined system is truly produced, polymerization activity and polymer properties can be tailored by rational structural variation. Immobilizing different boron compounds will provide insights into how the steric bulk and Lewis acidity of an activator affects the activity of the metallocene for polyolefin production. By creating supported, single-site borane and borate complexes, methods to rationally design and understand well-defined, single-site catalysts on oxide surfaces will be furthered, leading to improved methods of polyolefin production.

Metallocene cocatalyst research has focused, to some extent, on immobilizing perfluoroarylboranes (FAB) on various silica and polymeric supports. As discussed previously, tris(perfluorophenyl)borane has been directly reacted with the surface silanols to form a borate complex; this complex has been stabilized on the silica surface through the addition of a large counter ion. Up to this date, no work has been conducted to optimize the structure and spacing of a FAB on the support to provide better accessibility for the catalyst. By using distinct patterning techniques, an immobilized FAB can be studied to determine whether site-isolation produces a better heterogeneous cocatalyst.

When the patterned amine surface is reacted with the chlorobis(perfluorophenyl)borane, a reaction will occur with patterned amine functionalities and the borane, evolving HCl. As a result, the FAB will be patterned on the amine scaffold as the olefin polymerization cocatalyst. The borane will be reacted with the trityl or benzyl patterned aminosilica (Figure 7.1).

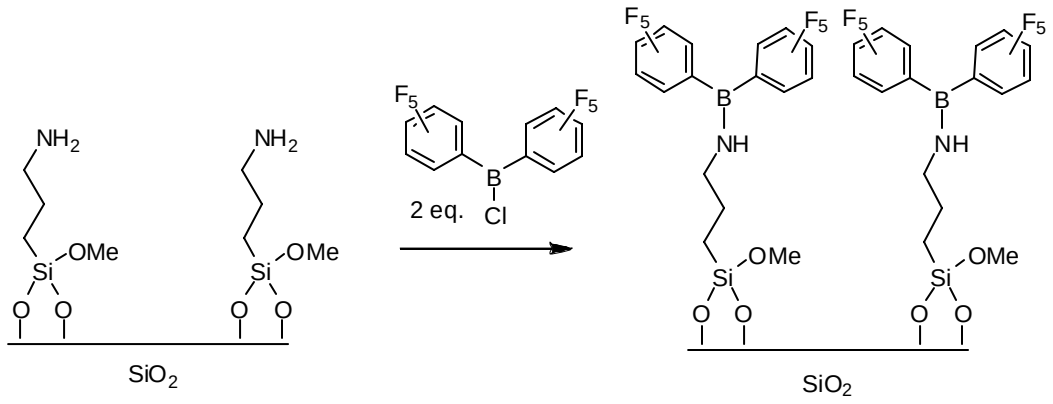

Figure 7.1. Method of borane immobilization on patterned aminosilicas.

To determine if site-isolation of the cocatalyst is a key factor in precatalyst activation, the two boranes on the spaced aminosilicas can be compared to boranes supported on traditional amine modified silica through catalytic tests. The disadvantage of the traditional aminosilica material is the potential interactions between the surface silanols with amines and adjacent amines with each other via hydrogen bonding. This may render many of the amine sites unreactive. Even though much has been published on this method due to its experimental simplicity, it is not an ideal support for most catalysts or cocatalysts due to the presence of multiple types of surface sites.

Boron and metal catalyst leaching tests on all of the boron-modified support reactions will provide information on the catalytically active species. This elucidation of the active species will help clarify the reaction mechanisms for the heterogeneous cocatalysts.

Molecular Design of Organic/Inorganic Hybrid Sorbents for CO_2 Capture

The difficulty with the hyperbranched aminosilica in Chapter 5 is the lack of control over the branching of the amine groups. In order to design a CO_2 capture material that can bind CO_2 with high capacities, the efficiency of the material must be controlled (i.e. synthesis of primary and secondary amines with no tertiary amines). One way to prevent hyperbranching is by protecting the aziridine before reaction with the surface (Figure 7.2).[21]

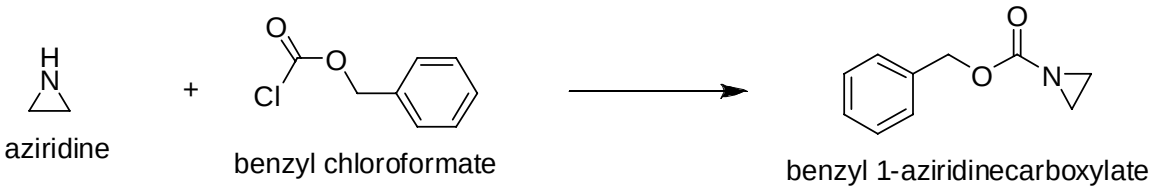

Figure 7.2. Protecting aziridine.

Secondly, either pure silica or an aminosilica can be used to ring-open the protected aziridine.[22] After the reaction with the surface, the protecting group can be cleaved with heat, trifluoroacetic acid, or piperidine to form the primary amine. Subsequently, the material can be reacted with another aliquot of the protected aziridine and repeated (Figure 7.3). In theory, the end result is a material that can be synthesized

with a specific amount of secondary amines, end capped with primary amines. This method will reduce the amount of tertiary amines on the sorbent, limiting the amount of "unusable" binding sites.

Well-defined scaffolds (aminosilicas produced by a protection/deprotection method with benzyl- and trityl-spacers) can be used to develop structure property relationships (Figure 7.4). The underlying support material should be as well-defined as possible in order to understand the role of amine separation for grafting. For instance, using supports 3-7 in Figure 7.4 will provide an aminosilica with fewer amine sites (e.g. prevention of amine-amine and amine-silanol interactions, while separating the amines a given distance apart).

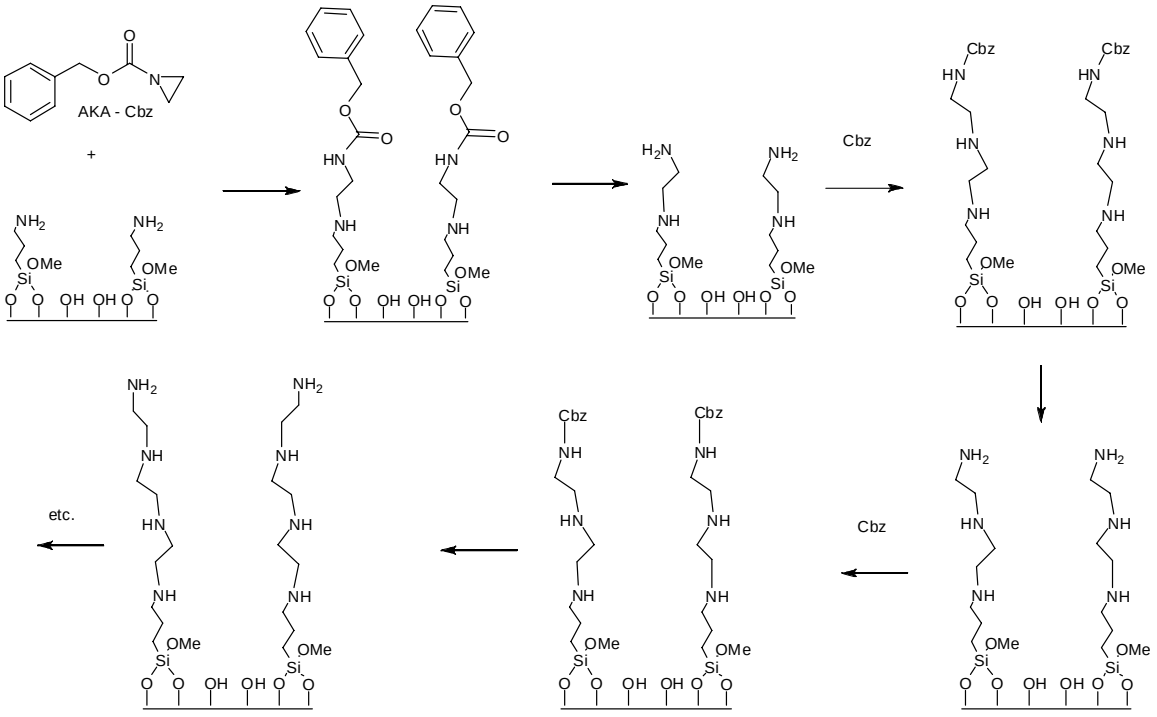

Figure 7.3. Synthesis of CO_2 sorbent with protected aziridine.

Also, this system can be tailored to create a CO_2 sorbent that surpasses current technology (adsorption of CO_2 greater than 4 mmol CO_2/g sorbent) by using different protection groups (Figure 7.5) to provide a high loading of secondary amines on the surface separated far enough to prevent diffusion effects. Overall, this method to produce aminosilicas via a step-wise protection/deprotection approach by changing the protecting group and aminosilica support has many advantages:

1) Heat can be used to thermolyze (as the deprotection method) the t-butyl carbamate and cyclohexyl carbamate. Piperidine or trifluoroacetic acid can also be used to deprotect the amine protecting group.
2) Various protected aziridine molecules can react differently.
3) The formation of a tertiary amine is limited due to the bulkiness of the protecting group on aziridine.
4) The result is a molecularly designed CO_2 sorbent that has mainly secondary amines.

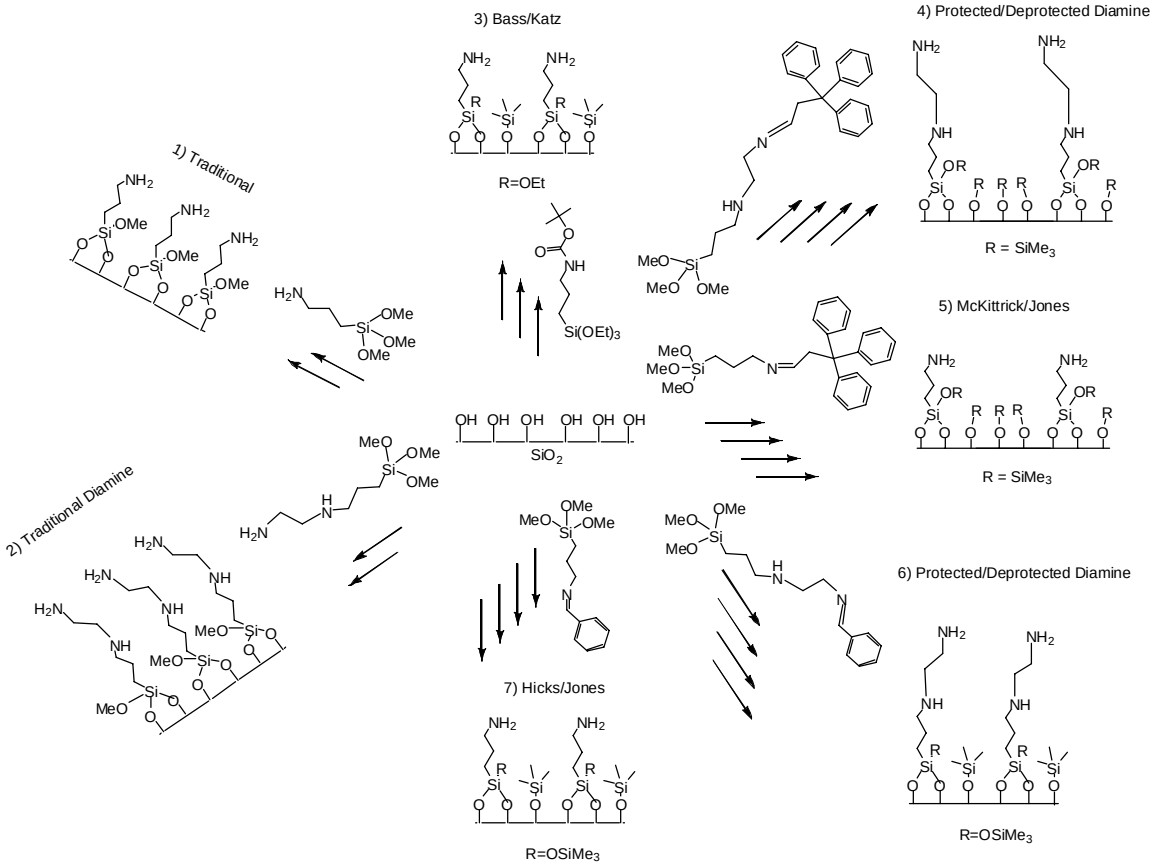

Figure 7.4. Aminosilicas for CO_2 study.

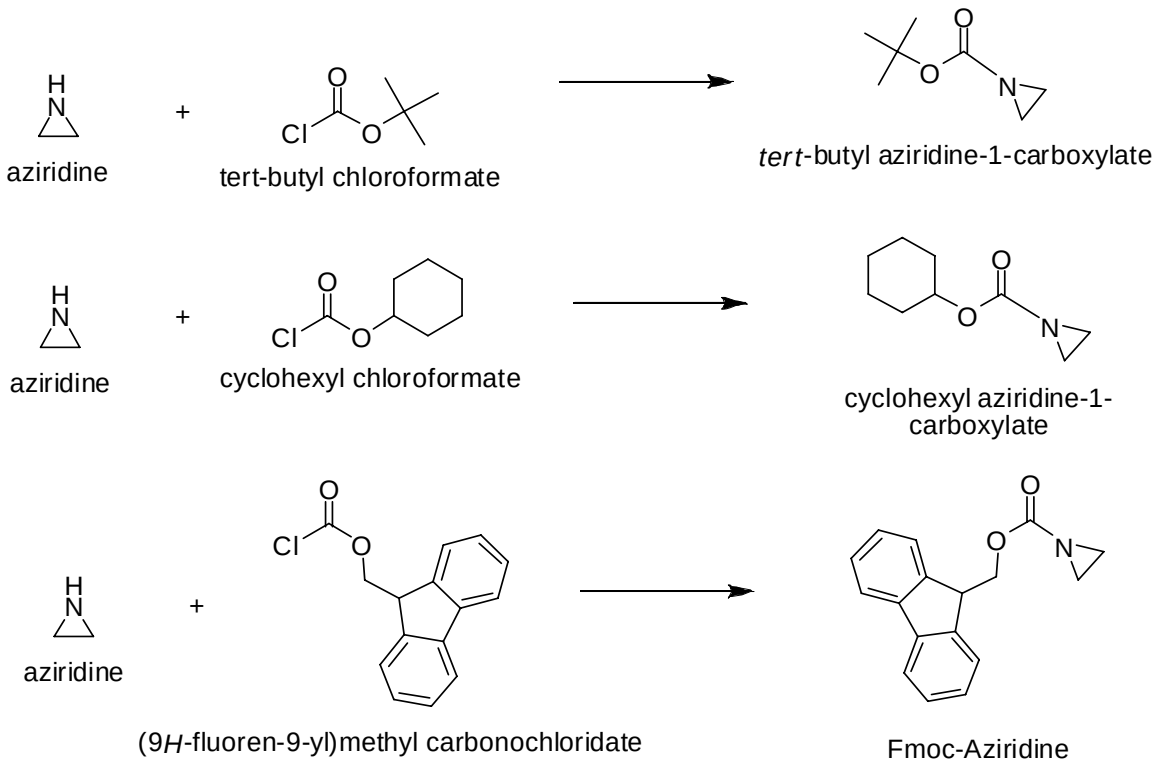

Figure 7.5. Protecting aziridine with different groups.

Bifunctional Materials using Spaced Aminosilicas

Acid-base cooperative catalysis is common for biological catalysts (such as enzymes).[11, 23-25] Due to their ability to perform multi-step reactions with high efficiency, much work as involved synthesis of acid-based cooperative catalysts that mimic nature.[11, 23-25] For instance, Katz and coworkers have synthesized isolated amine groups on silica surfaces (using a protection/deprotection method) that contain surface silanol groups.[11] The combination of the amine (base) and silanol (acid) produced a bifunctional material that showed an increase in efficiency for Michael and Henry reactions. Davis and coworkers reported the synthesis of bifunctional thiol and sulfonic acid tethered materials

that showed cooperation for condensation reactions.[24] Also, Davis and coworkers have reported the synthesis of an amine and sulfonic acid bifunctional catalyst by grafting the groups on a mesoporous silica surface.[25] These reported bifunctional materials showed reactivity for an aldol condensation reaction that could not be obtained with homogeneous compounds. Our amine spaced aminosilica could also be used to synthesize bifunctional materials. For instance, the trityl-spaced amines could be formed on the surface (materials synthesized without silanol capping). The resulting material could be used as a bifunctional material involving amines (base) and silanols (acid). Also, 3-mercaptopropyltrimethoxysilane could be reacted with the remaining surface silanols (between the trityl-spaced amines) in order to produce a bifunctional material consisting of a base (amine) and an acid (thiol) to perform heterogeneous multi-step reactions.

7.2.3 Continuation of Sulfonic Acid/TMA as Cocatalyst for Activation of Olefin Polymerization Precatalysts

As discussed in Chapter 6, the use of a perfluoroalkane sulfonic acid-functionalized silica material mixed with small amounts of trimethylaluminum acts as a dual activator/support by activating metallocenes for olefin polymerizations. Currently, it is proposed that the Bronsted acid (sulfonic acid) interacts with the Lewis acid (trimethylaluminum) creating a species capable of activating metallocenes by abstracting a methyl- group from the metal (i.e. Cp_2ZrMe_2). However, it would be advantageous to determine the species activating the metallocene. This could be determined using data obtained from EXAFS (extended X-ray fine structure) studies combined with solid state

NMR techniques (^{13}C, ^{27}Al, ^{17}O, etc.). For instance, a ^{13}C labeled metallocene could be used and monitored with ^{13}C NMR to determine the surface activation mechanism of the metallocene with the fluorinated alkanesulfonic acid groups and the alkylaluminum. The ^{27}Al NMR could be used to suggest a structure of the alkylaluminum/sulfonic acid groups. Also, ^{17}O NMR could possibly be used to investigate the oxygens bound to the sulfonic acid before and after addition of the trimethylaluminum. All of these experiments together could provide enough information to propose a more feasible activated catalyst structure on the silica surface.

Also, structure-property relationships between the sulfonic acid and aluminum source or between the sulfonic acid/alkylaluminum activator and the precatalyst could provide information critical to determining the structure of the surface bound cocatalyst. These studies could be performed by analyzing the effects of precatalyst activation by changing the aluminum source from trimethylaluminum to other sources (triethylaluminum, tri-n-propylaluminum, triisobutylaluminum, etc.). Also, different precatalysts could be studied to determine the types of organometallic complexes activated by the perfluoroalkane sulfonic acid/alkylaluminum tethered cocatalyst.

In conclusion, the synthesis, characterization, and application of various organic/inorganic hybrid amine-functionalized or sulfonic acid-functionalized materials have been studied. I have reported the synthesis of a benzyl-spaced aminosilica that is more reactive and more spaced compared to traditionally synthesized aminosilicas. These benzyl-spaced aminosilicas could be useful to researchers needing a relatively high loading of amines on the support that were synthesized to prevent multiple types of amine species on the surface. I have also reported the synthesis of an organic/inorganic hybrid

sulfonic acid functionalized silica material cocatalyst capable of activating metallocenes for the polymerization of ethylene when an alkylaluminum is present. The activated catalyst was found not to leach from the surface, preventing reactor fouling. These cocatalysts could be useful in industrial reactors where reactor fouling is a major concern. Lastly, I have reported the synthesis of a hyperbranched aminosilica with a high loading of amines sites tethered to the support capable of reversibly binding CO_2 from simulated flue gas streams. The hyperbranched aminosilica materials were synthesized in a one step reaction which created a material with an amine loading > 8 mmol/g. These materials have captured CO_2 reversibly with higher capacities than the best known organic/inorganic hybrid aminosilicas. All of the materials reported in this dissertation are important as catalysts, cocatalysts, adsorbents and/or reactive scaffolds for further functionalization. Overall, organic/inorganic hybrid materials have become important in a variety of fields, due to the ability to design these materials for specific applications. Due to their limitless application and design, organic/inorganic hybrids will continue to be a topic of much research for years to come.

7.3 References

1. White, L. D.; Tripp, C. P., *J. Colloid Interface Sci.* **2000,** 227, 237.

2. Kanan, S. M.; Tze, W. T. Y.; Tripp, C. P., *Langmuir* **2002,** 18, 6623.

3. Wulff, G.; Heide, B.; Helfmeier, G., *J. Am. Chem. Soc.* **1986,** 108, 1089.

4. Wulff, G.; Heide, B.; Helfmeier, G., *React. Polym.* **1987,** 6, 299.

5. Zaitsev, V. N.; Skopenko, V. V.; Kholin, Y. V.; Konskaya, N. D.; Mernyi, S. A., *Zh. Obshch. Khim.* **1995,** 65, 529.

6. Katz, A.; Davis, M. E., *Nature* **2000,** 403, 286.

7. McKittrick, M. W.; Jones, C. W., *Chem. Mater.* **2003,** 15, 1132.

8. Bass, J. D.; Anderson, S. L.; Katz, A., *Angew. Chem. Int. Ed.* **2003,** 42, 5219.

9. Bass, J. D.; Katz, A., *Chem. Mater.* **2003,** 15, 2757.

10. Bass, J. D.; Katz, A., *Chem. Mater.* **2006,** 18, 1611.

11. Bass, J. D.; Solovyov, A.; Pascall, A. J.; Katz, A., *J. Am. Chem. Soc.* **2006,** 128, 3737.

12. Defreese, J. L.; Hwang, S.-J.; Parra-Vasquez, A. N. G.; Katz, A., *J. Am. Chem. Soc.* **2006,** 128, 5687.

13. Hicks, J. C.; Jones, C. W., *Langmuir* **2006,** 22, 2676.

14. Hicks, J. C.; Dabestani, R.; Buchanan III, A. C.; Jones, C. W., *Chem. Mater.* **2006,** 18, 5022.

15. Luechinger, M.; Prins, R.; Pirngruber, G. D., *Microporous Mesoporous Mater.* **2005,** 85, 111.

16. Hicks, J. C.; Dabestani, R.; Buchanan III, A. C.; Jones, C. W., *J. Mater. Chem.* **2007,** submitted.

17. Hicks, J. C.; Mullis, B. A.; Jones, C. W., *J. Am. Chem. Soc.* **2007,** 129, 8426.

18. Chen, E. Y.-X.; Marks, T. J., *Chem. Rev.* **2000,** 100, 1391.

19. Hlatky, G. G., *Chem. Rev.* **2000,** 100, 1347.

20. Sinn, H.; Kaminsky, W.; Vollmer, H. J.; Woldt, R., *Angew. Chem. Int. Ed.* **1980,** 19, 390.

21. Dauban, P.; Dubois, L.; Elise Tran Huu Dau, M.; Dodd, R. H., *J. Org. Chem.* **1995,** 60, 2035.

22. Kim, H. J.; Moon, J. H.; Park, J. W., *J. Colloid Interface Sci.* **2000,** 227, 247.

23. Sharma, K. K.; Asefa, T., *Angew. Chem. Int. Ed.* **2007,** 46, 2879.

24. Zeidan, R. K.; Dufaud, V.; Davis, M. E., *J. Catal.* **2006,** 239, 299.

25. Zeidan, R. K.; Hwang, S.-J.; Davis, M. E., *Angew. Chem. Int. Ed.* **2006,** 45, 6332.

VITA

Jason C. Hicks was born in Owensboro, KY to John and Debbie Hicks. He graduated from McLean County High School (Calhoun, KY) in 1998. After graduation, he spent three years at Kentucky Wesleyan College in Owensboro, KY working towards his B.S. degree in chemistry (2003). He then attended Vanderbilt University in Nashville, TN to obtain a B.E degree in chemical engineering (2003) and to complete the required courses from Kentucky Wesleyan College. After performing much undergraduate research, Jason decided to attend the Georgia Institute of Technology the following fall to work toward a Ph.D. in chemical engineering. After his Ph.D., he plans to work for Chevron Energy Technology Company in the catalysis division.